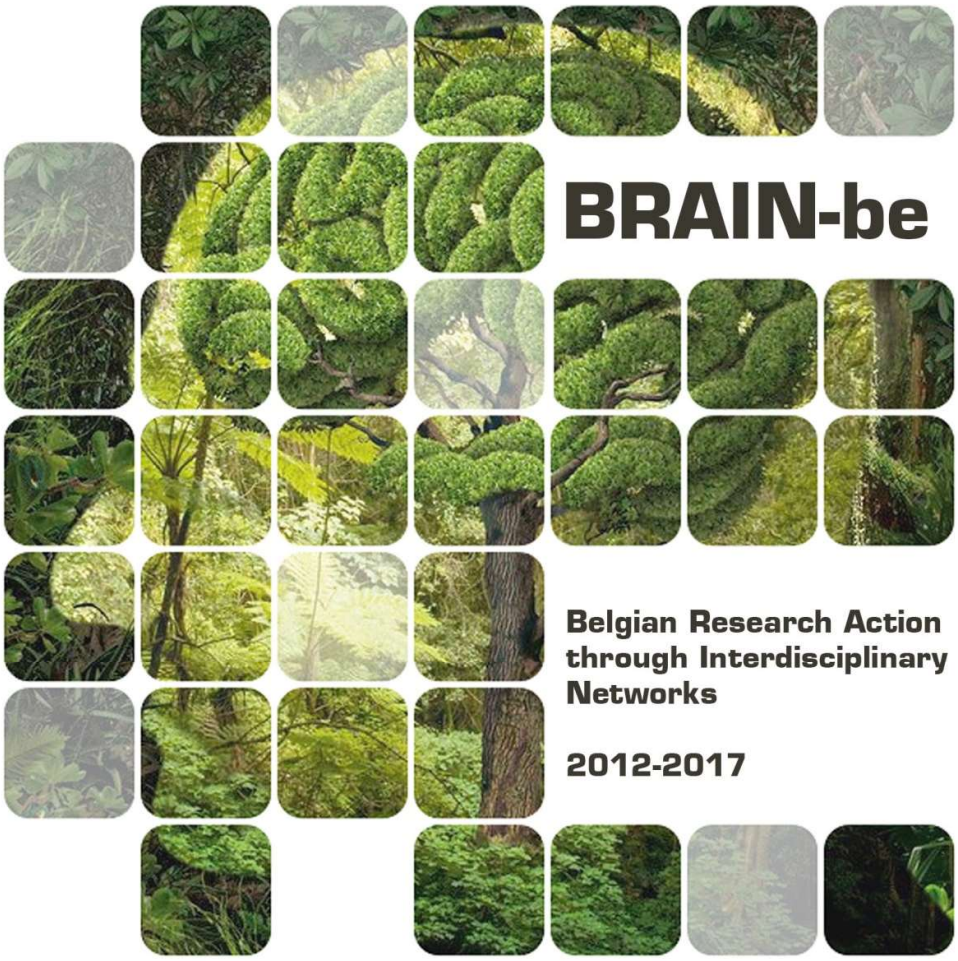

NewSTHEPS

New Strategies for monitoring and risk assessment of Hazardous chemicals in the marine Environment with Passive Samplers

Koen Parmentier (RBINS, ODNature) – Argiro Adamopoulou (RBINS, ODNature) – Patrick Roose (RBINS, ODNature) – Katrijn Baetens (RBINS, ODNature) – Geneviève Lacroix (RBINS, ODNature) – Samuel Moeris (UGent, GhEnToxLab) – Simon Hansul (UGent, GhEnToxLab) – Karel De Schamphelaere (UGent, GhEnToxLab) – Francis Vanryckeghem (UGent, EnVOC) – Kristof Demeestere (UGent, EnVOC) – Herman Van Langenhove (UGent, EnVOC) – Lynn Vanhaecke (UGent, Laboratory of Chemical Analysis) – Steve Huysman (UGent, Laboratory of Chemical Analysis) – Camille Gaulier (Vrije Universiteit Brussel, Analytical, Environmental and Geo-Chemistry Department – Lille University (France), Laboratory for Infrared and Raman Spectrochemistry) – Wei Guo (Vrije Universiteit Brussel, Analytical, Environmental and Geo-Chemistry Department) – Willy Baeyens (Vrije Universiteit Brussel, Analytical, Environmental and Geo-Chemistry Department) – Yue Gao (Vrije Universiteit Brussel, Analytical, Environmental and Geo-Chemistry Department) – Foppe Smedes, Masaryk University (Brno, Czech Republic), Faculty of Science, RECETOX.

Axis 2: Geosystems, universe and climate

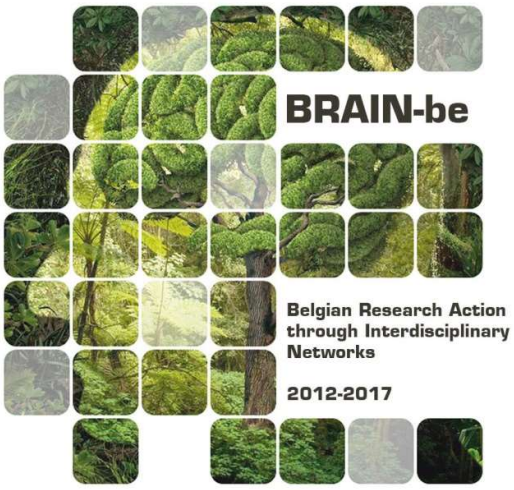

NETWORK PROJECT

NewSTHEPS

New Strategies for monitoring and risk assessment of Hazardous chemicals in the marine Environment with Passive Samplers

Contract - BR/143/A2

FINAL REPORT

PROMOTORS: Patrick Roose & Koen Parmentier (RBINS, ODNature)
Colin Janssen & Karel De Schamphelaere (UGent, GhEnToxLab)
Kristof Demeestere & Herman Van Langenhove (UGent, EnVOC)
Lynn Vanhaecke (UGent, Laboratory of Chemical Analysis)
Yue Gao & Willy Baeyens (VUB, AMGC)

AUTHORS: Koen Parmentier, Argiro Adamopoulou, Patrick Roose, Katrijn Baetens, Geneviève Lacroix (RBINS, ODNature)
Samuel Moeris, Simon Hansul, Karel De Schamphelaere (UGent, GhEnToxLab)
Francis Vanryckeghem, Kristof Demeestere, Herman Van Langenhove (UGent, EnVOC)
Lynn Vanhaecke, Steve Huysman (UGent, Laboratory of Chemical Analysis)
Camille Gaulier (Vrije Universiteit Brussel, Analytical, Environmental and Geo-Chemistry Department –Lille University (France), Laboratoire de Spectro-chimie Infrarouge et Raman)
Wei Guo, Willy Baeyens, Yue Gao (Vrije Universiteit Brussel, Analytical, Environmental and Geo-Chemistry Department)
Foppe Smedes, Masaryk University (Czech Republic, Brno), Faculty of Science, RECETOX

Published in 2021 by the Belgian Science Policy Office
WTC III, Simon Bolivarlaan 30 Bd Simon Bolivar
B-1000 Brussel | Bruxelles | Brussels
Belgium
Tel: +32 (0)2 238 34 11 - Fax: +32 (0)2 230 59 12
http://www.belspo.be
http://www.belspo.be/brain-be

Contact person: Koen Lefever
Tel: +32 (0)2 238 35 51

Neither the Belgian Science Policy Office nor any person acting on behalf of the Belgian Science Policy Office is responsible for the use which might be made of the following information. The authors are responsible for the content.

No part of this publication may be reproduced, stored in a retrieval system, or transmitted in any form or by any means, electronic, mechanical, photocopying, recording, or otherwise, without indicating the reference :

Parmentier, K., Adamopoulou, A., Roose, P., Baetens, K., Lacroix G., Moeris, S., Hansul, S., De Schamphelaere, K., Vanryckeghem, F., Demeestere, K., Van Langenhove, H., Vanhaecke, L., Huysman, S., Gaulier, C., Guo, W., Baeyens, W., Gao Y., Smedes, F. ***New Strategies for monitoring and risk assessment of Hazardous chemicals in the marine Environment with Passive Samplers.*** Final Report. Brussels : Belgian Science Policy Office 2020 – 136 p. (BRAIN-be - (Belgian Research Action through Interdisciplinary Networks)

TABLE OF CONTENTS

CONTENTS

ABSTRACT: 7
CONTEXT: 7
OBJECTIVES: 7
CONCLUSIONS: 7
KEYWORDS: 7
1. INTRODUCTION. 8
2. STATE OF THE ART AND OBJECTIVES. 9
3. METHODOLOGY. 11
3.1. SAMPLING AND SAMPLING CAMPAIGNS. 12
3.1.1. Preparation of sampling material. 13
3.1.2. Sampling campaigns: time, position, duration, parameters measured. 17
3.2. TRACE METAL ANALYSIS. 18
3.2.1. Chemicals and materials. 19
3.2.2. Passive sampling of trace metals: Diffusive Gradients in Thin-films (DGT) piston retrieval and treatment. 19
3.2.3. Grab sampling of trace metals: seawater filtration and treatment. 20
3.2.4. Trace metal analysis. 21
3.3. ESTROGENIC ACTIVITY ANALYSIS USING DGT TECHNIQUE AND ERE-CALUX BIOASSAY. 21
3.3.1. Experiment Chemicals and Materials. 21
3.3.2. o-DGT performance test and application. 22
3.3.3. Sample Extraction for the measurement of ERE-CALUX Bioassay. 23
3.4. ADVANCED ANALYSIS OF CONTAMINANTS OF EMERGING CONCERN (CECS) AND LEGACY POLLUTANTS. 24
3.4.1. Analysis of pesticides, pharmaceuticals and personal care products. 24
3.4.2. Analysis of Steroidal EDCs. 28
3.4.3. Analysis of plasticizers and plastics additives. 30
3.4.4. Analysis of Persistent Organic Pollutants (CBs, BFRs, PAHs, chlorinated pesticides, musk fragrances). 31
3.5. UPTAKE KINETICS AND EQUILIBRIUM OF MICROPOLLUTANTS ON PASSIVE SAMPLERS. 32
3.5.1. Silicone Rubber. 32
3.5.2. Hydrophilic DVB based passive samplers. 33
3.5.3. Multi-ratio experiment on bioavailability of HOCs. 35
3.6. PARTICULATE CARBON AND STABLE ISOTOPES. 40
3.6.1. Treatment for Suspended Particulate Matter (SPM). 41
3.6.2. Carbon and stable isotope ratio analysis. 41
3.7. ECOTOXICOLOGICAL EFFECTS. 41
3.7.1. Ecotoxicity testing of individual contaminants of emerging concern. 43
3.7.2. Ecotoxicity testing of environmental samples collected with Passive Samplers. 46

3.7.3. Integrated Environmental Risk Assessment. 48

3.8. MODELLING. 49

4. SCIENTIFIC RESULTS AND RECOMMENDATIONS. 51

4.1. NOVEL ANALYTICAL METHODS: ANALYTICAL PERFORMANCE CHARACTERISTICS. 51

4.1.1. Novel development of o-DGT and ERE-CALUX for EDCs analysis. 51

4.1.2. Analytical validation for pharmaceuticals, personal care products and pesticides. 52

4.1.3. Analytical validation for steroidal EDCs. 56

4.1.4. Analytical validation for steroidal plasticizers and plastic additives. 57

4.2. CALIBRATION DATA ON HYDROPHILIC DVB BASED PASSIVE SAMPLERS. 57

4.2.1. Characterization. 57

4.2.2. Sampling rate. 58

4.2.3. Equilibrium partitioning coefficients. 60

4.3. FIELD RESULTS OF MONITORING CAMPAIGNS. 62

4.3.1. Trace metals. 62

4.3.2. Estrogenic activity analysis using o-DGT coupled with ERE-CALUX bioassay. 70

4.3.3. Analysis of pharmaceuticals, personal care products and pesticides. 71

4.3.4. Analysis of steroidal EDCs, plasticizers and plastic additives. 75

4.3.5. Results for HOC (CBs, BFRs, PAHs, chlorinated pesticides, musk fragrances). 76

4.3.6. Particulate Carbon concentrations and stable isotope ratios. 82

4.4. ECOTOXICOLOGICAL EFFECTS. 83

4.4.1. Ecotoxicity testing of individual contaminants of emerging concern. 84

4.4.2. Ecotoxicity testing of environmental samples collected with passive sampler. 85

4.4.3. Speedisk extract testing approaches for ERCMs. 86

4.4.4. Integrated Environmental Risk Assessment. 89

4.5. EXPOSURE MODELLING OF POLLUTANTS: CASE STUDY AND RECOMMENDATIONS FOR FURTHER WORK....98

4.5.1. Exposure modelling of clothianidin in the BPNS (open sea): influence of sources and degradation. 98

4.5.2. Conclusions and further recommended work. 104

4.6. A NOVEL AND INTEGRATED PASSIVE SAMPLER-BASED APPROACH FOR CHEMICAL EXPOSURE AND BIOLOGICAL EFFECT ASSESSMENT. 105

5. DISSEMINATION AND VALORISATION. 110

5.1. ORAL PRESENTATIONS. 110

5.1.1. 2016. 110

5.1.2. 2017. 110

5.1.3. 2018. 110

5.1.4. 2019. 112

5.2. POSTER PRESENTATIONS....112

5.2.1. 2016. 112

5.2.2. 2017. 112

5.2.3. 2018. 113
5.2.4. 2019. 113
5.3. WEBSITE, ANNEXES AND RAW DATA ARCHIVE. 114
6. PUBLICATIONS. 115
6.1. PEER-REVIEWED PUBLICATIONS. 115
6.1.1. 2017. 115
6.1.2. 2019. 115
6.1.3. 2020. 116
6.2. OTHER PUBLICATIONS. 116
6.2.1. 2018. 116
6.2.2. 2019. 117
6.2.3. 2020. 117
7. ACKNOWLEDGEMENTS. 118
8. REFERENCES. 119
GLOSSARY 132

ABSTRACT:

Context:

The NewSTHEPS project focused on the use of alternative sampling techniques (passive samplers, sediment traps), combined with state-of-the-art analytical methodologies to quantify a wide variety of chemical compounds, including legacy pollutants, chemicals of emerging concern (CECs), metals as well as their potential ecotoxicity and risks to the marine environment. This was combined with stable isotope analysis of suspended particulate matter (SPM) and modelling techniques in harbours and along the coast of the Belgian Part of the North Sea (BPNS).

Objectives:

The main goal was to offer policy support tools that allows to monitor a multitude of chemicals, that remained previously undetected, to enable risk assessment, combined with distance to target assessment (in case of exceeding the Environmental Quality Standards (EQS)) or Margin of Safety (MoS) assessments of mixtures of substances in the field.

Conclusions:

New sampling materials and deployment configurations were tested, optimized and applied. Twenty-one chemicals of emerging concern (CECs), including neonicotinoids, pharmaceuticals, steroids and phthalates were detected above their marine PNEC (Probable No-Effect Level). In addition, ecotoxicity testing of sampler extracts, combined with the MoS approach also suggests ecological risks of realistic compound mixtures in the BPNS. Most legacy organic pollutants still present are in or close to equilibrium between the different environmental compartments (water, SPM, sediment). Labile metal concentrations were determined for the first time in the Belgian Part of the North Sea by using the DGT technique. Isotopic signature analysis revealed that most of the SPM was of marine origin. An existing sediment transport model was extended with a contaminant fate module, that allowed for exposure assessment of individual substances, but this exposure model requires further optimisation (related to degradation and adsorption processes) and validation to enable its full potential in policy making.

Keywords:

passive sampling - high-resolution mass spectrometry - ecotoxicity – environmental risk assessment – marine chemical fate and exposure model

1. INTRODUCTION.

The project aimed to develop innovative approaches and novel practical techniques to address the current fundamental scientific and methodological issues related to the evaluation if Good Environmental Status (GES) for Descriptor 8 of the Marine Strategy Framework Directive in national and European waters (EU, 2008).

This included the development, application and testing of different passive sampler (PS) materials, the study of their kinetic and equilibration behaviour in different matrices, the use of PS-based sampling techniques in both harbour and open sea sampling sites in the Belgian part of the North Sea (BPNS), and the development of state-of-the-art analytical techniques for legacy pollutants, priority substances and chemicals of emerging concern (CECs; organics: both hydrophobic and more soluble compounds and inorganics).

This was expanded with ecotoxicity testing of a wide range of detected single organic substances and of enriched passive sampler extracts to represent environmentally relevant organic contaminant mixtures (ERCMs). The latter allowed the calculation of the "Margin of Safety" (MoS) of environmental samples. Also, an automated method for estimating the Predicted No Effect Concentration (PNEC) from a large ecotoxicity database was developed an applied to estimate single substance and mixture ecological risks for targeted compounds. In parallel with the analytical and ecotoxicological work, stable isotope analysis (carbon, nitrogen) of the collected suspended matter was performed to allow characterisation of its origin (marine or terrestrial).

Finally, a dedicated hydrodynamic advective and sediment transport model was adapted to and optimized for the study area (with focus on the harbour of Zeebrugge), and contaminant fate processes were added, i.e. degradation and sorption to suspended matter to simulate contaminant transport, distribution and concentrations in the BPNS.

Altogether, the project provides a wide suite of ready-to-use novel methods for GES assessment and the basis for an integrated assessment framework based on the use of passive sampling.

2. STATE OF THE ART AND OBJECTIVES.

The European Union (EU) by means of the Water Framework Directive (WFD; EU, 2000) and Marine Strategy Framework Directive (MSFD, EU, 2008) has as a main objective that the Member States reach the Good Environmental Status (GES) in their national waters (EU, 2008). However, this ambitious goal remains improperly described, despite several joint international efforts. This project aims to deliver (or at least to give substantial input for) a Belgian answer for the Descriptor 8, i.e. "concentrations of contaminants not giving rise to pollution effects". The marine environment acts as a sink for an extremely wide set of chemicals, used either on land or sea, spilled or released into the atmosphere, including a vast set of degradation and transformation products. The GES is far from defined with regard to descriptor 8, because under WFD and MSFD only limited Priority Substances, River Basin Specific Pollutants and Watch List substances are defined, and for many of those Environmental Quality Standard (EQS) or Predicted No Effect Concentrations (PNECs) are still not agreed upon. In addition, knowledge about the marine ecotoxicity of these substances is limited and fragmentary, and even less is known about the combined effect of the complex mixtures that are encountered in the marine environment.

The integrated approach applied in the NewSTHEPS project aimed to give at least a partial answer towards GES evaluation by the development of comprehensive environmental monitoring and risk assessment of a broad set of both priority and emerging contaminants in the marine environment. The project aimed to contribute to a more integrated, more efficient, cost-effective and scientifically relevant way to assess GES. It tried to achieve this by applying integrated passive sampler (PS)-based approaches (measurements) for both chemical exposure (monitoring) and biological effect assessment (passive dosing and extract spiking). Through the use and validation of a broad array of PS techniques, applicable in a wide polarity range, the project put focus on the quantification of a wide set of both priority and emerging organic micropollutants and metals (targeted approach). Additionally, the study of SPM was an integral part of this project because it constitutes an important adsorption phase for certain contaminants. To trace SPM to its origin, carbon ($^{12}C/^{13}C$) and nitrogen ($^{14}N/^{15}N$) stable isotope ratios were measured, as organic matter from marine and terrestrial origin has a quite different isotopic C signature and sometimes also a different isotopic N signature. The specific objective was to identify the sources of the organic matter present in the marine environment.

The new sampling methods were executed in parallel with traditional techniques, to allow comparison of both approaches. For metals this includes a comparison between the labile and total concentration. State-of-the-art analytical measurement techniques were used for determination of compounds down to or lower than MSFD required levels, where classical methods are still inadequate. Classic Environmental Risk Assessment (ERA) of individual compounds and mixtures of contaminants was performed based upon measured environmental concentrations and ecotoxicity data, and this was extended with a new Margin of Safety (MoS) approach addition based on direct ecotoxicity testing of

(enriched) passive sampler extracts, which allows taking into account cumulative effects of ERCMs, which – in contrast to conventional ERA – also takes into account compounds that are present but either not detected or targeted in the chemical analysis.

In addition, the foundation is laid for a hydrodynamic and sediment transport model to simulate the fate, transport and spatiotemporal distribution of selected pollutants. This model will ultimately help in taking appropriate measures to identify pollution sources in case of exceeding EQS. Altogether, the combination of all these tasks aimed to provide the basis for an integrated assessment framework, consisting of a suite of methods to evaluate anthropogenic chemical environmental pressure and to quantify the environmental status of the Belgian coastal zone.

3. METHODOLOGY.

A diversity of Passive Sampler devices (Silicone Sheets (SS), Speedisks, Simple Teabag Equilibrium Passive Sampler (STEPS) and Diffusive Gradient in Thin films (DGT) samplers) are deployed for several weeks at the individual sampling stations. During the same period, SPM is collected through specially designed traps. Water (Niskin) and sediment (Van Veen) samples are collected at the start and end of every sampling period.

Samples are collected from the different compartments (water, SPM, sediment) and analysed for metals, nonpolar and polar organics through dedicated protocols. SPM is analysed both by non-destructive (Nuclear Magnetic Resonance (NMR), X-ray) as classic analysis (metals, stable isotopes, Malvern grain size, equilibrium experiments with SS). Equilibrium constants and calibration of samplers is performed wherever these data are not available from open literature.

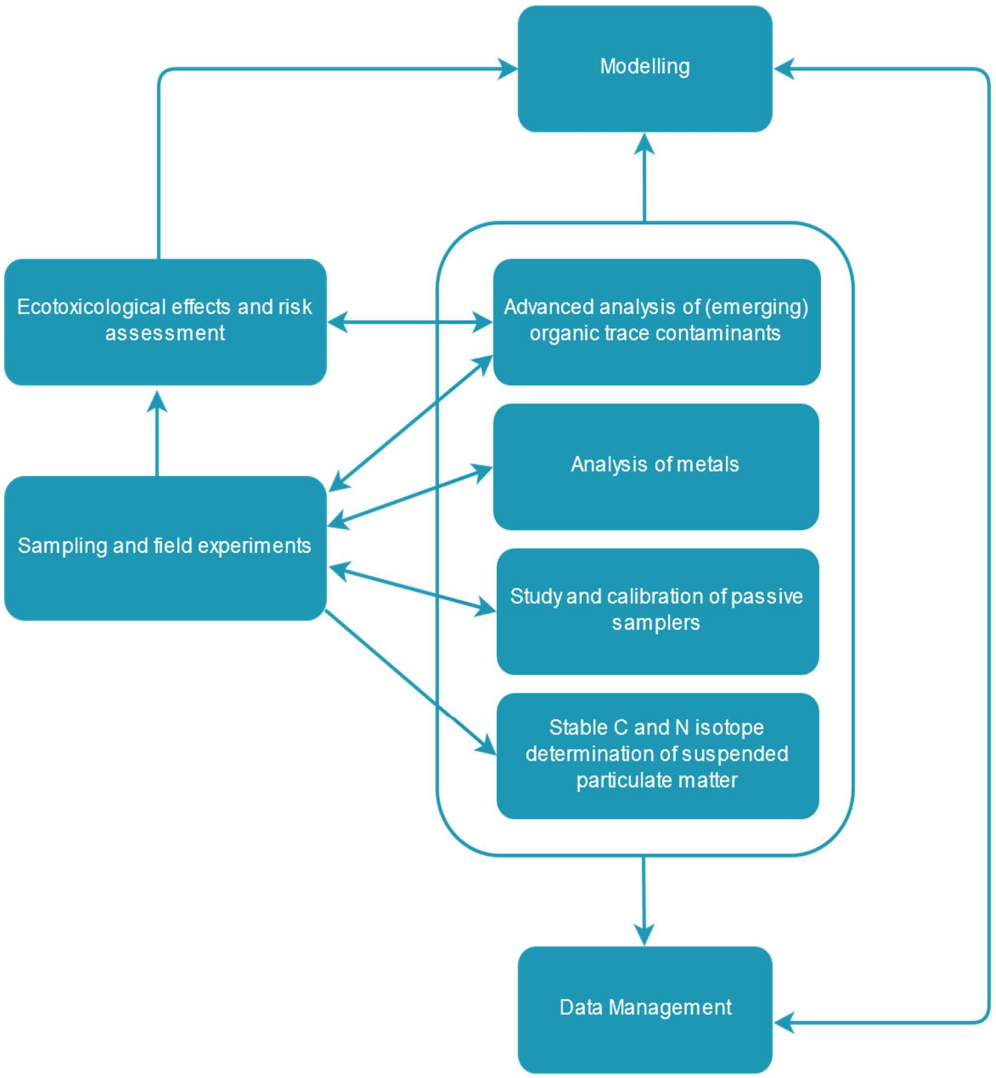

Figure 1. Overview of the different work packages constituting the NewSTHEPS project and their interactions.

Samples are used in toxicity testing, both as obtained as in processed form (e.g. concentrates) in order to reveal actual and potential environmental effects. In combination with the modelling of the sediment transport through the water column and exchange with the underlying sediment layer in combination with exchange of contaminants, this should result in a better understanding of the factors that govern the behaviour of different classes of contaminants in the marine and harbour environment, and proper assessment of the risks involved. An overview of the project's structure, indicating the different work packages (WPs) and their interactions is depicted in Figure 1.

3.1. Sampling and sampling campaigns.

For sampling, the Ostend and Zeebrugge region were selected, each consisting of 2 harbour stations and a nearshore open sea station, so 6 stations in total. The choice was driven by the intensive port activities and the nearby Scheldt estuary for Zeebrugge, and the presence of a large wastewater treatment plant (WWTP; capacity of 165000 Inhabitant Equivalents) and the port infrastructure for Ostend.

The harbour stations had to fulfil the requirements of being relevant, reachable and with restricted access to avoid theft or loss. The open sea stations had to be approved by the Shipping Assistance Division (SAD) of the Marine Rescue and Coordination Centre (MRCC), situated near but not attached to a buoy, with limited traffic and within 2–5 km of the related harbour. Due to that reason, the station near Ostend had to be replaced, as the first designed location was not reachable for the Research Vessel and the deployed tripod prone to displacement by the strong currents and intense fishing activity. The different stations and their coordinates are presented in Table I, and their location on the map is depicted in Figure 2.Open Sea station Ostend was moved three times due to accessibility and recovery issues.

Table I. Overview of the different sampling stations and their coordinates over the different sampling campaigns.

Sampling Stations	Coordinates	Code
Ostend	51°N 13.58 2°E 56.14	**HO_1**
Ostend	51°N 14.07 2°E 55.63	**HO_2**
Zeebrugge	51°N 20.40 3°E 12.20	**HZ_1**
Zeebrugge	51°N 19.85 3°E 11.98	**HZ_2**
MOW1	51°N 21.50 3°E 7.67	**OZ_MOW1**
aKUST39 (2nd)	51°N 14.81 2°E 55.66	**OO_aKust39**
Obstn14 (3rd)	51°N 15.55 2°E 58.02	**OO_Obstn14**
Buitenstroombank (4th)	51°N 15.17' 2°E 51.72'	**OO_Bstbk**

Both grab sampling and passive sampling were carried out. Grab sampling consists of a single sample collected at a certain station, and constitutes the observation restricted to one moment in time and space. This can be either water sampling with Niskin bottles or sediment collected with Van Veen samplers. Passive samplers are deployed for a longer period, typically 2 weeks (metals by DGT) or 8

weeks (all different sampler types) for organic analysis. In parallel with Passive Samplers, SPM traps were deployed, they collect an image of the SPM over the sampling period, which is especially interesting for less soluble substances.

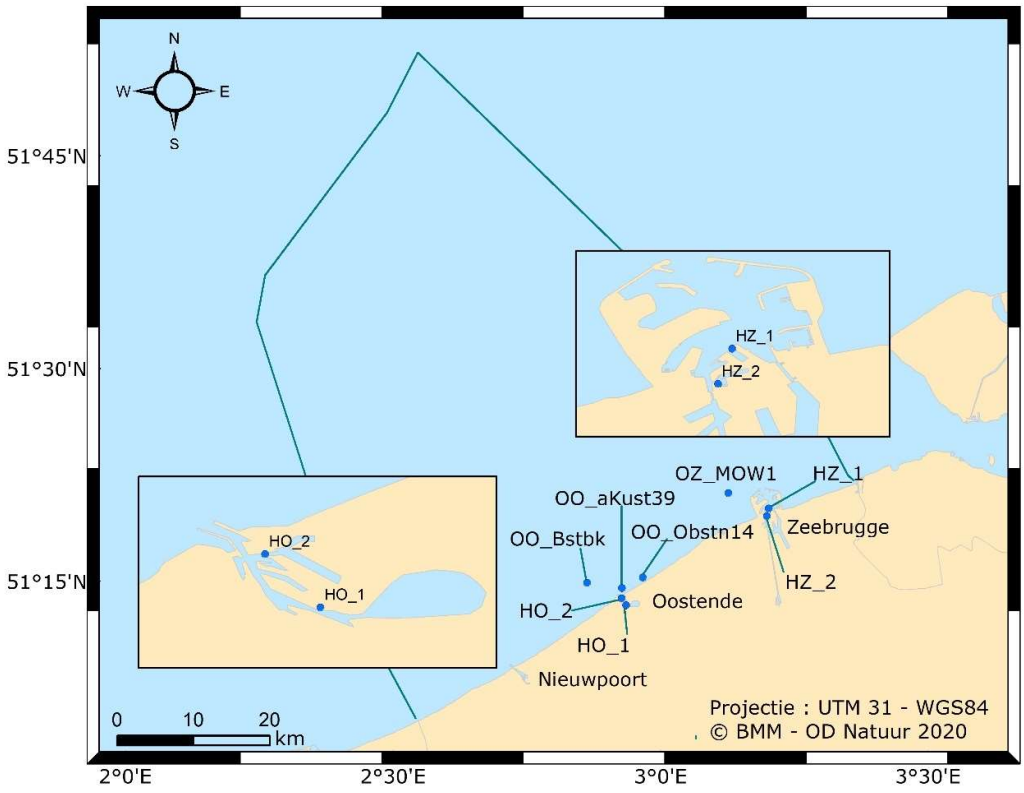

Figure 2. Map depicting the different sampling locations of the NewSTHEPS Project. The black line marks the boundaries of the Belgian Part of the North Sea.

3.1.1. Preparation of sampling material.

3.1.1.1. Preparation of Silicone Polymer sheets.

Altesil® sheets were Soxhlet pre-extracted during 96h in ethyl acetate, dried and spiked with Performance Reference Compounds (PRCs). Approximately 70 sheets are put in a wide mouth glass bottle and 500 mL of methanol is added together with individual CBs at concentration of 100mg L^{-1}: (International Union of Pure and Applied Chemistry (IUPAC) numbers 10, 14, 50 (100µL) and 104, 145, 204 (50µL)), individual deuterated PAHs all at concentration of 200mg L^{-1}: Fluorene-D10, Fluoranthene-D10, Phenantrene-D10 (all 100µL), Benzo(e)pyrene-D12 and Coronene-D12 (both 50µL) are added, shaken for 24h. Ultrapure water (Resistivity normalised to 25° C of 18.2MΩcm) is added (200mL), shaken for another 24h, again 100 mL of ultrapure water is added, shaken for 24h and kept refrigerated until use.

3.1.1.2. Preparation of Speedisk samplers.

The Bakerbond hydrophilic divinylbenzene (h-DVB) Speedisks, which can be used for large-volume Solid Phase Extraction (SPE) of seawater samples, can also be used as passive samplers. Speedisks consist of DVB sorbent sandwiched between two glass fibre filters and held together by two screens and a retaining ring (Figure 3A). To enable the use of Speedisks as passive samplers, the configuration was slightly altered; *i.e.* the top-part of the Speedisk was removed to allow a more efficient contact of the receiving sorbent phase with the bulk water and fixing holes were made in the lower-part (Figure 3B). The Speedisks were pre-conditioned with 20 mL of methanol/acetonitrile (50/50, v/v%) and subsequently with 20 mL of HPLC grade water under vacuum. After pre-conditioning, the outlet of the Speedisk was closed with a Luer lock tip and placed in a pre-rinsed wide mouth glass jar filled to the top with deionized water. The adjusted Speedisks were kept submerged in deionized water until usage.

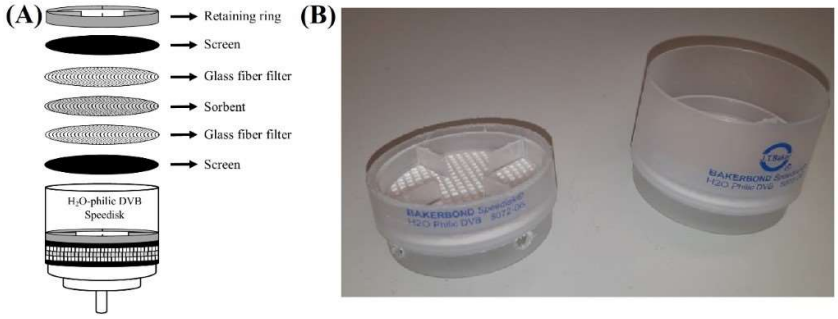

Figure 3. (A) Schematic representation of the hydrophilic divinylbenzene (h-DVB) Speedisk with its different components. (B) Adjusted Speedisk to be used as passive sampler with removed top part and fixing holes (left) compared to normal Speedisk (right).

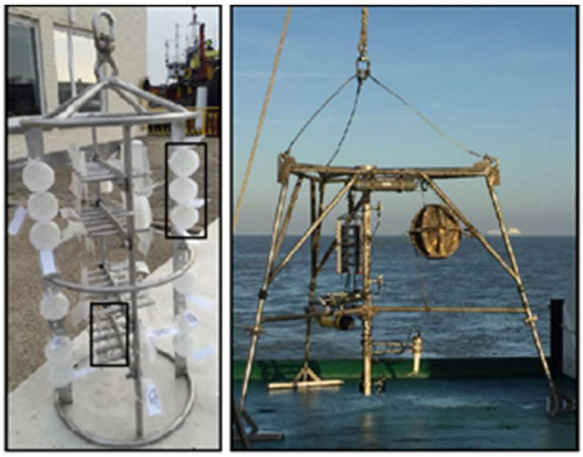

Figure 4. Speedisks and STEPS were mounted on a deployment cage (left) and subsequently attached to a tripod which was lowered onto the seabed at an approximate depth of 10 m (right).

The h-DVB Speedisks were deployed as described in Table II. They were all attached onto a stainless-steel cage facing the same orientation and deployed on a tripod as depicted in Figure 4 for a period up to 2 months.

3.1.1.3. Preparation of STEPS.

A novel STEPS sampler was developed in the project. STEPS samplers were prepared as follows. Nylon net filters with a pore size of 20 µm were pre-cleaned by soaking them in methanol/acetonitrile (50/50, v/v%) and let them dry under room temperature for approximately 1 hour. A 20 mg portion of pre-conditioned (See Section 3.4.1.2.2) hydrophilic DVB sorbent (same sorbent as in the Speedisks in 3.1.1.2) was then enclosed by the net filter which was later heat-sealed (Figure 5). Afterwards, holes were made in the net filter - by heat-sealing - to allow the STEPS to be fixed, and finally the STEPS were submerged in wide mouth glass jars filled with deionized water until usage.

The STEPS were deployed similarly to the h-DVB Speedisks as described in Figure 4 during sampling campaign 5 (Table II and Figure 7), giving a total of 24 STEPS.

Figure 5. STEPS developed using heat-sealed nylon net filters with dimensions 4x4 cm. The h-DVB sorbent is visible in the lower left corner of the STEPS, yet will be freely dispersed within the nylon mesh when deployed in the water column.

3.1.1.4. Preparation of DGT samplers.

3.1.1.4.1. DGT for trace metal assessment.

The labile fractions of trace metal complexes were studied by passive sampling using the technique of Diffusive Gradients in Thin films (DGT) (Davison, 2016). The DGT technique relies on controlled diffusive transport of the analyte and is here deployed in the water column (e.g. Baeyens et al., 2011; Zhang and Davison, 1995) to assess labile trace metal fractions (the size of the dissolved compounds that can enter the diffusive gel layer is smaller than 10 to 20 nm). The device is composed of a filter and two hydrogel layers: a polyacrylamide hydrogel that is backed up by a second polyacrylamide hydrogel layer containing the metal-selective Chelex®-100 accumulative resin.

For the material cleaning and preparation (Niskin and Teflon bottles, Teflon and glass plates), nitric acid (HNO_3; Fisher Scientific, Trace Metal Grade, 65%), distilled nitric acid (distilled in the laboratory), and ultrapure water (Millipore) were used. For DGT preparation, Chelex®-100 (Bio-Rad, 200-400 mesh size), cross-linker (DGT Research, Lancaster), acrylamide (40%, Merck), ammonium persulfate (APS; Merck), tetramethyl ethylenediamine (TEMED;Merck, >99%), DGT pistons (caps and bases, DGT research, Lancaster), 0.45 µm-pore size filter membranes (0.45 µm Polyvinylidene Fluoride (PVdF) membrane, Merck Millipore,) and NaCl (Merck, Suprapur) were used. The diffusive hydrogel, the resin gel and DGT probes were prepared and handled under a laminar flow hood in a clean laboratory room before each campaign and according to the method reported by Zhang and Davison (1995) and described in the Supplementary Information (SI).

The DGT piston (DGT research) consists of a round plastic moulding (a cap and a piston base, both assembled), holding together three successive layers, which are, from the cap to the bottom piston: a membrane filter (0.45 µm pore size cellulose acetate - 0.125 mm thick), a diffusive hydrogel (polyacrylamide hydrogel - 0.8 mm thick) and finally a resin gel (binding Chelex®-100 resin - 0.4 mm thick) (Figure 6).

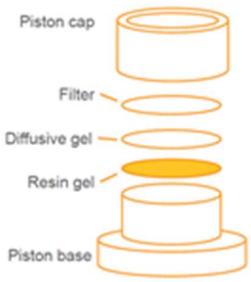

Figure 6. Diffusive Gradients in Thin-films (DGT) moulding

At each sampling station, 6 DGT pistons were enclosed in a plastic cage which was held with a nylon rope 2 m below the water surface, anchored to the seabed using a weight and lifted to the surface with the help of a buoy. The time and temperature at deployment and removal of the devices were recorded at each station (see Table II for the deployment time) and were further used for DGT concentration calculations. In recent years, this technique has been applied in aquatic systems for the assessment of organic pollutants as well, for example Endocrine Disrupting Chemicals (EDCs).

3.1.1.4.2. o-DGT (organic DGT) for EDCs assessment.

o-DGT preparation was carried out according to Guo et al. (2017, 2019). o-DGT moulding were fabricated in-house using Teflon (PTFE or Polytetrafluoroethylene) as the inert material of choice. A Teflon base (2.5 cm diameter) was stacked with resin gel, diffusive gel and filter membrane (PVdF, 0.45 µm) and then a Teflon cap tightly closed the sampler. Similar as for labile trace metal measurement using "classic" DGTs, the o-DGT (Figure 6) is based on the organic solute

accumulation on a binding resin layer after passage through a diffusive gel which acts as a well-defined diffusion layer.

3.1.1.5. Preparation of water and sediment sampling equipment.

For the collection of water samples for analysis of organic substances, Niskin bottles are cleaned using a 2M HCl solution and rinsed with ultrapure water prior to sampling. Sampling bottles are dish-washed, acid-rinsed followed by a rinse with ultrapure water, dried, capped with aluminium foil and heated in a muffle furnace at 450° C for 4h. Sediment traps are precleaned with 2M HCl and rinsed with ultrapure water. Van Veen samplers are cleaned and rinsed with local seawater prior to sampling.

For metal analysis, Niskin bottles and Teflon bottles are cleaned with 10% HNO_3, rinsed three times with ultrapure water in the laboratory and with seawater in the field, prior to sampling.

3.1.2. Sampling campaigns: time, position, duration, parameters measured.

Sampling was performed twice a year starting in 2016 and presented in Table II. The Sampling campaign (SC) number, location, start and end dates, calculated deployment time in days and type of samples taken or samplers deployed. At each time-point, grab samples were taken in triplicate.

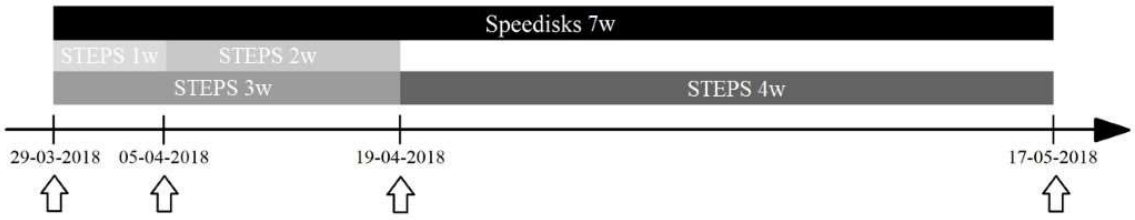

Figure 7. Deployment scheme of the Speedisks and STEPS in the BPNS during SC4. Triplicate STEPS were deployed for 1, 2, 3 and 4 weeks in the harbours of Zeebrugge and Ostend, whereas the Speedisks were deployed for 6-8 weeks.

Table II. Overview of the sampling campaigns (SC) at the harbours of Zeebrugge (HZ; both locations) and Ostend (HO; both locations) and at open sea Zeebrugge (OZ_MOW1) and Ostend (OO; all locations). Grab samples were taken at deployment (D) and retrieval (R) of the Speedisk passive samplers (SpD) and DGT samplers (DGT). In addition, intermediate grab samples were taken at 05-04-2018 (I_1) and 19-04-2018 (I_2) during SC5. STEPS (ST) were only deployed during SC5 in the harbours, according to the scheme in Figure 7. The √ and - symbolizes the presence or absence of samples, respectively. The NA (not available) means no samples were taken due to unavailability of the R.V. Belgica.

SC	Location	Start	End	Deployment time (days) [DGT]	D	I_1	I_2	R	SpD	ST	DGT
SC1	HZ	14-03-2016	20-05-2016	67 [14]	-	-	-	√	-	-	√
	OZ_MOW1	14-03-2016	20-05-2016	67 [14]	-	-	-	√	-	-	√
	HO	14-03-2016	20-05-2016	67 [14]	-	-	-	-	-	-	√
	OO	NA	NA	-	-	-	-	-	-	-	-
SC2	HZ	25-11-2016	02-02-2017	69 [18]	√	-	-	√	√	-	√
	OZ_MOW1	23-11-2016	06-02-2017	75 [16]	√	-	-	√	√	-	√
	HO	25-11-2016	02-02-2017	69 [18]	√	-	-	√	√	-	√
	OO	23-11-2016	NA	-	√	-	-	-	-	-	-
SC3	HZ	13-04-2017	20-06-2017	68 [14]	√	-	-	√	√	-	√
	OZ_MOW1	23-05-2017	14-07-2017	52 [17]	√	-	-	-	√	-	√
	HO	13-04-2017	20-06-2017	68 [14]	√	-	-	√	√	-	√
	OO	02-05-2017	26-07-2017	85	√	-	-	√	√	-	lost
SC4	HZ	16-10-2017	18-12-2017	63 [14]	√	-	-	√	√	-	√
	OZ_MOW1	26-10-2017	19-12-2017	54	√	-	-	√	√	-	lost
	HO	16-10-2017	18-12-2017	63 [14]	√	-	-	√	√	-	√
	OO	26-10-2017	10-04-2018*	-	√	-	-	√	-	-	-
SC5	HZ	29-03-2018	17-05-2018	49 [7]	√	√	√	√	√	√	√
	OZ_MOW1	29-03-2018	NA	-	√	-	-	-	-	-	-
	HO	29-03-2018	17-05-2018	49 [7]	√	√	√	√	√	√	√
	OO	29-03-2018	NA	-	√	-	-	-	-	-	-
SC6	HZ	18-10-2018	31-10-2018	[13]	√	-	-	-	-	-	√
	OZ_MOW1	NA	NA	-	-	-	-	-	-	-	-
	HO	18-10-2018	31-10-2018	[13]	√	-	-	-	-	-	√
	OO	NA	NA	-	-	-	-	-	-	-	-

* Due to loss of the tripod, no passive samplers were retrieved at this time-point.

3.2. Trace metal analysis.

Trace metal speciation in the water column (in samples collected by both passive (3.2.2.) and grab (3.2.3.) sampling) was investigated (Figure 8), considering three main pools: labile metal species (3.2.2.), total dissolved metals (3.2.3.1.) and particulate bound metals (3.2.3.2.). Taking into account the labile trace metals should provide a better understanding of their bioavailable potential due to the fraction size of nanometre level, closely linked to their toxicity potential and impact on marine ecosystems (Baeyens et al., 2018; Simpson et al., 2012; Tessier and Turner, 1995).

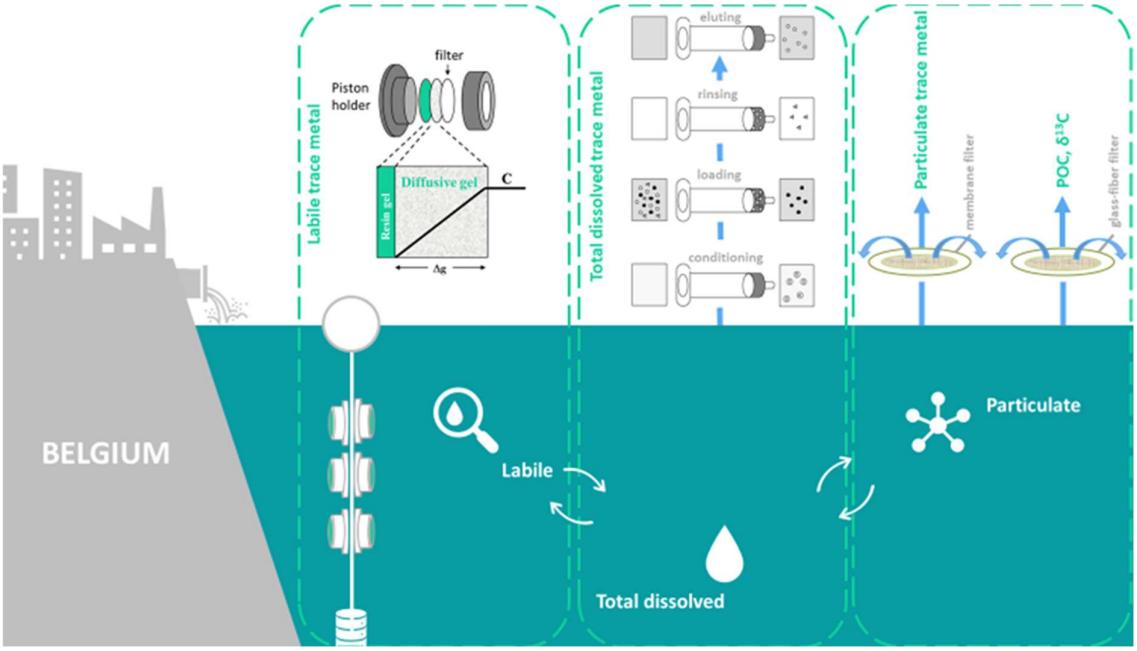

Figure 8. Graphical abstract of the different steps followed for the trace metal analyses (3.2.) and the particulate carbon analyses (3.6.) of the NewSTHEPS project.

3.2.1. Chemicals and materials.

For the material cleaning and preparation (Teflon bottles, Teflon and glass plates), nitric acid (HNO_3; Fisher, Trace Metal Grade, 65%), distilled nitric acid (distilled in the laboratory), and ultrapure water (Millipore) were used. For the elution of DGT Chelex-100 resin gels, 1M HNO_3 was prepared by diluting 63 mL HNO_3 (Fisher, Trace Metal Grade, 65%) in 937 mL ultrapure water. For sample treatments, distilled nitric acid (HNO_3; Fisher, Trace Metal Grade, 65%; distilled in the laboratory), ultrapure water (Millipore), ammonia (NH_3; Merck, Suprapur, 25%), glacial acetic acid (CH_3COOH; Fisher, Trace Metal Grade, >99%), HCl (Fisher, Trace Metal Grade, 37%), HF (Fischer, Trace Metal Grade, 40%) and H_3BO_3 (Fischer, Trace Metal Grade, 4%) were used.

3.2.2. Passive sampling of trace metals: Diffusive Gradients in Thin-films (DGT) piston retrieval and treatment.

After deployment and recovery of the DGT devices in the field, the labile trace metals, accumulated on the resin gel, were eluted in 1 mL of 1M HNO_3 for at least 24 hours. The eluents were then diluted ten times with ultrapure water prior to analysis (see 3.2.4.). From the total mass of accumulated metal, the average labile trace metal concentration was calculated following Fick's law (Eq. 1), assuming perfect sink conditions (i.e. all metal ions arriving at the interface between the diffusive hydrogel and the resin gel are immediately bound to the resin):

$$C_{DGT} = m.\Delta G.(D.A.t)^{-1} \qquad \text{Eq. 1}$$

where C_{DGT} is the labile metal concentration in the seawater in µg L^{-1}, m is the trace metal mass accumulated on the resin gel (µg), ΔG is the total thickness of the diffusive domain in cm [diffusive

gel, membrane filter, Diffusive Boundary Layer (DBL, 0.01 cm; see SI for details)], D is the diffusion coefficient of the trace metal in 10^{-6} cm^2 s^{-1}, A is the DGT piston window area in cm^2 and t is the deployment time of the piston in s.

DGT samplers allow to obtain a time-integrated concentration of the labile trace metal fractions in an aquatic system Davison (2016). The labile metal concentrations obtained from DGT measurement are good indicators of the element bioavailability in the environment (Bade et al., 2012; Roig et al., 2011; Sierra et al., 2017; Simpson et al., 2012), i.e. as a general case, the bioavailability is dependent on the labile metal concentration, as estimated by C_{DGT} in previous work (Baeyens et al., 2018).

3.2.3. Grab sampling of trace metals: seawater filtration and treatment.

3.2.3.1. Treatment for dissolved trace metals.

At the same time when DGTs were deployed, seawater samples were taken 2 m below the surface using High Density Polyethylene (HDPE) Niskin bottles (see 3.1.1.5. for preparation prior to use). 500 mL of seawater samples were then filtered using 0.45 µm pre-weighted PVdF membranes. The solution was acidified with 0.2% distilled HNO_3 and then stored in clean Teflon bottles (see 3.2.1.). The filters were later treated for the analysis of particulate compounds. Procedural blank filters were handled at the same time as the samples, following the same methods in order to guarantee against any contamination.

As dissolved trace metals are generally present in the BPNS at ng L^{-1} levels (Baeyens et al., 1998), their concentrations are often close to the detection limit of most analytical instruments. Moreover, the complexity of the seawater matrix represents a second challenging issue for Inductively Coupled Plasma Mass Spectrometry (ICP-MS) analysis. The salt matrix can crystallize and cause clogging of instrument tubing and nebulizer, and even damage some parts of the instrument. To circumvent the analytical disturbance of the high NaCl concentration, target metals were isolated by a pre-concentration method using a solid-phase extraction (SPE) of the trace element from the seawater sample with a cation-exchange resin (Chelex®-100, 200-400 mesh size). To 100 mL of filtered and acidified seawater sample, 2.5 mL of concentrated ammonium acetate buffer were added to reach pH5. Next, a succession of treatments was carried out on the Chelex-100 resin all at a flow rate of 4 mL min^{-1}: (1) the pre-conditioning of the home-made column with 10 mL 2M HNO_3 / 1M HCl, 10 mL ultrapure water, 10 mL diluted NH_4Ac (pH 5) and 10 mL ultrapure water; (2) loading of the samples on the column, with retention of the metals on the resin; (3) rinsing of the column with 10 mL of diluted NH_4Ac (pH 5) and 10 mL ultrapure water, in order to remove the salt matrix and also other interfering elements from the resin; (4) elution of the trace metals from the column using 2M HNO_3 as eluting agent. The reagent preparations are described in the Supplementary Information. The acidic eluent resulting from this last step was stored at 4° C prior to analysis. In order to validate the method, a multi-element standard solution (Merck, ICP-MS standard XIII, 1 mg L^{-1}; including Cd, Cu, Pb, Ni, Co) was used as a spike in North Sea samples, reaching a concentration of

10 µg L^{-1} and then introduced into the SPE system before testing the real seawater samples. The recovery of Cd, Cu, Pb, Ni, Co was respectively 90, 95, 86, 96, and 96%.

3.2.3.2. Treatment for particulate trace metals.

The filters used for seawater sample filtration were dried under a laminar flow hood for 2 days and weighted again. The mass difference of the filters was recorded for the calculation of particulate metal concentrations and provide data on the concentration of suspended particulate matter in the water column (for the values, see the Supplementary Information). The filters were then introduced into clean Teflon tubes where 3 mL of concentrated HF (40%), 3 mL of concentrated HCl (37%) and 1 mL of concentrated HNO_3 (65%) were added. The solution was heated at 70° C overnight and finally after cooling down, 20 mL of H_3BO_3 (4%) were added to the Teflon bottles. This solution was then heated at 70° C for three hours. Once the solution was cooled down again, it was transferred to PE vessels and further diluted for analysis. To validate the process, two certified reference materials MESS-3 (marine sediment, National Research Council (NRC), Canada) and IAEA-405 (estuarine sediment, International Atomic Energy Agency) were treated in the same way as samples. All the certified reference concentrations were within the same range as the actual measured concentrations.

3.2.4. Trace metal analysis.

In the final solutions – *i.e.* eluents from the DGT passive sampler (3.2.2.), grab seawater samples (3.2.3.1.) and eluents from filter digestion (3.2.3.2.) – trace metals (Cd, Cu, Pb, Ni, Co and Al) were determined using a High Resolution-Inductively Coupled Plasma Mass Spectrometer instrument (HR-ICP-MS, Thermo Finnigan Element II). Calibration was carried out with appropriate dilutions of an acidified multi-element stock solution (Merck, ICP-MS standard XIII). Indium was used as an internal standard. Method Detection Limits (MDL) were around 0.002 µg L^{-1} for Cd, 0.05 µg L^{-1} for Cu, 0.011 µg L^{-1} for Pb, 0.005 µg L^{-1} for Co, 0.033 µg L^{-1} for Ni and 6.8 µg L^{-1} for Al. The relative standard deviation (RSD) was about 10% for all metals.

3.3. Estrogenic activity analysis using DGT technique and ERE-CALUX bioassay.

o-DGT in aquatic systems was developed for measurement of estrogenic activity in seawater. In this study, 17 β-estradiol (E2) was used as the only target compound since it is often used as the reference chemical for estrogenic activity and potency (Kudlak et al., 2015) and due to its recent status as a watch list chemical under the EU WFD (EU, 2013).

3.3.1. Experiment Chemicals and Materials.

Hexane (minimum 96.0%), and acetone (minimum 99.9%) were purchased from Biosolve. 17 β-estradiol (E2, minimum 98.0%), methyl *tert*-butyl ether (MTBE, HPLC grade), methanol (MeOH, HLPC grade), hydrochloric acid (HCl), humic acid (H1675-2, Lot#131078), glass fibre thimbles (Whatman, 19×90 mm), and D-glucose (minimum 99.5%) were purchased from Sigma-Aldrich. Dimethyl sulphoxide (DMSO, minimum 99.7%) and sodium hydroxide (NaOH) were purchased from Merck. Amberlite™ XAD18™ was obtained from Rohm and Haas Company and agarose was obtained

from Bio-Rad Laboratories. Dulbecco's Modified Eagle Medium (DMEM without phenol red (Gibco)), sodium pyruvate (100 mM, sterile-filtered), alpha-Minimal Essential Medium (α-MEM (Gibco)), penicillin-streptomycin, foetal bovine serum (FBS), charcoal-stripped FBS, L-glutamine (200 mM), trypsin (0.5% (Gibco)), phosphate buffered saline (PBS, 1 X, pH 7.4), and trypsin without phenol red (10 X, 0.5% (Gibco)) were purchased from Life Technologies. Luciferin reagent and lysis reagent were obtained from Promega. Stabilizing buffer A, B and NucleoCounter cartridges were purchased from Chemometec.

3.3.2. o-DGT performance test and application.

In order to validate this novel methodology for E2 measurements in aquatic systems, the following laboratory experiments were carried out: (1) adsorption of E2 on DGT holders, diffusive gels and membrane filters; (2) uptake and capacity of E2 by the XAD18 resin; (3) determination of diffusion coefficient of E2 in the diffusive gel of the DGT and (4) analysis of effects of pH, ionic strength and dissolved organic matter (DOM, mainly humic acid) concentration on the adsorption characteristics of E2 on the XAD18 resin. Thus, for optimal measurement, o-DGT materials including DGT holders, diffusive gels and filter membranes should not adsorb E2. o-DGT holders were immersed in a Ultra-Violet (UV) protecting bottle containing 1 L of 4.3 ng L^{-1} E2 solution (in ultrapure water, 23 ° C) and were then shaken for 48 h. Diffusive gels and filter membranes were separately immersed in 40 mL of 4.3 ng L^{-1} E2 solution (in ultrapure water, 23 ° C) and were also shaken for 48 h. Aliquots (10 mL) of each E2 solution were collected at 0 and 48 h and were extracted with a Hydrophilic Lipophilic Bond (HLB) cartridge, followed by ERE-CALUX bioanalysis to examine possible changes in E2 response of the spiked solution over time. Resin gels used in the DGT samplers should, ideally, present high adsorption capacities for target compounds. XAD18 resin gels were immersed in a beaker containing 1 L of E2 solution (in ultrapure water, 23 ° C) at various concentration levels (2, 4, 8, 16, 32 and 64 ng L^{-1}) and were then shaken at room temperature for 48 h. Aliquots (10 mL) of the E2 solution were collected before and after the XAD18 resin gel deployment and extracted with an HLB cartridge as described above. The XAD18 resin gel samples were retrieved from the E2 solutions, gently dried and extracted using the ASE200 unit and the extracts were analysed by ERE-CALUX. In order to test the diffusion coefficient of E2 and also the diffusive boundary layer (DBL), DGT samplers with diffusive gels of different thickness (0.025, 0.05, 0.075, 0.10 and 0.125 cm) were deployed in 9 L of solution (in ultrapure water, 23 ° C) containing 16 ng L^{-1} E2 in 0.03 M NaCl at a stir rate of 300 rpm for 4 h. To avoid a decrease of the E2 concentration during the experiment, we used a concentration of 16 ng L^{-1}, which is almost 4 times higher than in the adsorption experiments, as well as a sufficiently large volume (9 L). Aliquots (10 mL) of the aqueous phase were collected before and after DGT deployment in the solution and were extracted with HLB cartridges as described above. The XAD18 resin gel samples were peeled off from the o-DGT devices, dried gently and extracted using an Accelerated Solvent Extraction (ASE) ASE200 unit and extracts analysed by ERE-CALUX. DBL thickness measurements in the field were carried out in the station of HO-1 in the Belgian Ostend Harbour for 14 days (no biofouling effect was observed) using o-DGT samplers with

diffusive gels of different thickness (0.025, 0.05, 0.075, 0.10 and 0.125 cm). The influence of pH, ionic strength, and DOM on o-DGT samplers was tested at in the range of 5-8, ionic strength is generally tested in the range of 0.001 M to 0.5 M NaCl, and DOM concentration ranges from 0 mg L^{1} to 30 mg L^{-1}. After this validation study, the DGT devices were deployed at the HO-1 (Belgian Ostend Harbour) and MOW-1 (the North Sea) in Sept. and Oct. 2016 and the measured estrogenic activities were compared with those from conventional spot sampling.

3.3.3. Sample Extraction for the measurement of ERE-CALUX Bioassay.

All glassware used in the experiment was rinsed 3-5 times with ultrapure water and capped with aluminium foil prior to baking at 450° C for 8 h and stored until further use. Aqueous samples were extracted with Oasis HLB cartridges (5 mL, 200 mg, glass cartridge, Waters), while XAD18 resin gels were extracted automatically using the ASE unit (ASE200 from Dionex, Thermo Scientific). More details on the extraction procedures are available in the Supporting Information. In the last step, all extracts (approx. 60 mL) were evaporated to dryness using a vacuum centrifuge (Genevac MiVac Quattro) and re-suspended into a defined volume of hexane. VM7Luc4E2 cells (formerly known as BG1Luc4E2 cells) were used to carry out the ERE-CALUX bioassay, and the method was performed according to the XDS LUMI-CELL agonist protocol and OECD TG 455 guidelines but with certain modifications.

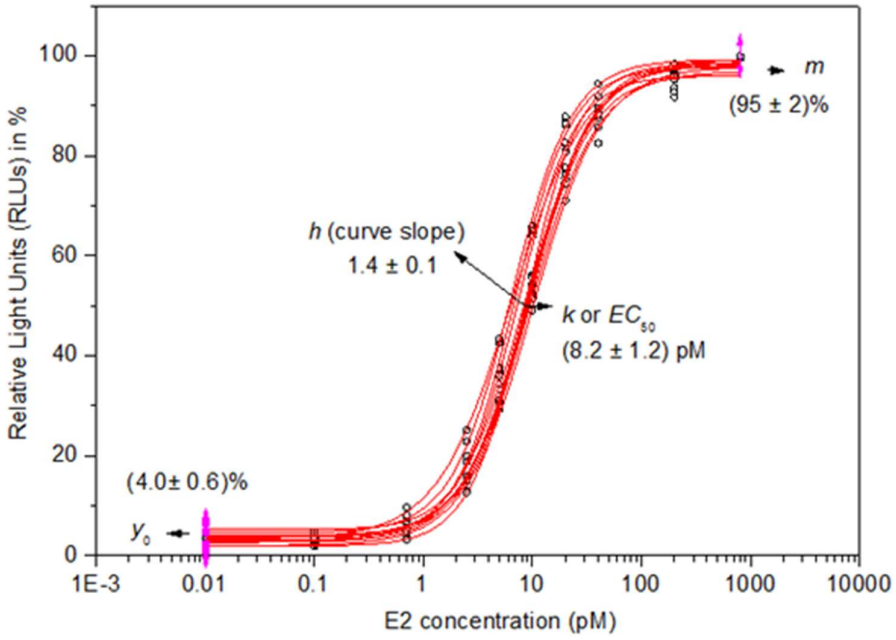

Figure 9. Concentration-response curve of E2 standard solutions measured with the ERE-CALUX bioassay (n=15). The 4 parameters of the sigmoid Hill plot are indicated as the background (y_0), the maximum induction (m), the effective concentration at half-maximal induction (EC_{50}) in pM and corresponding to an induction percentage equal to [y_0 + (1/2*(m-y_0))]. The hill parameter (h) equals the slope of the sigmoid curve at the inflection point (which equals the EC_{50}).

The response of those genetically modified cells towards estrogenic ligands is of biological/toxicological nature and ultimately yields photochemical signals directly proportional to the administered dose or compound concentration in the assay. The calibration curve for these types of assays consists of a 4-parameter sigmoidal equation and is depicted in Figure 9 (for each parameter, the average values along with their corresponding standard deviation (SD) were calculated). Based on 15 independent full concentration-response E2 standard curves, the mean EC_{50} value from these analyses amounted to 8.2 ± 1.2 pM.

3.4. Advanced analysis of contaminants of emerging concern (CECs) and legacy pollutants.

This section describes the sample preparation and instrumental methods used for trace quantification of contaminants of emerging concern (CECs) and legacy pollutants in samples collected by both grab and passive sampling.

3.4.1. Analysis of pesticides, pharmaceuticals and personal care products.

3.4.1.1. Chemicals and materials.

Eighty-nine pharmaceuticals (PhACs), personal care products (PCPs) and pesticides were selected based on their occurrence in natural waters, high consumption/usage, persistence in wastewater treatment plants (Jia et al., 2012; Vergeynst et al., 2015), and legislative frameworks such as the European Union Watchlist (EU, 2015; EU, 2018a,b). The selected compounds (52 PhACs, 9 PCPs and 28 pesticides), their subclass, the partitioning coefficient between octanol and water of the unionized molecular form (log K_{ow}), and the pK_a are listed in Annex 1. Individual stock solutions for the 89 target compounds were prepared at a concentration of 1 g L^{-1}. A standard mixture of all 89 compounds was prepared at a concentration of 2 mg L^{-1} in methanol/water (10/90, v/v %) with 0.1% (v/v %) formic acid and 0.1 g L^{-1} $Na_2EDTA.2H_2O$. The standard mixture was stored at −18° C in dark amber bottles for maximum 3 months. Working solutions (0.01, 0.03, 0.1, 0.3, 1, 3, 10, 30, 100, 300 and 1000 µg L^{-1}) of the mixture of all 89 compounds were prepared by appropriate dilution of the 2 mg L^{-1} standard mixture.

Reference seawater was prepared according to the American Society for Testing and Materials (ASTM) D1141-98 standard procedure (ASTM International, 2003) using deionized water and adjusted to a pH of 8.0 ± 0.2 with a 5M NaOH solution. Following materials were used: Bakerbond (h-DVB Speedisks® (each disk containing 400 ± 5 mg sorbent, Avantor Materials), Oasis® HLB cartridges (6 mL, 200 mg sorbent, Waters; for composition of sorbents: see Section 4.2.1), Whatman GF/D glass fiber filters (90 x 90 mm) and nylon net filters (20 µm ; Merck Chemicals). As solvents LC-MS grade water, LC-MS grade methanol, LC-MS grade acetonitrile, HPLC grade water and HPLC grade methanol (all VWR International) and LC-MS grade isopropanol, formic acid and $Na_2EDTA.2H_2O$ (Sigma Aldrich) were used. Deionized water (< 2 µS cm^{-1}) was produced from Aquadem ion exchange cartridges (Werner, Germany).

3.4.1.2. Sample preparation following grab sampling.

Seawater samples were taken using Niskin bottles (volume = 5L) at a depth of 2 m and were stored in pre-rinsed (using methanol/acetonitrile (50/50, v/v %)) amber glass bottles. Upon arrival at the laboratory, samples were filtered using a Whatman GF/D glass fiber filter (nominal particle retention 2.7 µm) to remove debris and sediment. Next, the samples were acidified with formic acid (pH 3) to prevent microbial activity during sample storage (at 4° C for maximum 4 days). Prior to SPE, $Na_2EDTA.2H_2O$ was added at a concentration of 1 g L^{-1} to increase the extraction efficiency of fluoroquinolone and tetracycline antibiotics (Gros et al., 2009), and the pH of the samples was adjusted to 7. Two separate SPE-methods were developed (3.4.1.2.1 and 3.4.1.2.2).

3.4.1.2.1. SPE protocol on Oasis® HLB cartridges.

The first method, a low volume SPE method, was developed using Oasis HLB cartridges based on a modified protocol for wastewater extraction developed by Vergeynst et al. (2017). This SPE-procedure was performed on an automated GX-271 ASPEC™ instrument (Gilson). The final protocol started with conditioning the cartridges with 6 mL High Performance Liquid Chromatography (HPLC) grade methanol and, subsequently, with 6 mL of HPLC grade water. Next, 200 mL of sample (prepared as described in the previous paragraph) was loaded on the cartridge, which was subsequently washed with 18 mL of HPLC grade water and vacuum dried with a nitrogen gas stream for 5 min. Afterwards, the cartridges were eluted with 5 mL of HPLC grade methanol/acetonitrile (50/50, v/v %) to obtain the eluent (SPE extract).

3.4.1.2.2. SPE protocol on DVB Speedisk.

A second novel method was a large volume extraction method using the Bakerbond hydrophilic DVB Speedisk. The full extraction of the Speedisks was performed on a six-port vacuum manifold extraction station (Avantor Materials). The final SPE-procedure started with conditioning the Speedisk with 20 mL of methanol/acetonitrile (50/50, v/v %) and, subsequently, with 20 mL of HPLC grade water under vacuum. Subsequently, the Speedisk was loaded with 1000 mL of sample, followed by a washing step using 18 mL HPLC grade water. Next, residual water droplets were removed by vacuum drying for 5 min. Finally, elution was performed with 10 mL of methanol/acetonitrile (50/50, v/v %). The eluent was treated in the same manner as described for the SPE protocol on Oasis HLB cartridges.

3.4.1.2.3. Handling of extracts.

In the next part of the preparation process, the eluent (SPE extract) was collected in pre-rinsed glass tubes and placed in a TurboVap (at 25° C) to be concentrated by evaporation under a gentle nitrogen gas stream just until complete dryness. After reconstitution in 1 mL of methanol/water (10/90, v/v %) containing 0.1% (v/v %) formic acid and 0.1 g L^{-1} $Na_2EDTA.2H_2O$, the glass tubes were sonicated for 1 min, vortexed for 20 s, and centrifuged at 870g for 5 min. Lastly, 0.8 mL of supernatant of this reconstituted extract was transferred into a HPLC vial for further instrumental analysis.

3.4.1.3. Sample preparation following passive sampling.

3.4.1.3.1. Speedisk passive sampler.

The Speedisk passive samplers were used in the field and in lab experiments as elaborated in Section 3.1.1.2. After usage, the Speedisks were handled and extracted according to the high-volume extraction procedure as described in Section 3.4.1.2.2 and 3.4.1.2.3.

3.4.1.3.2. Simple Teabag Equilibrium Passive Sampler (STEPS).

At the end of the lab experiments or deployment in the field, the STEPS were removed from the water phase and handled as follows: each STEPS was cut open using pre-rinsed (using methanol/acetonitrile (50/50, v/v %)) scissors and the sorbent together with the Teabag net filter was loaded on an empty Speedisk housing (without DVB sorbent) containing a Whatman GF/D glass fiber filter. The sorbent phase was washed with 18 mL of HPLC grade water followed by vacuum drying, and finally followed by elution using 10 mL methanol/acetonitrile (50/50, v/v %). The extracts were then treated according to Section 3.4.1.2.3.

3.4.1.4. Instrumental analysis.

Chromatographic separation was achieved by injecting 10 µL of the reconstituted extract (as obtained as described in 3.4.1.2) on an ultra-high performance liquid chromatography (UHPLC) reversed phase Hypersil Gold column (1.9 µm particle diameter, 2.1 x 50 mm, Thermo Scientific). The mobile phase used during the instrumental analysis operated at a flow rate of 350 µL min^{-1} (Accela 1250 pump, Thermo Scientific) and consisted of (A) water and (B) methanol both acidified with 0.1% and 0.01% formic acid for the positive and negative ionization mode, respectively. The following gradient was used: 0-1.5 min 10% B and 90% A, 1.5—15 min linear gradient to 100% B, and 15-16 min 100% B. The gradient ended with a cleaning phase (16-21 min 100% C) using (C) a mixture of equal volumetric amounts of water, methanol, acetonitrile and isopropanol each acidified with 0.5% formic acid, and a conditioning phase (21-26 min 10% B and 90% A). Mass spectrometric detection was performed on a hybrid quadrupole-Orbitrap High-Resolution Mass Spectrometer (HRMS Q-Exactive™, Thermo Scientific) equipped with a heated electrospray ionization (HESI-II) source and operating in full scan mode (120-760 *m/z* for HESI-positive; 100-760 *m/z* for HESI-negative) at a resolving power of 70,000 Full Width at Half Maximum (FWHM) at 200 *m/z*. External mass calibration of the HRMS was performed daily using the Calmix solution from Thermo Scientific (benzoic acid was added for analysis in the negative ion mode) over a mass range of 138-1721 Da and 21-1479 Da in the positive and negative ion mode, respectively. In the positive ion mode, online mass calibration using di-iso-octyl phthalate ($C_{24}H_{38}O_4$) as a lock mass was enabled. No appropriate lock mass could be found for the negative ion mode. The optimal HESI-II parameters of the final method were: spray voltage: ± 3.5 kV; sheath gas flow rate: 45 arbitrary units (a.u.); auxiliary gas flow rate: 10 a.u.; capillary temperature: 350 ° C; heater temperature: 375 ° C; S-lens RF-level: 60%. The automatic gain control (AGC) target was set at 3,000,000 ions with a maximal injection time of 200 ms.

3.4.1.5. Validation procedure.

3.4.1.5.1. Instrumental validation.

Preceding the method validation, an instrumental validation was performed consisting of analysing blank (methanol/water (10/90, v/v %) containing 0.1% (v/v %) formic acid and 0.1 g L^{-1} $Na_2EDTA.2H_2O$) and standard solutions and evaluating the instrumental precision and linearity, and the instrumental detection and quantification limits (IDL and IQL). The instrumental precision was defined as the relative standard deviation (RSD) of triplicate samples under inter-day repeatable conditions. The instrumental detection limits (IDL; Eq. 2) were estimated according to the Eurachem Guide (Magnusson and Örnemark, 2014) and correspond to the definition of the detection capability (CC β) of the EU, which is based on integrating non-noise peaks:

$$IDL = b + 2 * t_{1-\beta,n-1} * SD \qquad \text{Eq. 2}$$

where b is the mean blank level (n = 3). The Student t-value with β = 0.05 and n = 3 is 2.92, and SD is the standard deviation of the lowest concentration where a non-noise peak could be integrated. The instrumental quantification limit (IQL) is defined as the lowest concentration level equal to or above the IDL that could be measured with a precision (RSD) better than 15% (Vergeynst et al., 2017). The linearity of the standard curves was evaluated based on the lack of fit by comparing a linear and quadratic function, both characterized by a $1/x^2$ weighted least squared regression and by analysis of variance (ANOVA). The root-mean-square of the relative errors (RMSE) was used as a tool to account for (im)precision and (non)linearity of the calibration curves:

$$RMSE = \sqrt{\frac{\sum_i^n \left(\frac{y_i - \hat{y}_i}{\hat{y}_i}\right)^2}{n-p}} \qquad \text{Eq. 3}$$

In Eq. 3, y_i stands for the peak area of the i^{th} peak, whereas is the predicted peak area of the regression function with p parameters through n data points.

3.4.1.5.2. Method validation.

During method validation, the final analytical methods (Section 3.4.1.2. and 3.4.1.4.) were validated with spiked reference seawater, according to the standard addition approach described by Matuszewski et al. (2003) and further elaborated by Vergeynst et al. (2017) for wastewater. Briefly, procedural blanks (deionized water) and non-spiked samples (reference seawater), along with samples spiked before (pre-spiked, 11 concentrations: 0.05 to 5000 ng L^{-1} on Oasis HLB cartridges, 0.01 to 1000 ng L^{-1} on Speedisks) and after (post-spiked, at 100 µg L^{-1}) extraction, were analysed in triplicate on three different days. Daily external standard calibration was used to convert peak areas into concentrations, also taking the SPE concentration factor into account. This concentration factor depends on the loading volume and reconstitution volume of the SPE procedure (see Section 3.4.1.2). Matrix curves were made by plotting the concentrations - determined using daily external standard calibration - of the non-spiked ($C_{exp,ns}$) and the pre-spiked samples ($C_{exp,pre}$) as function of the

theoretical pre-spiked concentrations ($C_{the,pre}$). The slope of the matrix curves (Eq. 4) was used to determine the overall analytical process efficiency (PE), including both the SPE extraction recovery (RE) and the matrix suppression or enhancement factor (ME). ME and RE were also separately determined using Eq. 5 and 6, where $C_{exp,post}$ is the calibrated concentration of the post-spiked sample.

$$C_{exp,pre} = PE * C_{the,pre} + C_{exp,ns} \quad \text{Eq. 4}$$

$$ME = \frac{C_{exp,post} - C_{exp,ns}}{100\ \mu g\ L^{-1}} \quad \text{Eq. 5}$$

$$RE = \frac{PE}{ME} \quad \text{Eq. 6}$$

The linearity of the matrix curves was evaluated using ANOVA, whereas the method precision was evaluated as the RSD (n = 3) of the calibrated concentrations. Finally, method detection limits (MDL) - defined as detection capability (CC β) - were determined in the same way as the IDL (see 3.4.1.5.1).

3.4.2. Analysis of Steroidal EDCs.

3.4.2.1. Chemicals and materials.

70 steroidal EDCs (Steraloids Inc and Sigma Aldrich) were included in Annex 1. The selected EDCs covered 4 classes, i.e. 33 androgens, 14 oestrogens, 12 progestins and 11 corticosteroids. The selected deuterated internal standards (Steraloids Inc and Sigma Aldrich) for each class comprised 6 androgens, 5 oestrogens, 4 progestins, and 2 corticosteroids.

Primary stock solutions and standard mixtures were prepared in methanol, thereby reaching concentrations between 0.01 and 1000 ng μL^{-1}. The solutions were stored in dark glass bottles at -20° C. The organic solvents were of optima UPLC-MS grade (Fisher Scientific). Reference seawater was prepared according to ASTM D-1141. Ultrapure water was obtained from a water-purifying system (Millipore). Reference seawater was prepared by dissolving inorganic salts (Sigma Aldrich) into ultrapure water.

3.4.2.2. Final extraction protocol.

2.5 L grab samples were filtered (Glass Microfibre Filters Whatman™, Grade GF/F, 90 x 90 mm), acidified with 1 M HCl and stored in dark amber glass bottles at 4 ° C. Upon extraction, samples were brought to room temperature by vibrating. Thereafter, the pH was adjusted to 7 using 1 M NaOH and a mixture of deuterated internal standards was spiked (n = 17, 25 µL of 10 ng μL^{-1}) to the grab samples. Subsequently, the h-DVB sorbents were conditioned with 20 mL of 5% acetonitrile and 20 mL of ultrapure water under vacuum. Next, the samples were drawn through the h- DVB Speedisks under vacuum, followed by a washing step with 20 mL of ultrapure water, upon which a vacuum was applied on the Speedisks to remove residual water drops. Afterwards, elution was performed by

gravity using sequential 5 mL of pure acetonitrile and 5 mL of acetonitrile, with the latter being acidified with 0.1% formic acid. The combined extracts were vaporized in a TurboVap under a gentle stream of nitrogen at a temperature of 50° C until dry, reconstituted in 150 µL of methanol and ultrapure water (40/60, v/v), centrifuged at 2430 g, and the supernatant was transferred into LC-MS glass vial prior to analysis.

3.4.2.3. Instrumental analysis.

The EDCs were chromatographically separated using an UHPLC system, consisting of an Ultimate 3000 XRS pumping system, coupled to a Ultimate 3000 RS column compartment and autosampler (Dionex, Thermo Scientific). Chromatographic separation was achieved using reversed phase chromatography with gradient elution. Separation of EDCs was carried out using a Hypersil Gold column (1.9 µm, 100 x 2.1 mm, Thermo Scientific) at a temperature of 45° C. Furthermore, the mobile phase consisted of a mixture of water (Eluent A) and methanol (Eluent B) both containing 0.1% formic acid, pumped at a flow rate of 0.55 mL min^{-1}. The linear gradient program was as follows: 0 min, 40% B; 0-5.8 min, 40-65% B; 5.8-9.0min, 65-100% B; 9.0-10.5 min, 100% B; 10.5-10.6 min, 100-40% B; 10.5-12.5 min, 40% B. The injection volume was 2 µL.

The detection of EDCs was carried out using a Q-Exactive™ Benchtop HRMS (Thermo Scientific) fitted with an atmospheric-pressure chemical ionisation (APCI) source. Optimal positive and negative ionisation source working parameters were sheath gas flow 33 a.u. (arbitrary units), auxiliary gas flow 15 a.u., sweep gas flow 2 a.u., discharge current +/- 4 kV, capillary temperature 250° C, and vapour temperature 250° C. The optimal MS parameters of the Q-Exactive™ were S-lens RF-level 70, full-scan events and operated in polarity switching mode. Both scans were performed with a resolution of 70.000 FWHM at 1 Hz (1 scan per sec) and scan ranges from 60 to 900 Da. Furthermore, the scans were applied by targeting the automatic gain control (AGC) at ultimate mass accuracy (1 x 10^5 ions) and a maximum injection time of 50 ms. Initial instrument calibration was carried out by infusing calibration mixtures for the positive and negative ion mode (LTQ Velos ESI positive and negative ion calibration solution, Thermo Scientific). Instrument control and data processing were carried out by Xcalibur 4.0 software.

3.4.2.4. Method validation.

The analytical method was validated on reference seawater in order to evaluate its fitness-for-purpose. Currently, no specific criteria for the validation of methods for analysis of CECs in the marine environment are available. The only European guideline available for analytical evaluation of the water status is CD 2009/90/EC (EU, 2009), in which it is stated that the variation coefficient at the reported concentration must be below 50%. Furthermore, it stipulates that the detection limit has to be 0.3 times the EQS, which is defined by the concentration in water that a substance should not exceed to maintain the environmental quality objective. Currently, limited EQS values are available concerning the occurrence of steroidal EDCs, phthalates and alkylphenols in the marine environment. Therefore, stricter guidelines were consulted for additional performance criteria in

analytical method validation, i.e. CD 2002/657/EC (EU, 2002), Eurachem guidelines (Magnusson et al., 2014) and review articles (Kruve et al., 2015a; Kruve et al. 2015b).

Evaluation criteria included the empirical method detection (MDL) and quantification limit (MQL), linearity, specificity and selectivity, trueness, and precision. The MDL, MQL and the linearity were investigated by constructing three times a 13-point matrix-matched calibration curve (0, 0.125, 0.25, 0.50, 0.75, 1.0, 2.5, 5.0, 10, 20, 30, 40 and 50 ng L^{-1}). Furthermore, the specificity, selectivity, trueness and precision were examined by spiking the seawater at 1.5, 2.0 and 2.5 times the MQL-level in six-fold. This procedure was repeated on three different days by two different operators. In addition, also 20 blanks, i.e. non-spiked reference seawater, were analysed.

In parallel, a cross-validation on fresh tap water was performed to assess the matrix-versatility of the presented method. During this cross-validation, a 13-point matrix-matched calibration curve was constructed twice to determine the linearity performance, while the specificity, selectivity, trueness and precision were investigated by enriching samples with 1.5 times the MQL-level (n = 18).

3.4.3. Analysis of plasticizers and plastics additives.

3.4.3.1. Chemicals and materials.

A total of 27 target compounds (Accustandard and Sigma Aldrich) were considered (Annex 1). The target compounds were selected based on relevant literature, and covered 3 different classes, i.e. 7 phenols, 11 di-phthalates and 9 mono-phthalates. The selected internal deuterated standards comprised of 2 phenols, i.e. 2-chlorophenol-d_4 and phenol-d_5; and 2 phthalates, i.e. di-cyclohexyl phthalate-3,4,5,6-d_4 and diethyl phthalate-3,4,5,6-d_4. Primary stock solutions and mixed standards, reaching concentrations between 1 and 1000 ng μL^{-1}, were prepared in optima grade acetonitrile. The solutions were stored in amber glass bottles at -20° C. The organic solvents were of optima UHPLC-MS grade (Fisher Scientific).

3.4.3.2. Final extraction protocol.

Grab samples of 0.5 L were acidified to pH 3 using 1 M HCl and stored in dark amber glass bottles at 4° C. Upon extraction, samples were brought to room temperature. Afterwards, samples were spiked with a mixture of deuterated internal standards, i.e. 100 ng L^{-1} for the deuterated phthalates and 400 ng L^{-1} for the phenols. Subsequently, Oasis® HLB cartridges (6 cc, 500 mg sorbent, 60 µm particle size; Waters) were conditioned with 6 mL 5 % CH_3CN diluted in ultrapure water and 7 mL ultrapure water under vacuum. Next, samples were drawn through the cartridges under vacuum (10 mL min^{-1}), followed by a washing step of 8 mL ultrapure water and applying a vacuum (20 min) to remove residual water drops. Afterwards, elution was executed by using 9 mL of 0.1% formic acid in CH_3CN. The extracts were vaporized under a mild stream of nitrogen at a temperature of 40° C until dry. Consequently, the extracts were reconstituted in 150 µL of CH_3CN/H_2O (95/5, v/v), centrifuged at 2430 g. Finally, supernatants were transferred into LC-MS vials prior to analysis.

3.4.3.2. Instrumentation.

Chromatographic separation of target compounds was executed using a UHPLC system, consisting of an UltiMate 3000 XRS pumping system, coupled to an UltiMate 3000 RS column compartment and autosampler (Dionex). Separation of the target compounds was carried out using a Hypersil Gold column (1.9 µm, 100 x 2.1 mm) (Thermo Scientific) at a temperature of 45° C based on gradient elution. The mobile phase consisted of a mixture of water (Eluent A) and acetonitrile (Eluent B) both containing 0.1% ammonium hydroxide, pumped at a flow rate of 300 µL min^{-1}. The linear gradient program was as follows: 0–1 min, 5 % B; 1–2 min, 5–40 % B; 2–2.3 min, 40–90 % B; 2.3–6.1min, 90–96 % B; 6.1–8 min, 96 % B and 8–10 min, 5 % B. The injection volume was 10 µL. Additionally, a Hypersil Gold trap column (1.9 µm, 50 x 2.1 mm, Thermo Scientific) was placed between the UHPLC pump and the injection valve for retarding phenols and phthalic acid esters (PAEs) originating from the mobile phase and analytical instrument.

The detection of target compounds was carried out using a Q-Exactive™ Benchtop HRMS (Thermo Scientific) fitted with a Heated Electrospray Ionization (HESI-II) source. Analysis was realized through full-scan events with following optimal operating conditions for positive and negative ionization (polarity switching mode); auxiliary gas flow 30 a.u., sweep gas flow 2 a.u., discharge current (-)3.5 kV, capillary temperature 250 ° C and heater temperature 350 ° C. Optimal MS parameters of the Q-Exactive™ were an S-lens Radio Frequency (RF) level of 70, a resolution of 70,000 FWHM at 1 Hz, and an m/z scan-range of 60 – 900 Da. Moreover, balanced scans were applied by targeting the automatic gain control (AGC) to 5.10^5 ions and a maximum injection time of 50 ms. Calibration of the instrument was carried out by infusing calibration mixtures for the positive and negative ion mode (LTQ Velos ESI positive and negative ion calibration solution, Thermo Scientific).

Tentative identification of unknowns, that were related to the backbone of plasticizers and plastics additives, was obtained by combining the full-scan events at a resolution of 70,000 FWHM with an additional Parallel Reaction Monitoring (PRM) HRMS event at a resolution of 17,500 FWHM and optimal Collision Energy (CE) of 20 eV.

3.4.3.4. Method validation.

Method validation was handled in the same manner as described under Section 3.4.2.4.

3.4.4. Analysis of Persistent Organic Pollutants (CBs, BFRs, PAHs, chlorinated pesticides, musk fragrances).

Polycyclic aromatic hydrocarbons (PAH), organochlorine pesticides (OCP), pentachloro benzene (PeCB), hexachlorobenzene (HCB), polychlorinated biphenyls (PCB), polycyclic musk fragrances, organophosphorus flame retardants (OPFR), polar pesticides, and PRC were purchased from Sigma-Aldrich, Ultra Scientific or Dr Ehrenstorfer. Naphthalene-d8, phenanthrene-d10, perylene-d12, PCB 4, 29 and 185 (Dr Ehrenstorfer) were used as recovery internal standards. PCB 121 and p-terphenyl (Ultra Scientific) were used as syringe internal standards for quantification of non-polar compounds.

All used solvents, i.e. methanol, hexane, acetone, ethyl acetate and dichloromethane were pesticide grade or equivalent (Sigma-Aldrich). Concentrated sulfuric acid (95-97 %) and high-purity grade silica gel (pore size 600 nm, 60-100 mesh) used in clean-up procedures was purchased from Sigma-Aldrich.

Polycyclic Aromatic Hydrocarbons (PAHs), Organo-Phosphorous Flame Retardants (OPFR) and polycyclic musk fragrances were analysed using GC 6890 (Agilent) coupled to MSD 5975 mass spectrometer (Agilent) operated in EI+ mode. Compounds were separated on the column HP-5MS (30m x 0.25mm x 0.25µm film thickness) in selected ion mode (SIM). Helium was used as mobile phase at constant pressure. One µL of extract was injected in pulsed splitless mode at 280ºC. GC temperature program started at 70° C (hold for 2 min), ramped by 25° C min^{-1} to 150° C, 3° C min^{-1} to 200° C and 8° C min^{-1} to 280° C and held for 10 min.

Analyses for Chlorinated Biphenyls (CBs), Organochlorine Pesticides (OCPs) and PRC-CBs were performed on GC-MS/MS (7890A GC/7000B MS, Agilent) operated in EI+ MRM mode equipped with a 60 m × 0.25 mm × 0.25 µm HT8 column (SGE). A volume of 3 µL of extract was injected in pulsed splitless mode at 280° C. Helium was used as carrier gas at 1.5 mL min^{-1}. The GC temperature program started at 80° C (1 min hold), and was then raised by 40° C min^{-1} to 200° C, and after 18 min hold raised further by 5° C min^{-1} to 305° C.

3.5. Uptake kinetics and equilibrium of micropollutants on Passive Samplers.

3.5.1. Silicone Rubber.

For passive sampling of hydrophobic organic compounds (HOC) in the aqueous phase, PS made from silicone rubber sheets are deployed in a cage in free contact with the surrounding water for periods of typically six weeks. Uptake of PS is controlled by diffusion through the water boundary layer (WBL), a thin stagnant water layer at the PS surface. The thinner the WBL (e.g. because of high turbulence), the higher the uptake rate. It should be noticed that for passive sampling of the aqueous phase, equilibrium is only attained for HOC with K_{ow} up to 10^5 and for HOC of higher K_{ow} knowledge of the exchange rate is required. Because the water-PS exchange of HOC is isotropic, the uptake and release of HOC follow the same exchange process. Consequently, the uptake rate can be quantified from the release rate of performance reference compounds (PRCs) dosed to the PS prior to exposure. Determination of the PRC release rate is essentially functioning as an in-situ calibration of the first order uptake kinetics. Subsequently, all PRC release and target uptake data are combined allowing the calculation of C_w for the target HOC (Smedes and Booij, 2012). This calculation needs the PS-water partition coefficients for al target HOCs and PRCs.

Silicone rubber (actually polydimethylsiloxane) sheets, especially Altesil®, have been extensively used for passive sampling of neutral organic compounds in water, sediment and biota. Their silicone-water equilibrium constants for a wide range of compounds have been determined (Smedes, 2007, Smedes et al., 2009, Smedes, 2018, Smedes, 2019, Smedes et al., 2020), while for a number of compounds also silicone-lipid partition coefficients are available (Jahnke et al., 2008, Smedes et al.,

2017). These K_{SW} were used in all calculations involving Chlorinated Biphenyls (CBs), Brominated Flame Retardants (BFRs), Polycyclic Aromatic Hydrocarbons (PAHs), chlorinated pesticides and synthetic musk fragrances.

3.5.2. Hydrophilic DVB based passive samplers.

Although hydrophilic divinylbenzene (h-DVB) materials have been applied earlier as solid phase microextraction fibres, blades and membranes (Stiles et al., 2008; Kermani et al., 2013; Grandy et al., 2018), the potential of h-DVB for passive sampling of a broad range of CECs remains underexplored as opposed to the frequently applied Oasis HLB sorbent.

3.5.2.1. Characterization.

Sorbent characterization was performed to reveal the difference in chemical properties between the h-DVB surface and the frequently used Oasis HLB®. This was performed using a Thermo Scientific Nicolet iS50 spectrophotometer recording the FTIR (Fourier transform infrared) and Raman spectra within the ranges of 400 - 4000 cm^{-1}, 400 - 4000 cm^{-1} and 3000 - 12000 cm^{-1}, respectively. Other acquisition parameters were: number of scans: 256, number of background scans: 256, background gain: 4.0, and resolution: 4.0 (FTIR) / 8.0 (Raman). Acquisition was repeated 3 times, and spectral data were averaged prior to further data processing.

3.5.2.2. Calibration using static exposure batch experiments.

Investigation of the sampling rate (R_s) and equilibrium partitioning of the target CECs between the water and sorbent phase (K_{sw}) was performed using a static exposure batch set-up that can be used to describe CEC uptake by the sampler through quantitative analysis of both the water and sorbent phase. The batch experiments consisted of eleven 1 L glass beakers with aqueous solutions of reference seawater spiked with a mixture of target compounds placed under continuous stirring (100 rpm) inside a temperature-controlled (at 6° C) dark room. Three passive sampling configurations were investigated during calibration, i.e. freely dispersed h-DVB sorbent, h-DVB sorbent incorporated in the reconfigured Speedisks (Section 3.1.1.2), and h-DVB enclosed in the novel STEPS (Section 3.1.1.3). Experimental conditions used to investigate the uptake of CECs by the three passive sampling designs are reported in Table III. The sorbent/water ratios and initial spiked concentrations of the compounds were selected based on environmental relevant concentrations and analytical considerations (method detection limits).

Table III. Experimental conditions during the static exposure batch experiments used for calibration of CEC uptake on freely dispersed h-DVB, reconfigured Speedisks and the novel STEPS.

	Freely dispersed h-DVB	Speedisk	STEPS
Initial CECs concentration [nmol L^{-1}]	1.5	7.0	1.5
Sorbent mass [mg_s]	20	400	20
Sorbent concentration [mg_s L^{-1}]	25	500	25

The residual concentrations in water and the amounts accumulated by the sorbent were measured at 0, 1, 2, 4, 6, 8, 12, 24, 48, 96 and 168h (Figure 10-1). For the batch experiments with freely dispersed h-DVB sorbent, at each time-point the sorbent was separated from the aqueous phase by filtering the beakers' content over a Whatman GF/D filter. The glass fibre filter with the sorbent and aqueous phases were separately extracted, eluted and analysed, to provide sorbent and aqueous concentrations, respectively. Speedisks and STEPS were isolated from the water phase by removing them from the beakers. Afterwards, the water and passive samplers were separately handled according to the procedures described under Sections 3.4.1, 3.4.2 and 3.4.3. To elucidate the effect of possible evaporation and/or light degradation, parallel experiments were performed using spiked beakers without the addition of a sorbent phase. Furthermore, separate batch experiments were performed with the glass fiber filters of the Speedisk and nylon mesh of the STEPS added to spiked beakers in order to clarify if sorption occurred on the membrane/mesh.

3.5.2.3. Partitioning at different compounds concentrations and environmental conditions.

It was also studied how compound concentration and environmental factors affected the K_{sw}-values of CECs on freely dispersed h-DVB sorbent. To investigate the effect of compound concentration on the K_{sw}, at a contact time of 48h, multiple equilibrations were performed under similar conditions at various concentration levels, i.e. 0.75, 1.5, 3.0, 6.0, 12, 24 and 48 nmol L^{-1} (Figure 10-2). This experiment was executed at a water temperature of 6° C at pH 8.

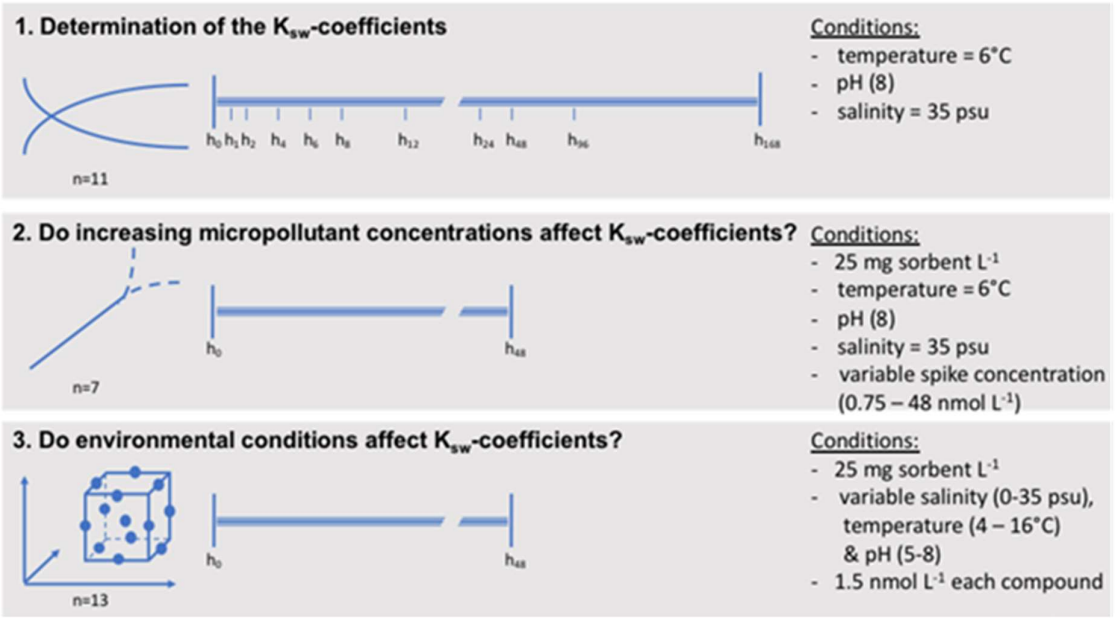

Figure 10. Schematic representation of the different experimental conditions used to determine the K_{sw}. The large ticks represent the start and end of the experiments, with the corresponding sampling of water and sorbent phase. The small ticks represent intermediate sampling points of water and sorbent phase. The 'h' corresponds to the contact time in hours.

To evaluate the impact of varying environmental conditions on the K_{sw} (48h contact time), three parameters were investigated within environmentally relevant ranges, i.e. pH, temperature and salinity respectively ranging from 5 to 8, from 4 to 16° C, and from 0 to 35 psu (Figure 10-3) using response surface modelling and Box-Behnken experimental designs. More details can be consulted in Huysman (2019) and Vanryckeghem (2020).

3.5.2.4. Determination of equilibrium partitioning coefficients and sampling rate.

During calibration of the passive samplers the R_S (L d^{-1}) and the K_{sw} (L kg^{-1}) were determined. After confirming that quality criteria - e.g. closed mass balances, insignificant losses related to non-sorptive processes, and attainment of equilibrium (Vanryckeghem, 2020) - were met, uptake calibration parameters could be determined for 92, 121 and 74 target compounds on freely dispersed h-DVB sorbent, Speedisk and STEPS, respectively.

K_{sw}-values were calculated according to Eq. 7:

$$K_{sw} = \frac{N_{w,t=0} - N_{w,eq}}{C_{w,eq} \cdot M_s} \qquad \text{Eq. 7}$$

with $N_{w,t=0}$ and $N_{w,eq}$ the amount of CEC (nmol) measured in the water phase at the beginning of the experiment and at equilibrium respectively, $C_{w,eq}$ the equilibrium concentration in the water phase (nmol L^{-1}), and M_s the mass of sorbent incorporated in the passive sampler (kg). Reported K_{sw} values (± standard deviation, SD) were calculated as an average from measurements at 96h and 168h.

The R_S was estimated using Eq. 8 by fitting modelled values to the measured dissolved aqueous concentration by non-linear regression through minimizing the sum of squared differences between the measured and modelled:

$$C_{w,t} = \frac{C_{w,t=0}\left\{1 + \frac{K_{sw}M_s}{V_w} exp\left[-\left(1 + \frac{K_{sw}M_s}{V_w}\right)\frac{R_s t}{K_{sw}M_s}\right]\right\}}{1 + \frac{K_{sw}M_s}{V_w}} \qquad \text{Eq. 8}$$

where $C_{w,t}$ represents the measured concentration in the water phase (nmol L^{-1}) at an exposure time t (d), $C_{w,t=0}$ the measured start concentration in the water phase (nmol L^{-1}), K_{sw} the calculated equilibrium partitioning coefficient (L kg^{-1}; Eq. 7), M_s the amount of sorbent incorporated in the passive sampler (kg), and V_w the water volume (L). The non-linear regression model was statistically evaluated based on goodness-of-fit and normality of residuals.

3.5.3. Multi-ratio experiment on bioavailability of HOCs.

3.5.3.1. Relevance of the experiment.

It is important to take the sediment compartment into consideration, either direct or through sampling the SPM that governs the exchange between sediment and the overlaying water column. Especially for hydrophobic organic compounds and poorly soluble metals, the sediment acts as a sink/source buffer for metals and hydrophobic/accumulative contaminants (Figure 11).

Sediment is variable in composition, giving different associated contaminant concentrations (C_{sed}). Sandy sediment give rise to low C_{sed} while fine-grained sediments or SPM have higher C_{sed}. In areas with heterogeneous sediment compositions, the variation in C_{sed} can be as large, or even larger, than between different areas. Therefore, C_{sed} results are often corrected for the sediment composition, to allow a more balanced risk assessment by comparing to EQS, EAC or other assessment values proposed by, a.o., OSPAR (OSPAR, 2008). Hereto, the concentrations of contaminants in sediment are expressed relative to the organic carbon (OC) content of the sediment or converted to a fixed OC content, e.g. 2.5% (OSPAR, 2008), as the majority of the hydrophobic organic compounds is assumed to be associated with OC. Through its partitioning with the aqueous phase, the hydrophobic organic compounds concentration bound to sediment organic matter reflects the water quality because of its relationship with the freely dissolved concentration (C_w) (Ditoro et al. 1991). As C_w is proportional to the chemical activity, it represents the partitioning exposure of hydrophobic organic compounds to organisms (Reichenberg and Mayer, 2006).

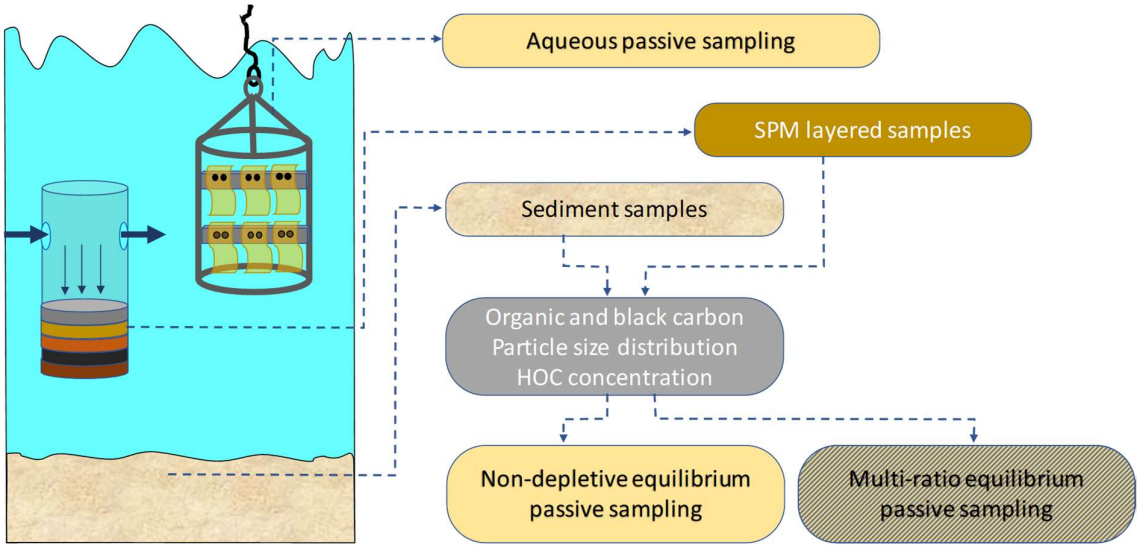

Figure 11. Sampling setup over the different compartments and sample flow.

However, hydrophobic organic compound concentrations in the aqueous phase are very low, and similar to sediment, depending on the composition of the water phase. For hydrophobic organic compounds with K_{OW} higher than 10^6, the amount in the water phase is dominantly bound to SPM. Consequently, the SPM amount present in the aqueous phase determines C_{total} in the water column, while the risk posed by hydrophobic organic compounds for organisms is more related to C_w. This does not mean that uptake by organisms takes place solely through the freely dissolved phase. C_w only expresses the exposure pressure organisms experience, i.e. the partitioning driven uptake, whether that is in sediment or water, also called the chemical activity. Similarly, uptake by PS, made from silicones or LDPE (Low Density Polyethylene), is driven by the same partitioning pressure and, consequently, when equilibrated with the aqueous environment, also represent the exposure pressure

or chemical activity. Equilibrium concentrations in the passive sampler (C_{ps}) can be converted to C_w through division by the PS-water partition coefficient ($K_{ps/w}$):

$$C_w = \frac{C_{ps}}{K_{ps/w}} \quad \text{Eq. 9}$$

For C_{ps} in equilibrium with the aqueous phase, C_w applies to the freely dissolved concentration in the water phase. For PS equilibrated with sediment Eq. 9 provides the C_w for water that would be in equilibrium with the sediment, mostly referred to as the pore water C_w. However, C_{ps} can also be converted to lipid basis (C_L; Eq. 10) by multiplication with the lipid-PS partition coefficient:

$$C_L = C_{ps} K_{L/ps} \quad \text{Eq. 10}$$

Here C_L is the concentration in lipid that would be in equilibrium with the phase the PS was equilibrated with and allows direct comparison with lipid-based concentrations in organisms. Differences between C_L in organisms and C_L for water or sediment are directly proportional to the thermodynamic level in the organism and the sampled phase. This is of great importance for assessing environmental quality as results can be directly related to levels in bioassays used to set EQS.

The passive sampling approach allows to compare the hydrophobic organic compound levels in water, in sediments, as well as in SPM in units of the C_w, irrespective of sample composition. These C_w are proportional to the thermodynamic concentration levels and its differences in space indicate the diffusive transport direction of the hydrophobic organic compounds and as said represent the exposure pressure on organisms, an assessment that is impossible with classical analysis. On the other hand, for estimating the mass transport of hydrophobic organic compounds, passive sampling is not suitable as this is dominated by sediment and SPM transport by water currents and tidal processes.

3.5.3.2 Description of the sediment/SPM passive sampling modes.

To assess what fraction of the organic load is available for partitioning, and as such is bio-available, sediment is allowed to equilibrate with a quantity of silicone polymer material in a number of vials where the proportion of sampler is gradually decreased. As the presence of an amount of sampler, how tiny it may be, is always partly depleting the sediment, this experiment allows for extrapolation to no added samplers, and as such the amount on the sediment that can be exchanged (the chemical activity of the compound in the sediment).

Non-depletive equilibrium passive sampling (ND-EPS) of sediment is performed in the laboratory by equilibration of a small PS with excess sediment. At such a ratio, that the uptake of the PS depletes the concentration level in the system by no more than 5%. After equilibrium, C_w can be calculated from C_{ps} using Eq. 9. The release of PRC from the sampler indicates whether equilibrium was obtained or depletion occurred. A full release of PRC from the PS to the sediment confirms both absence of sediment depletion for target hydrophobic organic compounds as well as equilibrium.

Opposite to ND-EPS *multi-ratio equilibrium passive sampling* (MR-EPS) of sediment uses depletion. By equilibrations applying different sampler to sediment ratios, , various levels of depletion are obtained, ranging from low to highly depletive. When plotting the concentration in the sampler versus the calculated concentration extracted from the sediment, a linear regression to no sampler added yields the available concentration in the sediment. The slope of this relation equals the reciprocal of the partitioning coefficient between sampler and sediment). Comparison to the total concentration in the sediment, obtained by total extraction methods, the fraction available for release to the water phase can be calculated.. Setting up MR-EPS it has to be assured that suitable depletion levels (*D*) are applied. Ideally D should range from <0.1 to >0.8, achieved by stirring sampler-sediment mass ratios following Smedes, et al. (2013).

$$\frac{m_P}{m_S} = \frac{0.63 \ K_{OW} f_{OC}}{K_{PW} \left(^1/_D - 1\right)} \qquad \text{Eq. 11}$$

where m_P/m_S is the ratio of sampler mass to dry sediment mass, f_{OC} the expected sediment's organic carbon fraction, K_{OW} and K_{PW} are the octanol-water and the polymer-water partition coefficients, respectively. The product of 0.63 and K_{OW} is considered to be an estimate of the organic carbon-water partition coefficient (K_{OC}) (Karickhoff et al., 1979). If the assumption that K_{OC} is in the same range as K_{PW} is right, will simplify Eq. 11 to:

$$\frac{m_P}{m_S} = \frac{f_{OC}}{\left(^1/_D - 1\right)} \qquad \text{Eq. 12}$$

The m_P/m_S ratios were estimated to achieve D levels of 0.1, 0.3, 0.5 and 0.9 expecting a f_{OC} of 0.02. To assure sufficient detectability of the hydrophobic organic compounds, minimum sampler masses were estimated for mixing with wet sediment to obtain final dry weight m_P/m_S ratios (g sampler/g dry sediment) of 1/500, 2.3/250, 3/150 and 5.5/20 for equilibrations PS1, PS2, PS3 and PS4, respectively.

Exposure of silicone samplers to homogenized sediment suspensions was carried out in glass bottles of various sizes (50—1000 mL) selected to be approximately 60 % full to allow adequate mixing during shaking. To reduce potential oxidation the bottles were purged with nitrogen just before closing with the aluminium foil lined lid. Shaking was performed in the dark with the bottles positioned horizontally on orbital shaker (GFL 3020) at 150 rpm for 6 weeks. After exposure, the silicone samplers were retrieved from the bottles, rinsed with ultrapure water and wiped dry with a paper tissue. The samplers were stored in glass jars with aluminium foil lined top at −20 °C until further processing.

3.5.3.3. Equilibration of passive samplers with SPM collected from SPM traps.

To study tidal variation of HOC in SPM, this material was collected by sedimentation traps providing layers related to individual tides. The SPM at low, high, spring and nick tide may have largely different composition, but the question is whether they also represent a different aqueous concentration, different chemical activity represented by C_w what could help to identify if HOC in SPM come from different sources depending on the type of tide and associated currents. If C_w corresponding to the sediment and SPM are similar, i,e. are of identical chemical activity for water, sediment and SPM, no

clear sources (or source direction) can be identified. Differences in C_w associated with slices of the SPM cores collected in the trap and, or sediment samples can be investigated by equilibrating them with small PS.

Hereto the cores collected in the SPM-trap were cut about every 5 cm and a 0.125 mm thick SSP silicone strip of approximately 5 mm wide and 30 mm long was mixed with an amount of wet sediment from the core (cores were cut +- every 5cm) containing at least 500 mg OC in a labelled glass bottle. Bottle size was selected such that it was not filled by more than 60%. Water of the same salinity as the location was added, until the sediment fluidized during shaking. The sample slurry is purged with nitrogen gas (to reduce potential oxidation) by means of a glass tube that was also used to stir the sediment. After 5 minutes of nitrogen bubbling and gentle stirring, 10 mL of 5% sodium azide solution per 100 mL of slurry is added. Then the nitrogen tube is slowly taken out and the bottle immediately capped with an aluminium lined screwcap, sealed with aluminium tape on top. The bottles were individually placed in a labelled sturdy plastic bag to prevent laboratory contamination if it would break due to biological activity or other cause. The samples were shaken in the dark with the bottles positioned horizontally on an orbital shaker (GFL 3020) at 150 rpm for 6 weeks. Subsequently, sampler strips were isolated from the sediment by sieving, rinsed with ultrapure water and cleaned with tissue and immediately placed in a weighed labelled vial with aluminium lined cap, and stored at 20° C until thermal desorption GC-MS analysis.

3.5.3.4. Sampler processing

Prior to extraction, recovery internal standards (RIS), i.e. PCB 4, 29, 185 (50 ng each), and naphthalene-d8, phenanthrene-d10 and perylene-d12 (250 ng each) were dosed on the surface of the silicone samplers placed in Erlenmeyer flasks. The samplers were extracted twice in methanol at room temperature by gentle swirling on an orbital shaker overnight. The volume of methanol used for extraction was tenfold of the sampler volume, i.e. 10, 20, 30 and 50 mL for PS1, 2, 3 and 4, respectively. Both extracts were combined in a point flask and the volume was reduced to about 2 mL on water bath using Kuderna-Danish evaporation unit and further reduced to 1 mL under a gentle flow of nitrogen. The extracts were quantitatively split in two portions: a 20 % and a 80 % portion was used for analysis of polar pesticides and HOC, respectively. To the 80 % extract portion, 10 mL hexane was added, and methanol was azeotropically exchanged to 1-2 mL hexane by Kuderna-Danish evaporation. The extract was purified over a glass column containing 5 g of activated silica gel (dried overnight at 160 °C) by elution with 40 mL diethyl ether and 10 mL acetone. The eluate was Kuderna-Danish concentrated down to 1.5-2 mL and azeotropically transferred to hexane. After addition of p-terphenyl (250 ng) and PCB 121 (10 ng) as syringe internal standards, the volume of extracts was further reduced to approximately 0.5 mL under a gentle flow of nitrogen. Thereafter, the extracts were quantitatively transferred to GC-MS mini vials, and the final volume was adjusted to 1mL. Instrumental analyses for PAH, OPFR and polycyclic musk were performed as described in 3.4.4. Subsequently, the analysed extracts were further purified by elution with 30 mL of hexane-DCM mixture, (1:1, v:v) over a column containing 8 g silica gel, modified with concentrated sulfuric acid

(44 %, w:w). The eluates were concentrated by Kuderna-Danish evaporation, transferred to GC mini vials and after volume reduction to 100 µL by nitrogen flow, analysed for PCB and OCP (3.4.4.).

3.5.3.5. Sediment processing

Before subsampling, sediment samples were manually homogenised. Dry weight (by drying at 105 ° C), organic carbon and soot carbon were determined in sub-samples of the SPM and homogenized wet sediment. Further subsamples were freeze dried and used to determine the total HOC concentrations. For passive sampling, non-depletive- (ND-EPS) as well as Multi-ratio-equilibrium passive sampling (MR-EPS) the sediment was used without further treatment. After addition of RIS similarly as for samplers (4.6), the freeze-dried sediments (10 g) were Soxhlet extracted for 8 h with 100 mL acetone: hexane mixture (1:3, v/v). Thereafter, the solvent volume was reduced in a Kuderna-Danish evaporation unit to 1.5-2 mL and, after addition of approx. 100 mg activated copper powder, the extracts were placed in an ultrasonic bath for 30 min to remove sulphur. Subsequently, the extracts were processed and analysed similarly as for silicone samplers.

3.5.3.6. Analysis of sediment traps

On the material in the sediment traps, several parameters are determined as described in Adamopoulou et al. (in prep.). The sediment traps were scanned with a Siemens Somatom Definition Flash X-ray computed tomography (CT) scanner in order to visualise the density structure of the sampled SPM. The scanner was operated at 120 kV, with an effective mAs of 200 and a pitch of 0.45. A 'soft tissue' and 'bone' reconstruction scan was applied in each sediment trap. Volume Graphic's VG Studio 2.2 software was used to visualize the central scan of the trap (Cnudde and Boone, 2013; Van Daele et al., 2016). The traps were split lengthwise and analysed with a Geotek Multi - Sensor Core Logger (MSCL-S) for Colour Spectrophotometry, Gamma Densitometry, and Magnetic susceptibility.

Using the Volume Graphics' VGStudio 2.2 software a ruler was placed next to the real size photo allowing easily to sample every tide of interest. A low density polyethylene (LDPE) plastic circle (0.76 m diameter) and a metal spatula were used for the subsampling of the tidal layers. Grain size, TOC and PCB analysis were performed on every subsample from the traps and on the bed samples. Grain size analysis of the SPM and the seabed sediment has been carried out with a Malvern Mastersizer 3000 laser grain size analyser equipped with a Hydro MV dispersion unit. Organic carbon, calcium carbonate (CaCO3), and biogenic silica were removed prior to grain size analysis using H_2O_2, HCL, and NaOH to achieve total disaggregation of the particles. The carbon content composition of the samples was determined using Flash TCD 2000. Prior to TOC analysis, the inorganic carbon was removed with hydrochloric acid (35% w:w; Ultrex II, J.T. Baker).

3.6. Particulate Carbon and Stable isotopes.

Besides the assessment of various pollutant levels, particulate carbon and its isotopic signatures have been investigated too. Their concentrations in Suspended Particulate Matter (SPM) will help to determine the origin (marine or terrestrial) of particulate organic matter (Raymond and Bauer, 2001).

Hereunder, the sample preparation and instrumental methods used for quantification of particulate carbon and its stable isotopes in samples collected by grab sampling is described.

3.6.1. Treatment for Suspended Particulate Matter (SPM).

500 mL of seawater samples were collected in a similar way as for metals (see 3.1. and 3.2.), then filtered using 0.70 µm pre-treated (i.e. heated at 500 ° C for 2 hours) and pre-weighted glass-microfiber filters (GMF, Sartorius-Stedim Biotech, 0.70 µm Nominal Particle Retention (NPR)). After filtration, the GMF were dried in the oven at 50° C overnight and weighted again. The filters were then used for particulate organic carbon (POC) concentrations and isotope ratio determinations. Procedural blank filters were handled at the same time as the samples, following the same methods in order to guarantee against any contamination.

A subsample of each filter was placed for 24 hours in an acid-fume chamber (HCl fumes) to remove the carbonate fraction and therefore only organic carbon content was obtained. The acidified subsamples were then heated to 50 ° C during at least two hours, folded, enclosed in tin cups and analysed. Another subsample of each filter was also folded, enclosed in tin cups without any additional treatment and analysed, in order to measure its total carbon (inorganic and organic) content.

3.6.2. Carbon and stable isotope ratio analysis.

The amount of POC and the stable isotope ratio of the samples were determined using an Elemental Analyzer coupled with an Isotope Ratio Mass Spectrometry (EA-IRMS instrument, Flash EA112, Delta V Plus, Thermo Scientific). Isotope ratios are here reported in the conventional isotope terminology and calculated following the formula (Eq. 13):

$$\delta(‰) = \frac{R_{sample}}{R_{standard}} \times 1000 \qquad \text{Eq. 13}$$

where δ stands for $\delta\,^{13}C$ and R_{sample} and $R_{standard}$ are the $^{13}C/^{12}C$ ratios of the sample and the standard, respectively. For carbon measurements, the certified reference material IAEA-CH6 sucrose was used as internal standard. The RSD of the measurements was below 7%.

3.7. Ecotoxicological effects.

The ecotoxicological part of NewSTHEPS consisted of three parts: (1) ecotoxicity testing of individual contaminants of emerging concern (CEC) (see 3.7.1), (2) ecotoxicity testing of samples collected from harbour and open sea sites in the BPNS with passive samplers (see 3.7.2), and (3) estimation of marine PNEC's (which are equivalent to EQS values) of CEC based on ecotoxicity data reported in databases (see 3.7.3).

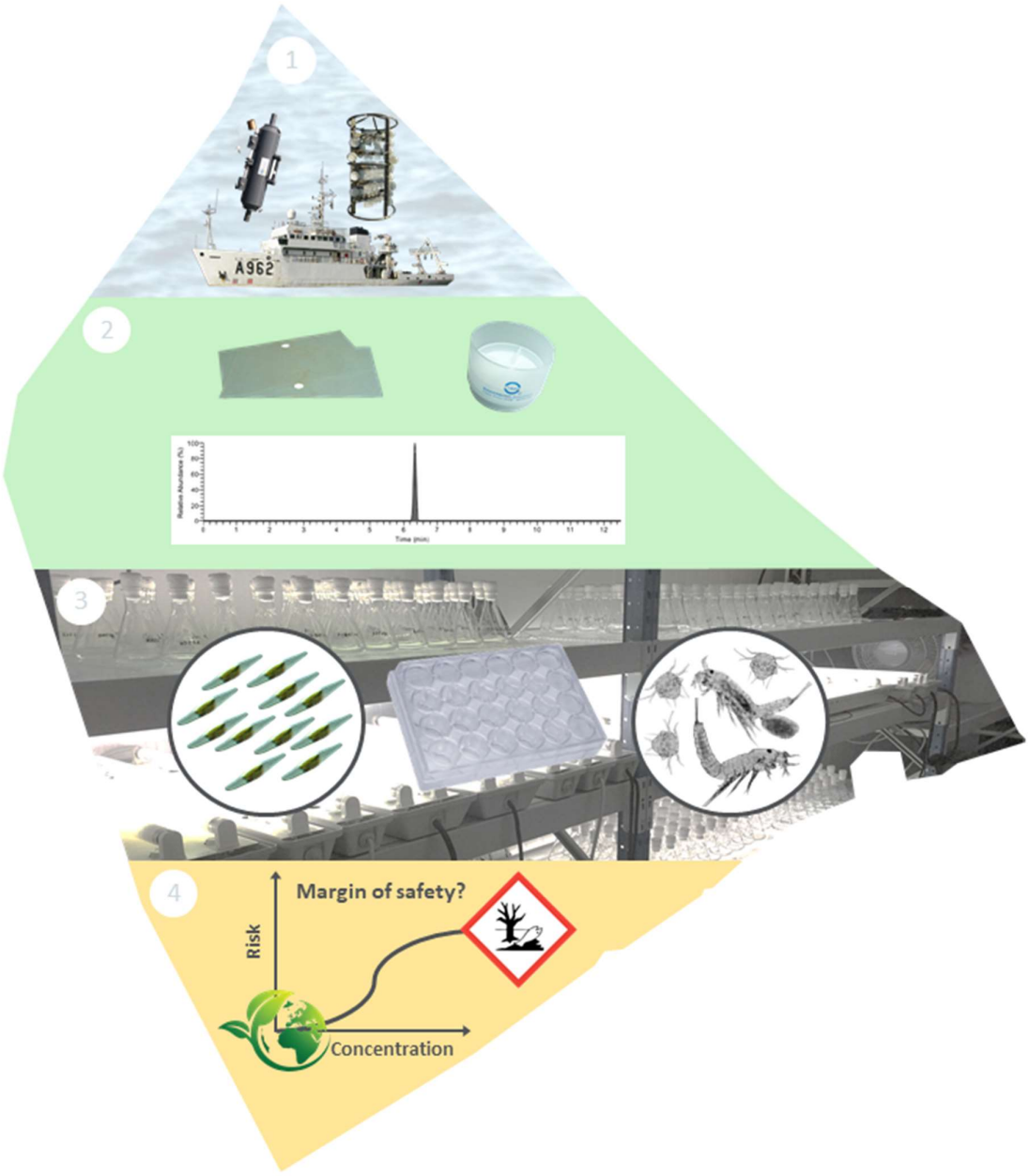

Figure 12. The position of ecotoxicological testing and effects assessment within the general NewSTHEPS project and within the full sequential workflow needed for integrated assessment of chemical contamination (in support of Descriptor 8 for GES assessment), comprising grab sampling and passive sampling of the marine environment (1), sample processing and chemical analysis (2), ecotoxicity testing of single compounds and ERCMs (as well as EQS derivation) (3), and risk characterisation, both conventional and using the new PS-based MoS approach (4).

The positioning of ecotoxicological testing in relation to the other parts of the workflow is visualised in Figure 12. This part of the project made use of the environmental samples taken with grab sampling and passive sampling (see 3.1) and the analytical results (see 3.4). Grab samples were used as a reference for the contaminants' occurrence and their realistic levels at the different sampling

locations. No ecotoxicity tests were performed with grab samples, but the analytical results of the grab samples of SC1 served as a selection criterion for individual substance testing (see 3.7.1), which were aimed at filling data gaps on CEC ecotoxicity for marine species. Ecotoxicity tests were run with two model species representing two trophic levels of marine ecosystems, i.e. *Phaeodactylum tricornutum* (a diatom) and *Nitocra spinipes* (a copepod).

Passive samples were taken using two devices: i) Bakerbond h-DVB Speedisks® (400 ± 5 mg sorbent, Avantor Materials) and ii) Altesil ® silicone rubber (SR) sheets (see 3.1 for details). Passive samples were used and processed in various ways to investigate the ecotoxicity of ERCM's. Details of their use and processing can be found at the beginning of the respective descriptions of the different ecotoxicity tests with passive samplers (see 3.7.2). Passive samples used for ecotoxicity testing originated from PS devices deployed and retrieved simultaneously with those taken for chemical analysis (see section 3.4). Active samples were also taken at the same time. More details about the different sampling campaigns can be found in section 3.1. For details on chemical analytical methods for the determination of pesticides, pharmaceuticals and personal care products, see section 3.4.

3.7.1. Ecotoxicity testing of individual contaminants of emerging concern.

3.7.1.1. Compound selection.

Compound selection for ecotoxicity testing was based on:

1. Analytical results of grab water samples from SC1 (see section 4.3): All substances without any detection above MDL were excluded.
2. Ecotoxicity data for marine crustaceans: Substances with ecotoxicity data for both marine algae and crustaceans available in the US-EPA ECOTOX database (US Environmental Protection Agency, 2019) were excluded since the main goal was to fill data gaps for marine species.
3. Log K_{OW}: Substances with a log K_{OW} > 3 were excluded with three exceptions, i.e. alachlor due to its detection frequency of 100 %, bezafibrate being the only representative of the sub-class of lipid-regulating pharmaceuticals and diclofenac due to high measured concentrations up to 269 ng L^{-1}. Other substances were excluded because a higher log K_{OW} can be associated with demanding test setups such as passive dosing to maintain constant exposure conditions (Smith et al., 2010).
4. Price: some substances (bisoprolol, gatifloxacin and sotalol) were excluded due to very high costs (>850 € per g) for the pure substance.

All substances were purchased from Sigma-Aldrich.

3.7.1.2. Test organisms and culture.

Phaeodactylum tricornutum Bohlin is a marine diatom algae and was obtained from the Culture Collection of Algae and Protozoa (CCAP 1052/1A, Oban, United Kingdom). Algae were cultured in marine algae growth medium according to the ISO 10253 guideline (ISO, 2006), where all details

about the medium composition and general culturing conditions can be found. Four days prior to test initiation, a preculture was prepared by inoculating fresh growth medium with 10,000 cells mL^{-1}. The pre-culture was allowed to grow under continuous white light (100 -120 µmol m^{-2} s^{-1}) at 22° C (± 1° C).

Nitocra spinipes Boeck is a harpacticoid copepod and was obtained from the Department of Environmental Science and Analytical Chemistry (ACES) at Stockholm University, Sweden, where *N. spinipes* has been in continuous culture since 1975 when it was isolated from the Tvären Bay in the Baltic Sea. A culture was established in our laboratory in 2016 (Koch and De Schamphelaere, 2019). *N. spinipes* is cultured according to methods described in Breitholtz and Bengtsson (2001) in natural seawater diluted to a salinity of 7 ‰ using deionized water. Natural seawater was collected 500 m offshore from the coast of Blankenberge, Belgium and filtered using 0.2 µm Pall Polyether sulfone (PES) membranes.

3.7.1.3. Algae growth inhibition testing with Phaeodactylum tricornutum.

Algae growth inhibition testing with *P. tricornutum* was performed as described in ISO 10253 (ISO, 2016). The 72-h growth inhibition test with *P. tricornutum* is a standardized test investigating potential effects of chemicals (or chemical mixtures) on algal growth. For testing, each substance was individually dissolved in marine algae growth medium (ISO 10253 guideline; ISO, 2006). Different concentration treatments were tested in triplicate by adding 50 mL spiked growth medium to 100 mL Erlenmeyer flasks. Test flasks were shaken manually twice a day and cell density measured daily during 72h with a Coulter counter. The specific growth rate μ was calculated for the different controls and each concentration treatment by applying the SLOPE function (Excel 2016) on the ln-transformed cell counts of the measurements of day 0 to day 3. The percentage of growth inhibition (I) for each replicate test flask ($I_{\mu,i}$) was then calculated as follows:

$$I_{\mu,i} = ((\text{mean } \mu_c - \mu_i) / \text{mean } \mu_c) * 100 \qquad \text{Eq. 14}$$

with mean μ_c the average growth rate [d^{-1}] of the controls (in this case the solvent controls) and μ_i as the growth rate [d^{-1}] of the individual test flasks.

For identification of differences in growth rates between concentrations and controls, one-way analysis of variance (one-way ANOVA, α = 0.05) was applied, followed by Dunnett's multiple comparisons test. This analysis as well as dose-response analysis with the four-parameter log-logistic dose-response model was performed in GraphPad Prism version 5.01 for Windows.

3.7.1.4. Acute lethal toxicity testing with Nitocra spinipes.

Acute lethal toxicity testing with *N. spinipes* was performed according to ISO 14669 (ISO, 1999). Briefly, 3 to 4 weeks old copepods were exposed to different concentrations of selected chemicals and mortality and immobility were monitored daily over 96 h. Immobility was defined as no swimming (vertical and horizontal movement) of copepods during 10 seconds of observation, whereas mortality was defined as no swimming and no appendages movement during 10 seconds of observation, as

described in ISO 14669 (ISO, 1999). During the test, organisms were permanently kept in darkness at 22° C (± 0.5° C). For each concentration treatment, 20 organisms were randomly selected regardless of gender (including egg-carrying females) and separated into 4 replicates of 5 organisms. They were exposed in 2.5 mL diluted (with deionized water) natural seawater (7 ‰) spiked with the respective test substance in sterilized non-treated 24-well cell culture plates.

First, a range-finding test was performed in which 5 adult copepods were exposed to 6 concentrations ranging from 0.01 to 100 mg L^{-1} in a geometric concentration series with spacing factor 10. For the actual test, substances were dissolved in diluted seawater (7 ‰) using ultra sonication if needed and a geometric dilution series was prepared directly in the well plates. For substances that resulted in no observed effects in the range-finding test, a limit test was performed by exposing 20 organisms to a nominal concentration of 100 mg L^{-1}. In addition, 24 wells distributed over different cell culture plates were filled with pure diluted natural seawater and 5 copepods each to serve as control treatments. pH was measured in one well of the lowest and highest test concentrations of each substance as well as two control wells at test start and end. Dose response models were fitted to the observed concentration response data using the "drc" package (Ritz et al. 2015) and visualizations were created with ggplot2 (Wickham 2016). For dose-response analysis, a two-parameter log-logistic model was used (fct = LL.2 (upper = 100), logDose = 10). The EC_{50} values with their 95 % confidence intervals were estimated from the fitted model.

3.7.1.5. Larval development testing with Nitocra spinipes.

Larval development tests with the harpacticoid copepod *N. spinipes* were performed according to the ISO 18220 standard (ISO, 2016). In short, nauplii younger than 24h were exposed to six different concentrations of four neonicotinoid insecticides: Clothianidin (CLO), Imidacloprid (IMI), Thiacloprid (TCP) and Thiamethoxam (TMX). These four compounds were selected because they exhibited the highest acute toxicity to *N. spinipes* among all tested individual CEC's (see 4.4.1.2). Nominal test concentrations of CLO ranged from 0.04 - 10 µg L^{-1} while those for IMI, TCP and TMX ranged from 0.33 - 100 µg L^{-1} . At test initiation 9 ± 1 nauplii were placed in eight replicate wells per concentration or control treatment for CLO, IMI, and TMX. Because of a limited availability of nauplii at test initiation of TCP only 6 ± 1 nauplii were used in the replicates and controls for TCP. Seventy percent of the test medium was refreshed once on day 4 and pH and salinity were measured at test start, day 4 and day 7. Organisms were exposed in 10 mL diluted (with deionized water) natural seawater (7 ‰) spiked with the respective test substance (or not spiked in case of control treatments) in sterilized non-treated 6-well cell culture plates. Copepods were fed on day 0 and day 4 with an algae suspension of *Rhodomonas salina* to achieve a concentration of 2.5 x 10^5 cells mL^{-1} in each well. During the tests, organisms were constantly kept in darkness at 22 ± 1° C and nauplii and copepodites were counted on day 5, 6 and 7. The larval development ratio (LDR) was defined as the ratio of live copepodites to the total number of live early-life stages (nauplii + copepodites) at the end of the test, which is defined as the day when control treatments reach an LDR of 60 ± 20 %. Statistical analysis was performed using non-parametric methods. Differences between specific

treatments and the control were assessed using the Mann-Whitney-U test. Based on this analysis, the no-observed effect concentration (NOEC) for each substance was defined as the highest concentration showing no statistically significant (Mann-Whitney-U-Test, α = 0.05) effect on larval development. The lowest-observed effect concentration (LOEC) was defined as the lowest concentration showing a statistically significant (Mann-Whitney-U-Test, α = 0.05) effect on larval development. In a separate analysis, a concentration-response model was fitted in R Studio using the "drc" package (Ritz et al. 2015) to determine the EC10. To this end, data were first transformed to a relative LDR by dividing the treatment LDR by the mean control LDR and expressing it as the relative LDR.

3.7.2. Ecotoxicity testing of environmental samples collected with Passive Samplers.

3.7.2.1. Silicone rubber sheet approaches for non-polar contaminant mixtures.

3.7.2.1.1. Passive dosing experiments with larval *Nitocra spinipes* for testing environmentally realistic contaminant concentrations.

Passive dosing experiments were performed using silicone rubber sheets deployed at HZ and OZ_MOW1 during SC1. After retrieval, SR sheets were rinsed with seawater on-site and stored in cooling boxes for transportation. Upon arrival in the laboratory, they were stored at -20 ° C until toxicity testing. In order to determine the ecotoxicity of the sampled environmentally realistic contaminant mixtures (ERCM), we passively dosed diluted natural seawater for testing of larval development of *N. spinipes* according to ISO 18220 (ISO, 2016). First, in a pre-equilibration step, four SR sheets (approximately 12.5 g in total) were added to 250 mL of diluted natural seawater (= test medium, 7 ‰, diluted with deionized water). The bottles were left on a rolling table at 20° C in darkness for 24h allowing equilibration between SR sheets and test medium. At test initiation, each of 6 replicate wells of a culture plate were filled with 7.5 mL of this pre-equilibrated test medium. In addition, pieces of 0.5 g SR sheet from the pre-equilibration beakers were cut into four equal pieces (4 x 0.125 g) and added to each of the 8 wells. At test start, 10 neonate (younger than 24h) nauplii of *N. spinipes* were added to each well and fed with 0.5 mL of an algae suspension of *Rhodomonas salina* to achieve a concentration of 2.5 x 10^5 cells mL^{-1} in each well. At day 2 and day 5 test medium was refreshed by replacing 5.6 mL medium with pre-equilibrated test medium and organisms were fed as described before. Organisms were counted on day 5 and day 6 and the larval development ratio was calculated as the ratio of live copepodites per total live organisms (nauplii plus copepodites).

3.7.2.1.2. Proof of principle study for testing of enriched ERCMs.

Claessens et al. (2015) have previously used SR sheets deployed in the North Sea to passively dose algae growth medium for ecotoxicity testing of ERCMs of non-polar compounds. A limitation of their passive dosing method is that only one concentration level of the ERCM can be tested, i.e. the environmental concentration that is being reconstituted by the passive dosing, with a relative enrichment factor (REF) equal to 1 (see 3.7.2.2 and Eq. 15 for further explanation). For samples with no observed ecotoxicity, this means it is impossible to derive an ecotoxicological margin of safety (MoS). In order to improve the usefulness of passive dosing ecotoxicity tests with SR sheets with

regard to documenting and interpreting trends in environmental monitoring, there is a need for sample enrichment. The aim of this experiment was therefore to conduct a proof of principle study for enrichment of mixtures of PAHs (as model non-polar compounds) on SR sheets in order to allow ecotoxicity testing of a concentration series rather than single concentrations. We attempted to achieve this via SR sheet size reduction. All methodological details can be found in Annex 2.

3.7.2.2. Speedisk extract testing approaches for ERCMs.

3.7.2.2.1. Toxicity identification evaluation (TIE) approach with Speedisk samplers.

This approach aimed to investigate effects of ERCMs (collected during SC1) on larval development of *N. spinipes* according to ISO 18220 (ISO, 2016) with the option to identify mixture toxicity driving chemical groups (from less to more polar) by fractionating the contaminant mixtures by means of the use of solvents with different polarity to extract the Speedisks. All methodological details can be found in annex 3.

3.7.2.2.2 Speedisk extract testing of enriched ERCMs as basis for MoS derivation.

This approach aimed to investigate effects of ERCMs extracted from Speedisks (that had been deployed in the field) on the growth of *P. tricornutum*. Our initial method consisted of extracting Speedisk according to the extraction protocol described in section 3.4.1.3 and ecotoxicity testing of a dilution series of those extracts with *P. tricornutum* in 50 mL of artificial seawater medium in Erlenmeyer flasks (method as in 3.7.1.3). This method was applied to samples from SC1 and SC4 and full methodological details are available in Moeris et al. (2019). This initial method for Speedisk extract testing, however, had an important limitation: the maximum Relative Enrichment Factor (REF) that could be tested was limited to about 2, because of the solvent content of the undiluted extract (as the solvent concentration in ecotoxicity testing needs to remain below 0.1 - 0.01%, depending on the test species) and because of the high testing volume. Therefore, the initial method was modified to allow testing of ERCMs (Speedisk extracts) that were enriched compared to the original field situation.

Our final method consisted of solvent-free ecotoxicity testing in 24 multi-well plates, where diatoms were exposed to dilution series of Speedisk extracts in smaller volumes (2 mL) and where fluorescence measurements instead of cell counting were used to monitor cell growth (See Annex 3). This method was applied to Speedisk samples from SC2, SC3, and SC5 and allowed to test REFs up to about 44. Briefly, Speedisk extractions took place as in our initial method (see section 3.4.1.3 and Moeris et al., 2019), but after evaporating the extract to complete dryness, the precipitate was reconstituted in 1 mL ultrapure HPLC water (instead of a methanol/water mixture). A comparative study with Speedisks from the Harbour of Ostend (SC2 HO) showed very good correspondence in chemical composition (39 target substances) in the final extracts between the initial and the final method, with an R^2 = 0.97 and 88% of the detected substances showing less than 2-fold difference between both methods (see Annex 3).

Following the reconstitution step, dilution series of the Speedisk extract were prepared in artificial seawater and brought into 24 multi-well plates. Media were inoculated with algae (10,000 cells mL^{-1}) and were left to grow under conditions as described in 3.7.1.3 and in accordance with the ISO guideline (ISO, 2006). Algae fluorescence was measured after 0, 24, 48 and 72 h of exposure using a microplate reader (TECAN Infinite 200 PRO microplate reader). At day 0 a calibration series ranging from 10,000 to 400,000 cells mL^{-1} was prepared (based on cell counts using an electronic particle counter, Coulter Counter model DN, Harpenden) to enable conversion of fluorescence measurements to cell numbers. Fluorescence measurement settings are provided in Annex 3.

In order to make the link to Margin of Safety (MoS) calculations, it is required to relate the various dilutions of the extracts that were tested to the environmentally realistic concentration levels that occurred during Speedisk passive sampling in the field. Therefore, exposure concentrations in these tests were expressed as Relative Enrichment Factor (REF). The individual REF per substance (REF_i) was calculated based on the concentrations measured in grab samples taken at the respective sampling location during sampler deployment and retrieval (mean of sampler deployment and retrieval):

$$REF_i = \frac{2.C_{i,extract}}{(C_{i,grab\ sample\ deployment} + C_{i,grab\ sample\ retrieval}).d} \qquad \text{Eq. 15}$$

Where d = the applied dilution factor for the treatment the ecotoxicity test. Then, the REF of the ERCM (as present in the Speedisk extract) was determined as geometric mean (Eq. 16) of the relative enrichment factors across all measured substances ($REF_{geomean}$):

$$REF_{geomean} = \sqrt[n]{\prod_{i=1}^{n} REF_i} \qquad \text{Eq. 16}$$

where n is the number of detected substances. Substances with concentrations below the method detection limit (MDL) were not included in the calculation of the REF. An REF = 1 corresponds to the environmental concentrations (C_w) as measured in the field, as applied in previous research (Kim Tiam et al. 2014).

Finally, diatom growth rates in all dilutions where calculated (Eq. 14) and statistically compared with those in the control using one-way ANOVA, followed by Dunnett's multiple comparisons test (α = 0.05). The $NOEC_{REF}$ (NOEC expressed as $REF_{geomean}$) was defined as the highest $REF_{geomean}$ with no significant reduction of diatom growth rate compared to a control. The $NOEC_{REF}$ is also equal to the MoS for this diatom species (see 3.7.2.1).

3.7.3. Integrated Environmental Risk Assessment.

3.7.3.1. Margin of Safety (MoS) approach for assessing risks through direct toxicity testing of ERCMs collected with Speedisks.

The Margin of Safety (MoS) for a given species is defined as being equal to the $NOEC_{REF}$, as explained in 3.7.2.2.2.

3.7.3.2. Risk characterisation for substances with existing EQS or PNEC values.

For a number of CEC's either EQS or PNECs are already available. In this section we performed risk characterisation by comparing measured concentrations of CECs (see Annex 4) with:

- AA-EQS values for WFD priority substances for 'other surface waters' (meaning salt water under the WFD (EU, 2013).
- (Adjusted) PNEC values for freshwater for WFD watch list substances (EU, 2018a & b)
- The lowest of two PNECs for antibiotics ($PNEC_{antibiotic}$), i.e. $PNEC_{ENV}$ (typical freshwater PNEC for aquatic organisms) and $PNEC_{MIC}$ (PNEC protecting against development of antibiotic resistance; Tell et al. 2019).

Risk quotients (RQ) of each individual substance *i* were defined as follows:

$RQ_i = C_i/PNEC_i$ or $RQ_i = C_i/EQS_i$ Eq. 17

3.7.3.3. Marine PNECs and risk assessment for neonicotinoids and their mixture.

Specific Marine EQS (equivalent to PNEC) were derived for four neonicotinoid insecticides according to the Technical guidance document for deriving environmental quality standards (European Commission 2011). Toxicity data were obtained from two databases: the US EPA ECOTOX database (US EPA, 2019) and the US EPA Office of Pesticide Programs (OPP) Pesticide Ecotoxicity database (US EPA, 2018). More details about the methodology can be found in Annex 5. Risk assessment of mixtures of neonicotinoids was performed using the concentration addition model (also called the toxic unit approach, TU; Eq. 18), i.e. by summation of RQ values:

$$RQ_{mix} = \sum_{i=1}^{n} TU_{i,x} = \sum_{i=1}^{n} \frac{C_i}{PNEC_i} \quad \text{Eq. 18}$$

Where TU_i is the toxic unit for substance *I*, or the ratio between the measured concentration of that substance (c_i) and the PNEC of that substance ($PNEC_i$), and *n* is the number of substance considered.

3.7.3.4. Screening-level marine PNECs and screening-level risk characterisation for CECs.

We developed an automated calculation algorithm and programmed it in R to derive screening-level PNECs for all CEC's. Briefly, the estimation entails a data selection and filtering step applied on the US EPA ecotoxicological database, assignment of organism classes, discrimination between acute (short-term) and chronic (long-term) toxicity data, selection of the most sensitive ecotoxicity value and appropriate assessment factor. To allow automation, it was necessary to somewhat simplify the rule set for deriving marine EQS as compared to the guidance (EU, 2011). Therefore, PNECs (and RQ's based on it) are to be considered as screening-level with the purpose of prioritisation for further work or PNEC refinement. Detailed methodology is available in Annex 6.

3.8. Modelling.

A pollutant fate model that describes the phase changes and transport of non-conservative pollutants was developed. Non-conservative pollutants are defined as pollutants that can switch between a dissolved phase and an adsorbed phase. In the adsorbed phase they are either connected to the

suspended sediments of the water column or to the sediments of the seabed. To describe the transport of non-conservative pollutants, a sediment transport model coupled to a hydrodynamic model is needed. The numerical model used in this work is the "COupled Hydrodynamic Ecological model for REgioNal Shelf seas (COHERENS)", an open source, three-dimensional, hydrodynamic model with a sediment module included. For a detailed description we refer to the online manual of the numerical code (http://odnature.naturalsciences.be/coherens/manual). The pollutant model developed within this project is based on the 2D model described in Periañez et al. (2013). The 2D model was converted to 3D, the degradation (decay) of pollutants in the dissolved phase was added and we coupled the adsorbed phase or 'particulate phase' (attached to suspended sediment or seabed sediment) to the sediment module of COHERENS. The concept of the model is illustrated in Figure 13. For a more in-depth explanation of the model modification we refer to Annex 7. The model was tested for correct implementation under several set-up testing conditions to check for mass conservation.

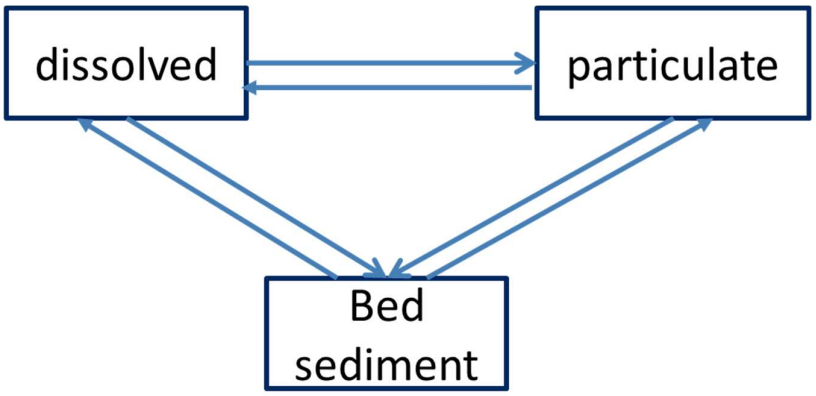

Figure 13. Concept of the pollutant exposure model. The exchanges with the dissolved phase are governed by diffusion, adsorption and desorption processes. The exchange between the particulate phase and the bed sediment are governed by advection processes (deposition and erosion).

4. SCIENTIFIC RESULTS AND RECOMMENDATIONS.

In this section, the major outcome of the project is presented, limited to real achievements. The rest of the results is presented in the different annexes or available on the NewSTHEPS website.

4.1. Novel analytical methods: analytical performance characteristics.

4.1.1. Novel development of o-DGT and ERE-CALUX for EDCs analysis.

The combination of o-DGT and ERE-CALUX bioassay is ideally suited to get an integrated view of the total estrogenic activity of all compounds in an aquatic system, but without details of individual compounds or small scale spatial and temporal variations. The o-DGT component allows for spatial and temporal integration while the bioassay encompasses the estrogenic activity of the individual compounds present in any given study area. In the validation experiment, a small decrease of 5% of the E2 concentration in solution was observed after 48 h when DGT holders and agarose diffusive gels were immersed in the solution, while a small increase of 2.4% was observed when the filter membranes were immersed. The adsorption/desorption effect onto the DGT has been always verified in the subsequent experiments but never influenced the obtained results. The XAD18 binding affinity to E2 was tested at increasing E2 concentrations of 2, 4, 8, 16, 32 and 64 ng L^{-1} of E2 (with 64 ng L^{-1} as a maximum based on literature). The uptake of E2 by XAD18 resin gel increased linearly from 2 to 64 ng L^{-1} of E2 (R^2 = 0.999) and was very close to the value of 100% recovery.

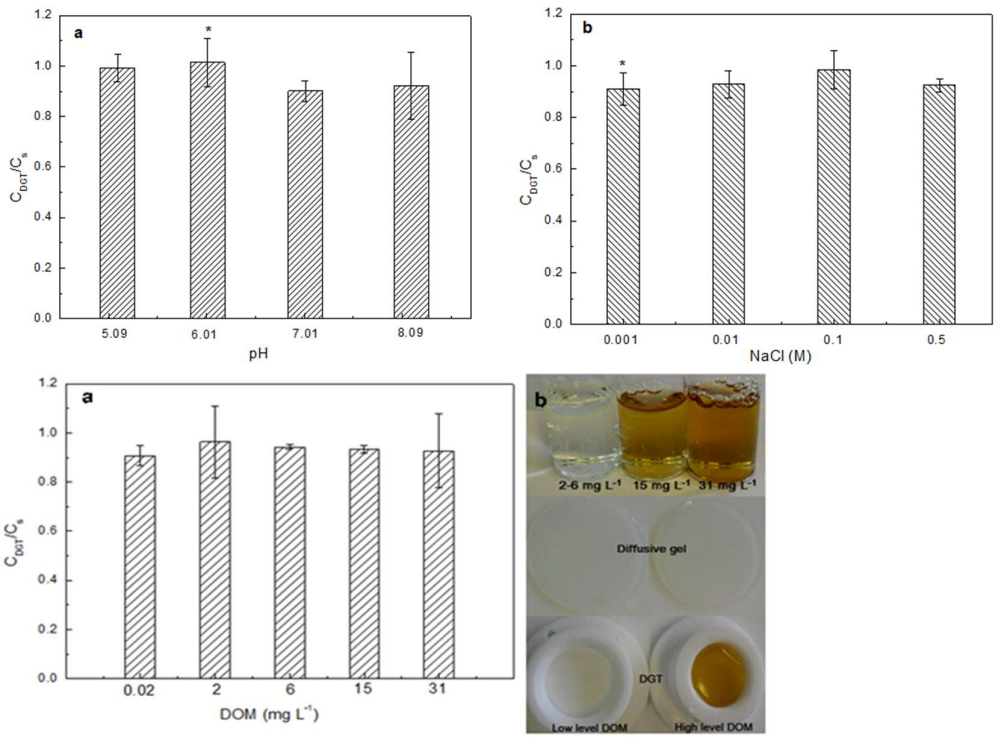

Figure 14. Effect of pH, ionic strength and dissolved organic matter (DOM) on the ratio of the E2 concentration assessed with DGT(C_{DGT}) to the bulk E2 concentration (C_s).

Since saturation of the XAD18 resin gel by E2 was never observed, even at the highest E2 concentration ever reported, it is reasonable to assume that a DGT with XAD18 resin gel will be

suitable for monitoring steroid hormones in natural waters without concerns of resin saturation by E2. The measured effective diffusion coefficient of E2 of $4.65 \pm 0.37 \times 10^{-6}$ cm^2 s^{-1} was slightly lower than the theoretical calculated diffusion (D_t) coefficient of 5.17×10^{-6} cm^2 s^{-1} but was within 10%. Due to similarities in molecular structure and chemical characteristics, the D_t values of many steroid hormones (Estrone (E1), E2, Estriol (E3) and 17-alpha-ethinyl-estradiol (EE2)) are very similar, yielding an average value of $5.16 \pm 0.05 \times 10^{-6}$ cm^2 s^{-1} based on 4 steroid hormones (Guo et al., 2016). A pH range from 5-8, ionic strength ranged from 0.001 M to 0.5 and DOM concentration ranges from 0 mg L^1 to 30 mg L^{-1} do not influence of the performance of o-DGT samplers (Figure 14).

4.1.2. Analytical validation for pharmaceuticals, personal care products and pesticides.

4.1.2.1. Instrumental validation.

Among the 89 target compounds, 63 and 17 compounds could be analysed either in the HESI positive and negative ionization mode, respectively. The remaining 9 compounds (i.e. acyclovir, bezafibrate, chloridazon, diclofenac, diuron, efavirenz, imidacloprid, indomethacin and naproxen) could be analysed in both ionization modes leading to a total of 98 combinations of compound and ionization mode (hereafter called analytes), which were used to evaluate the method validation parameters.

The instrumental precision was found to be better than 10% for 86% of the values in Annex 8. The IDLs and IQLs ranged from 0.01 to 1 µg L^{-1} except for 13 out of 98 analytes with values between 3 and 100 µg L^{-1}. Regarding instrumental linearity, the statistical tests showed significant deviation from linearity (p-value < 0.01) for 55 out of the 98 analytes, and RMSE calculated for the 'entire' calibration range (*i.e.* from the IQL up to the maximum standard concentration of 1000 µg L^{-1}) was higher than 10% for 77 analytes when using a linear function. Instead of using a quadratic function ($a+bx+x^2$) that can yield several solutions when calculating concentrations from peak areas and is not monotonously increasing, a power function ($a+bx^c$) was introduced which improved the fit, with RMSEs < 10% for 51 analytes. A closer inspection of the calibration and residual plots pointed out that the response factor reduced with higher intensities, leading to negative residuals. Therefore, the 'entire' calibration range of 69 analytes having an IQL < 1 µg L^{-1} - meaning that the calibration range was wider than a factor of 1000 - was divided into a 'low' (*i.e.* from IQL to 10 µg L^{-1}) and a 'high' (*i.e.* from 10 to 1000 µg L^{-1}) calibration range. For the remaining 29 analytes, the calibration range was not split as the IQL was equal or higher than 1 µg L^{-1}. This resulted in a total of 167 (69 x 2 + 29) calibration curves, where non-linearity was still concluded for 78 calibration curves (p-value < 0.01). The RMSEs were larger than 10% for 72 curves when using a linear function, while a power function showed to fit the calibration curves better with RMSEs > 10% for only 18 out of 167 curves. The final instrumental calibration parameter for each compound is reported in Annex 8.

4.1.2.2. Method validation.

The (large-volume) Speedisk extraction (Section 3.4.1.2.2) clearly showed improved method precision and linearity as compared to the commonly used (low-volume) Oasis HLB extraction technique

(section 3.4.1.2.1). The RSD at 10 ng L^{-1} was better than 20% for 79% of the analytes (Annex 9). The Oasis HLB method (Annex 10) clearly showed lower precision (RSD > 20%) for analytes with Log K_{ow} values above 4 (e.g. indomethacin, diclofenac, efavirenz), whereas the Speedisk method performed better over the entire polarity range of the analytes (Log K_{ow} ranging from -1.6 to 5.1). To correct for the curvature of the instrumental response, a multi-point external calibration strategy was implemented using the power function fitted to the instrumental standard curves for external calibration. An improved method linearity was obtained with the Speedisks compared to Oasis HLB cartridges, as the number of analytes showing linear matrix curves (p-value > 0.01) reached 84 instead of 52 out of 98 analytes. The optimized sample loading volume of 1000 mL on Speedisks ensured a high concentration factor (CF = 1000) during sample preparation, leading to MDLs lower than 1 ng L^{-1} for 56 analytes (Annex 9), compared to 33 analytes upon extraction with Oasis HLB (Annex 10). PE values ranged from 1.4% to 76% for the target analytes extracted with the Speedisk method while for the Oasis HLB extraction, PE values between 0.06% and 103% were obtained. Although the most non-polar analytes (Log $K_{ow} \geq 4$) attained higher Pes following Speedisk extraction, it could be noticed that in general, Pes were lower than for Oasis HLB extraction: 16 versus 59 analytes having a PE > 60% for Speedisk and Oasis HLB, respectively. This could be mainly attributed to the extraction recovery (RE) rather than matrix effects (ME). Whereas ME is found to be between 80 and 120% for at least 70 analytes using both methods, RE is lower than 60% for 65 and 33 analytes when respectively using Speedisk and Oasis HLB extraction (Figures 15, 16). This may be linked to different chemical characteristics of the polymeric sorbent resulting in different interactions between analytes and sorbents and/or to partial breakthrough for some analytes when using a loading volume of 1000 mL. For quantitative analysis of real samples, analytes having PE values < 10% (14 and 9 analytes for the Speedisk and Oasis HLB method, respectively) were excluded from further data interpretation and for field measurements (Vergeynst et al., 2015).

The analyte concentration in grab samples (C_w, ng L^{-1}) was calculated based on the calibrated concentration ($C_{exp,sample}$, in ng L^{-1}) resulting from the instrumental analysis, the analytical process efficiency (PE) determined during validation, and the concentration factor (CF) following extraction of a 1000 mL sample (Section 3.4.1.2.2; Eq. 19):

$$C_w = \frac{C_{exp,sample}}{PE * CF} \qquad \text{Eq. 19}$$

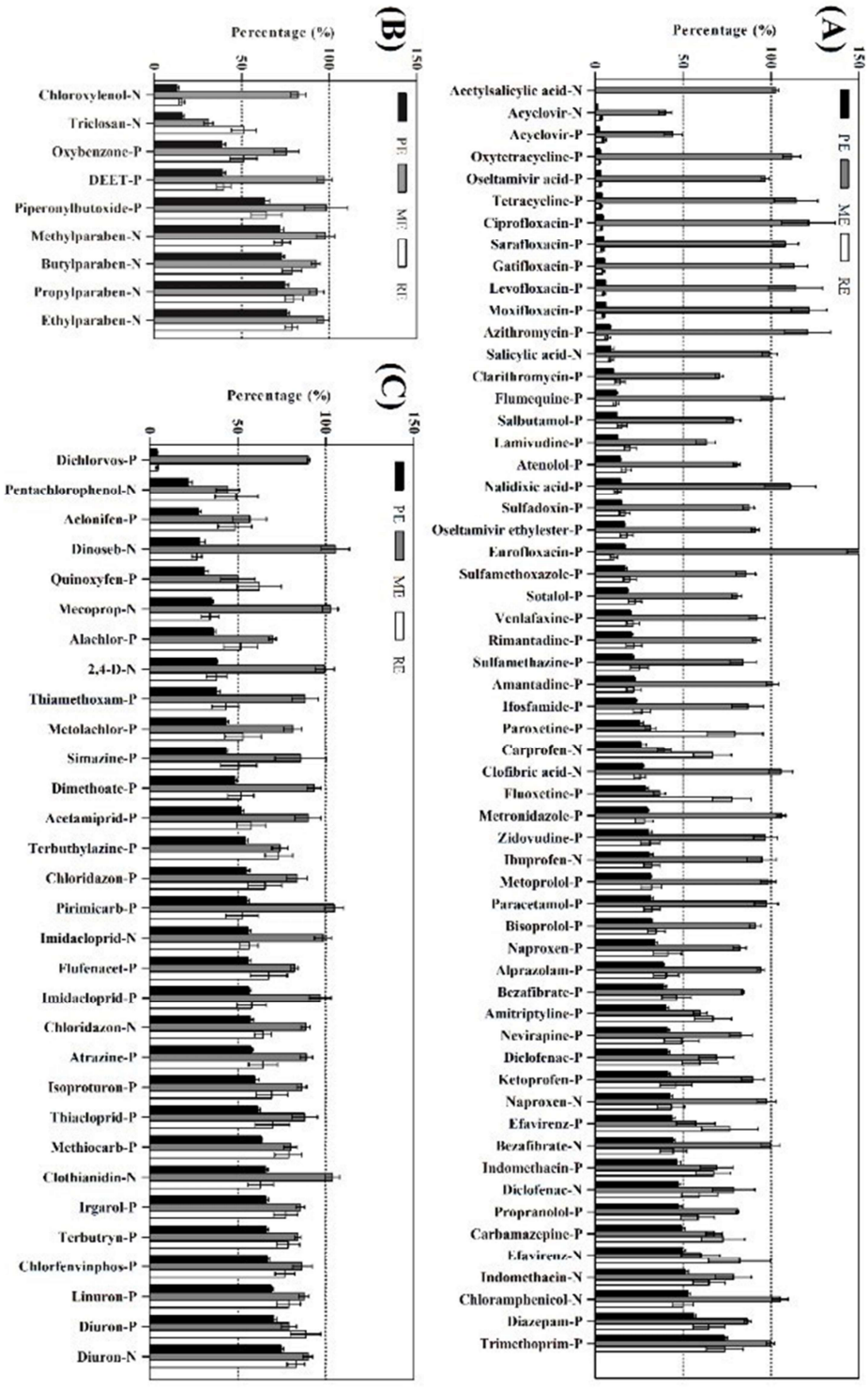

Figure 15. Decomposition of the analytical process efficiency (PE) into matrix effect (ME) and extraction recovery (RE) for the (A) pharmaceuticals, (B) PCPs and (C) pesticides, determined during the method validation with Speedisk extraction. The analytes are ordered according to increasing PE, and the error bars represent the standard deviation (n = 3).

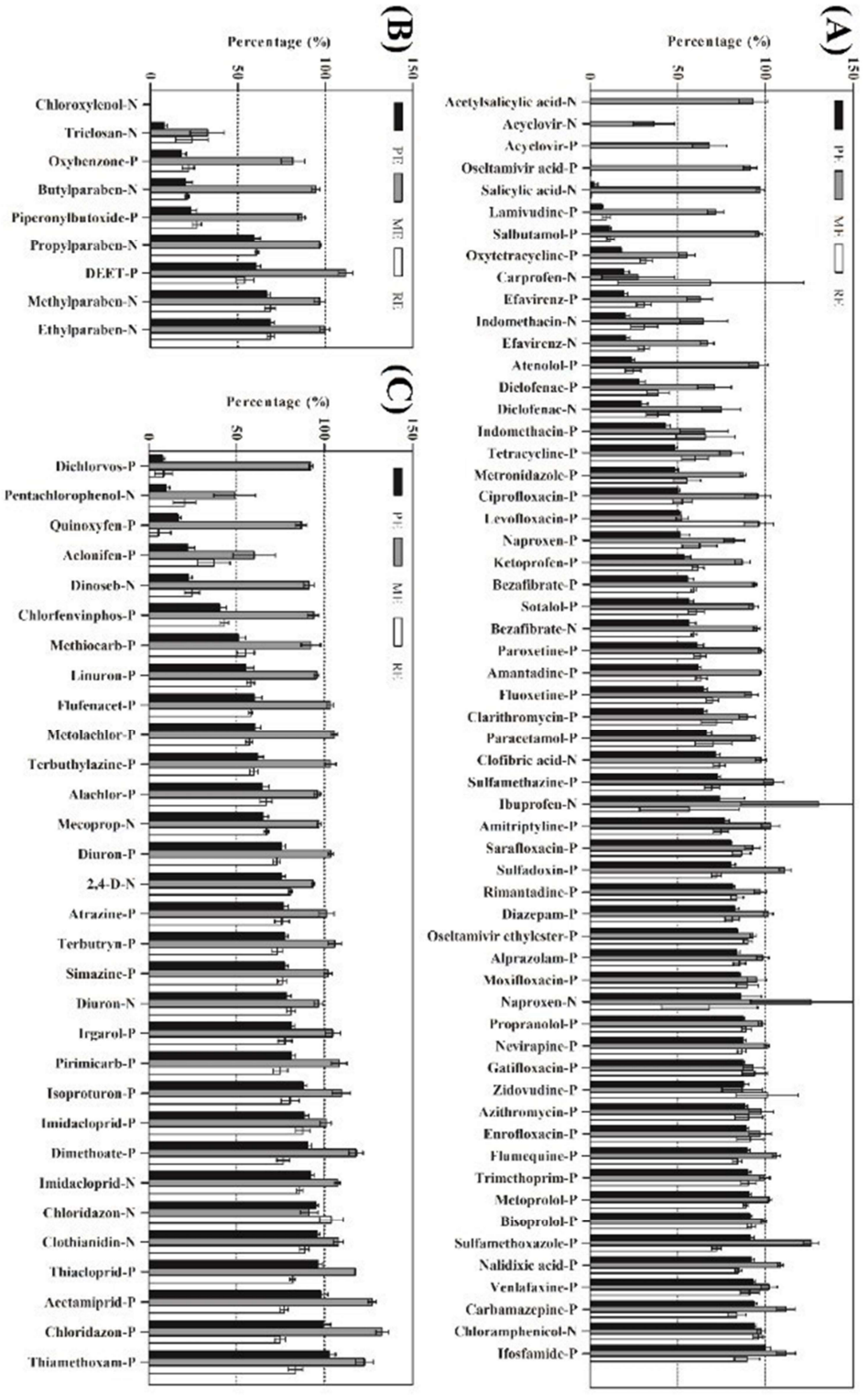

Figure 16. Decomposition of the analytical process efficiency (PE) into matrix effect (ME) and extraction recovery (RE) for the (A) pharmaceuticals, (B) PCPs and (C) pesticides, determined during the method validation with Oasis HLB extraction. The analytes are ordered according to increasing PE, and the error bars represent the standard deviation (n = 3).

4.1.3. Analytical validation for steroidal EDCs.

The detection and quantification of EDC residues using HRMS presents new challenges to the determination of MDLs and MQLs, as traditionally estimated by theoretical or empirical calculations based on signal-to-noise ratios. The signal-to-noise ratios obtained by HRMS are mainly of infinite magnitude, resulting in virtually low detection and quantification limits. To deal with these virtual estimations, new strategies are required based on more practical criteria. Therefore, the validation criteria stated in CD 2002/657/EC (food safety, EU 2002), CD 2009/90/EC (water monitoring, EU 2009) and Eurachem 2016 (general guidelines) - for measuring residues in the aquatic environment - were combined and refined as was previously described by Vergeynst et al. (2017), but with usage of an additional criterion, i.e. identity confirmation through the ^{13}C-isotope and the $^{13}C/^{12}C$-ratio of each target compound at the corresponding theoretical MDL. The MQLs for the androgens, oestrogens, progestins and corticosteroids ranged from, respectively, 0.13 to 5.00 ng L^{-1}, 0.25 to 5.00 ng L^{-1}, 0.25 to 2.50 ng L^{-1} and 0.50 to 5.00 ng L^{-1}, whereas the MDLs for all classes ranged from 0.06 to 2.50 ng L^{-1}.

The specificity and selectivity were evaluated by analysing blank samples as well as samples spiked at 1.5 times the MQL. As true blanks, reference seawater was used, containing no measurable residues of exogenous EDCs at their accurate mass and specific retention time. A significant increase was observed at the accurate mass and specific retention time when EDCs were added to the blank samples, taking into account a maximal RSD of 20%. The above-mentioned observations confirmed that the optimised method was selective for the 70 target EDCs in the presence of other matrix constituents. Identification was based on accurate mass and relative retention time, i.e. the ratio between retention time of the analyte and its deuterated internal standard, which ensured the high selectivity of the method. In addition, the mass deviation (< 1 ppm) and retention time deviation (< 0.05 min) confirmed the instrumental stability (n = 110, time period = 3 days) of the developed UHPLC-HRMS method.

Linearity was evaluated by setting up 13-point matrix-matched calibration curves in triplicate, with concentration levels ranging from 0 to 50 ng L^{-1} for the compounds of interest. The linearity was analysed by establishing weighted linear regression models. These regression models indicated good linearity ($R^2 < 0.99$) and no lack of fit (95% confidence interval; F-test, $p < 0.05$) (EU, 2002). During the evaluation of the linearity performance, appropriate deuterated internal standards were determined for each compound, thereby pursuing a RSD for the peak area ratio ≤ 20% and a good linearity ($R^2 > 0.99$ and no lack of fit).

Trueness and precision were assessed at different levels, which were 1.5, 2.0 and 2.5 times the MQL. In absence of certified reference material, trueness was investigated by calculating the recovery. For all compounds, the recovery ranged between 97% and 109%, with RSDs below 10% (n = 70). These recoveries are better in comparison to literature, ranging in aquatic matrices from 88 to 120 (Goh et al., 2016; Zhang et al., 2014; Ronan and McHugh, 2013).

The precision, covering the repeatability and within-laboratory reproducibility, was in line with the Horwitz equation. The RSDs of repeatability and within-laboratory reproducibility ranged, respectively, from 3.7 to 8.5% and 3.8 to 10.5% for all compounds. These values are comparable to the RSDs that have been described in literature for a rather limited number of EDCs, reporting repeatability RDSs from 4.2 to 8.3% and within-laboratory reproducibility RSDs from 3.6 to 12.0% (Goh et al., 2016; Zhang et al., 2014; Ronan and McHugh, 2013).

4.1.4. Analytical validation for steroidal plasticizers and plastic additives.

The MDLs for the phenols, di-phthalates and mono-phthalates ranged respectively from 10 to 150 ng L^{-1}, 5 to 25 ng L^{-1} and 5 to 25 ng L^{-1}, whereas the MQLs ranged respectively from 25 to 200 ng L^{-1}, 10 to 50 ng L^{-1} and 10 to 50 ng L^{-1}.

No detectable residues of exogenous Aps, Bisphenol A and PAEs at their accurate mass and specific retention time were observed in reference seawater used as a blank. Spiking the target analytes to the blanks resulted in a significant increase, taking into account a maximal RSD of 20%, confirming the selectivity of the optimised method for the 27 target compounds. The latter were identified based on their accurate mass and relative retention time, i.e. the ratio between retention time of the analyte and its deuterated internal standard. Moreover, the target low and high molecular phthalates were respectively corrected by using the diethyl phthalate-3,4,5,6-d_4 and di-cyclohexyl phthalate-3,4,5,6-d_4. The specific deuterated internal standard that was used for quantification of every target compound can be consulted in Annex 1. The observed retention time deviations (< 0.05 min) and observed mass deviations (< 1 ppm) confirm the excellent instrumental stability for the developed UHPLC-HRMS method. Weighted linear regression models indicated good linearity (R^2 > 0.99) and no lack of fit (95% confidence interval, F-test, p-value > 0.05) (EU, 2002).

The recovery ranged for all compounds between 98.5 and 105.8%, with RSDs below 10% (n = 70, independent extractions at 3 different days). These recoveries outperform these reported in related literature, ranging in aquatic matrices from 91.8 to 118% (Chen et al., 2016). The precision, encompassing the repeatability and within-laboratory reproducibility complied to the Horwitz equation. The RSDs of repeatability and within-laboratory reproducibility ranged for all the target compounds, respectively, from 1.6 to 9.5% and 2.4 to 9.9%. Comparing our results to reported literature, recovery and within-laboratory reproducibility ranges respectively from 4.1 to 17 % and 4.7 to 12 %, our precision can be considered as good (Esteve et al., 2016).

4.2. Calibration data on Hydrophilic DVB based Passive Samplers.

4.2.1. Characterization.

To the best of our knowledge, the surface chemistry of h-DVB has not been studied earlier. This work relied on spectral analysis (i.e. FTIR, Raman and NIR) to unravel surface functionalities of h-DVB. Additionally, the co-polymer poly(divinylbenzene-co-N-vinylpyrrolidone), also more familiar

under the tradename Oasis® HLB, was analysed for comparison. Multivariate statistical analysis of the obtained FTIR spectra demonstrated significant differences between the two sorbents (p-value < 0.05, $R^2(X)(cum) = 0.989$, $R^2(Y) = 0.99$, $Q^2(cum) = 0.974$). The main spectral differences were related to the presence of water adsorbed to amorphous regions of the polymer (Kizil et al., 2002; Guo et al., 2018), suggesting the presence of hydroxyl [-OH] and/or ketone [-C=O] groups and the presence of carboxyl [-COOH] groups (Mizuguchi et al., 1997; Taguchi and Noguchi., 2007). For Oasis HLB, the amide [C-N] stretching vibration of the pyrrolidine ring present in the PVP (poly-N-vinylpyrrolidone) moiety was observed. Complementary to the FTIR spectra, the Raman spectra also provided qualitative and quantitative information on the functional groups of the two sorbents. Raman analysis revealed and confirmed the presence of carboxyl [-COOH] moieties in the h-DVB co-polymer and the occurrence of vinyl-groups [CH2=CH2] in the Oasis HLB. On top of that more intense signals were marked for the h-DVB functional groups, revealing a higher degree of cross-linkage and functionalisation for h-DVB as compared to Oasis HLB.

4.2.2. Sampling rate.

Based on the decrease in aqueous concentrations as a function of contact time, as measured in our static exposure batch experiments, the R_S could be determined using the non-linear regression model depicted in Eq. 8. Overall, for the vast majority of compounds, residuals showed no heteroscedastic variance and appeared to be normally distributed by both visual assessments using QQ-plots as well as statistical evaluation using the Shapiro-Wilk test (p-value > 0.05). This shows that Eq. 8 confirms the model assumptions.

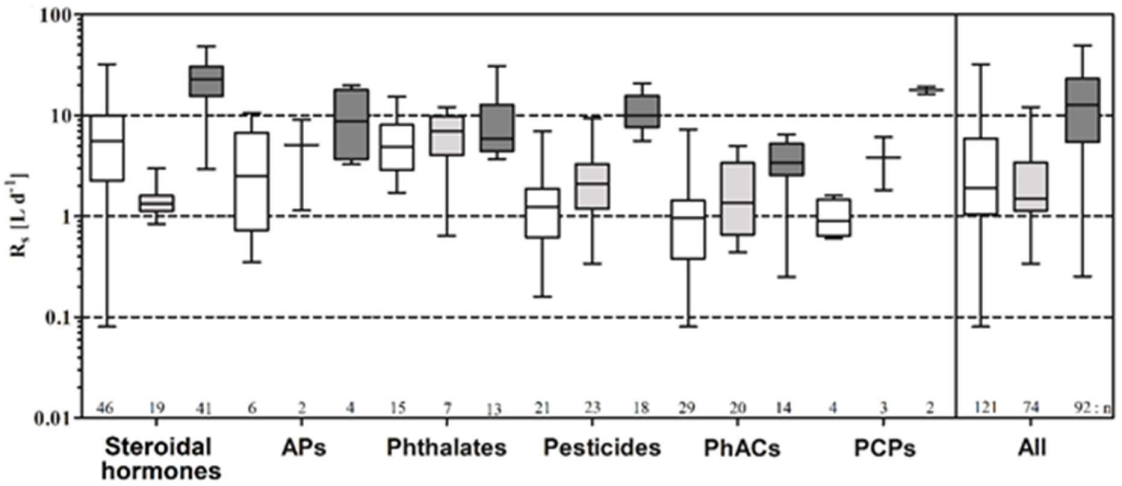

Figure 17. Overview of the sampling rates (R_S, L d^{-1}) for the steroidal hormones, (alkyl)phenols (Aps), phthalates, pharmaceuticals (PhACs), personal care products (PCPs) and pesticides on Speedisks (white), STEPS (light grey) and freely dispersed sorbent (dark grey). Horizontal black lines represent the median values, boxes represent the 25-75% quartiles, and the whiskers indicate minimum and maximum values. N represents the number of compounds included in the boxplots.

The R_S and associated standard deviations are summarized per compound class in Figure 17 and can be consulted in Annex 11. As can be seen on the right side of Figure 17, the R_S on Speedisks ranged from 0.08 to 32 L d^{-1} with a median value of 1.9 L d^{-1}. The R_S on STEPS ranged from 0.3 to 12 L d^{-1} with a median value of 1.5 L d^{-1}, whereas the R_S on freely dispersed sorbent had a median of 13 L d^{-1} and ranged from 0.3 to 49 L d^{-1}. Comparison between the STEPS and freely dispersed sorbent allows to pinpoint the effect of the nylon mesh on compound uptake. All compound classes showed significantly lower sampling rates (p-value < 0.05) when enclosing the h-DVB sorbent in a nylon mesh, aside from the phthalates for which no significant differences could be observed (Figure 17). The variation in the multi-stage mass transport of compounds from the bulk water to the sorbent phase most likely lies at the origin of these results. For the freely dispersed sorbent, mass transfer is only hindered by the formation of a water boundary layer at the surface of the sorbent particles. This in contrast to the STEPS where the nylon mesh presents an additional diffusive barrier prone to the formation of a second water boundary layer at its surface. This results in an increase in the overall mass transfer resistance, implying a decrease in the mass flux and thus sampling rate.

Experimental determination of uptake rates of rather polar organic compounds on STEPS or Speedisk passive samplers is difficult and literature data are very scarce. The sampling rates of 59 target compounds attained on Speedisk and STEPS in this study were compared with results of previous studies focusing on Oasis HLB sorbent enclosed in the POCIS passive sampler design (Figure 18). On average, uptake rates measured in our static exposure batch set-up are a factor of 9 and 13 higher for STEPS and Speedisk, respectively, than those reported in literature for POCIS.

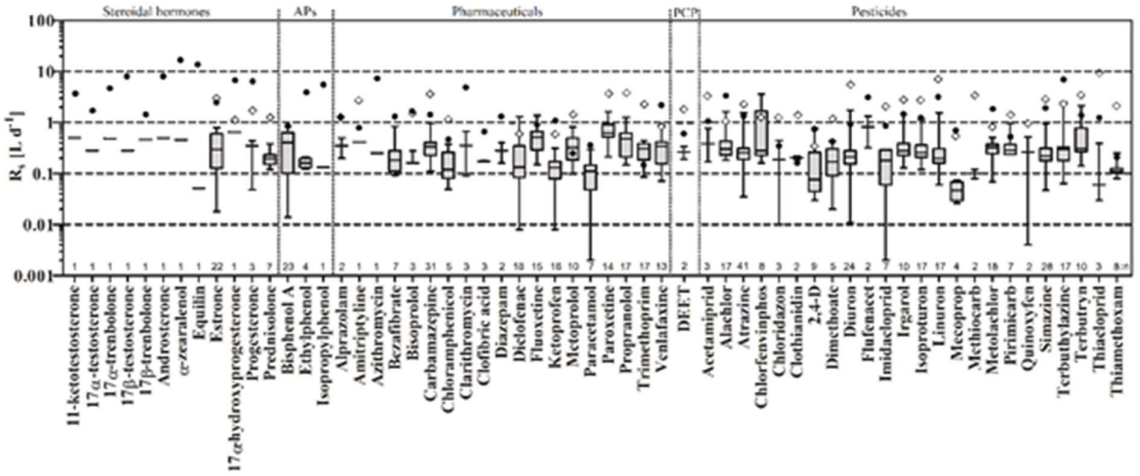

Figure 18. Comparison of STEPS (white diamonds) and Speedisk (black circles) sampling rates with sampling rates reported for POCIS passive samplers in literature. Horizontal black lines represent the median values, boxes represent the 25-75% quartiles, and the whiskers indicate minimum and maximum values. N represents the number of compounds included in the boxplots.

Based on an approach where Speedisk data are linked with data obtained from parallel exposed silicone rubbers in freshwater environment, Hamers et al. (2018) reported uptake rates for about 15

compounds up to 0.7 L d^{-1}. Direct comparison of STEPS sampling rates with previous studies is not possible as studies working with a nylon mesh and h-DVB sorbent as a receiving phase have not been reported yet. However, sampling rates on POCIS, in which PES membranes were replaced by nylon membranes (Belles et al., 2014; Morrison and Belden, 2016), are still up to a factor of 19 lower than those obtained here on STEPS. These observations of high sampling rates on the developed passive samplers suggest a short linear accumulation phase and hint at the importance of the equilibrium stage for the application in the real environment.

4.2.3. Equilibrium partitioning coefficients.

The calculated Log K_{sw} are listed in Annex 11. For Speedisk and STEPS, the Log K_{sw} ranged from 3.09 to 4.78 L kg^{-1} and from 4.14 to 6.51 L kg^{-1}, respectively. The latter is well within the range obtained with freely dispersed sorbent, ranging from Log K_{sw} 4.26 to 6.96 L kg^{-1} (Annex 11). No significant sorption was noticed on the Speedisk membrane and STEPS nylon mesh, thus indicating that only the h-DVB sorbent itself is responsible for the CEC-uptake. This is a clear advantage compared to POCIS, where the diffusion limiting PES membrane can act as a second receiving sorption phase and as such greatly influence the calculated partitioning coefficients (Vermeirssen et al. 2012). To the best of the author's knowledge, only one study of Jeong et al. (2017) determined the sorption of 28 organic compounds to freely dispersed SPE sorbent (*i.e.* Oasis HLB) in a static exposure design. The Log K_{sw}-values of specific compounds obtained in the NewSTHEPS project, *i.e.* metoprolol (5.65), isoproturon (6.44), flufenacet (6.16), diuron (6.81), atrazine (6.33), and terbutryn (6.42) are comparable or slightly higher (Log -difference ranged between 0.41 and 1.55 Log unit), than those reported by Jeong et al. (2017) (5.15; 6.03; 5.23; 5.26; 5.29; and 5.39, respectively). These data suggest that the investigated polar compounds (Log $K_{ow} < 4$) have a slightly higher sorption tendency to h-DVB as compared to the Oasis HLB sorbent. This agrees with the functional characterization data, which demonstrated that h-DVB comprises of more divinylbenzene groups (Section 4.2.1) and has hydrophilic moieties with a higher polarity as Oasis HLB, *i.e.* carboxyl [-COOH] as opposed to N-vinylpyrrolidone groups.

In line with the ever-increasing number of chemicals that is released into the environment, several passive sampling-based studies have attempted to mathematically model Log K_{sw} using various physicochemical properties of the compounds under investigation as input (Lohmann et al., 2012; Choi et al., 2013; Liu et al., 2017; Smedes et al., 2009). Up until now, Log K_{ow} and molecular weight (MW) have been correlated frequently to the Log K_{sw} ($R^2 = 0.92$, n = 65) (Lohmann et al., 2012; Choi et al., 2013; Smedes et al., 2009) for more non-polar compounds (Log $K_{ow} > 4$). However, using our dataset, lack-of-fit (p-value < 0.05) between Log K_{ow} or MW and Log K_{sw} was observed. Smedes (2018) observed similar findings for the PAHs, polychlorinated biphenyls (PCBs) and phthalates. Therefore, we evaluated the modelling potential of a number of other physicochemical properties; including V_x (molecular volume), qA^- (most negative charge on O, N, S, X atoms), H_y (hydrophilic factor), vapor pressure, bioconcentration factor, number of carbon atoms, pK_a, water solubility and polar surface area. No valid model ($R^2_{adj} = 0.36$, n = 92) was however obtained for predicting Log K_{sw}

with any of the above-mentioned parameters or combinations thereof using the dataset. Additionally, it should be highlighted that no quantitative effect of type and number of functional groups on the K_{sw} was observed (see Figure 19). The above-mentioned results lead to conclude that the partitioning of analytes towards h-DVB seems to be compound-specific and warrants individual experimental determination.

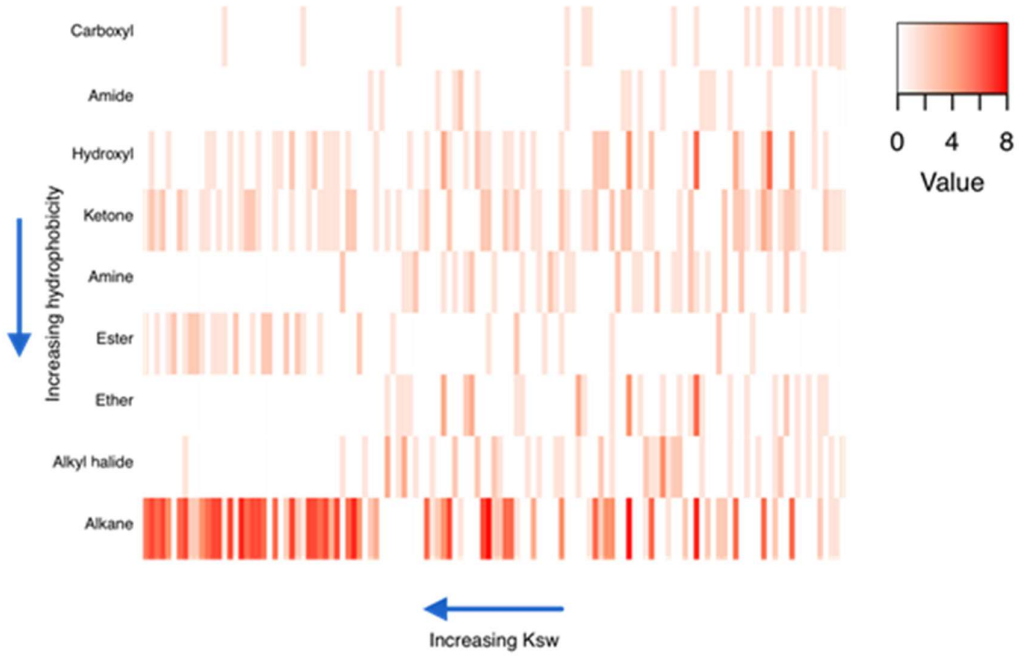

Figure 19. Chart depicting the effect of type (y-axis) and number of functional groups (colour intensity) on K_{sw} (x-axis) based on the complete dataset obtained with freely dispersed h-DVB.

The effect of increasing dissolved organic contaminant concentrations on the partitioning process was shown to be minimal as for the majority of the CECs the sorption process was linear up to 70 ng L^{-1} which is in the same order of magnitude than seawater concentrations measured in the BPNS (Section 4.3.2, 4.3.3 and 4.3.4). Dissolved concentrations exceeding the linear ranges of the isotherms resulted in higher K_{sw} for the steroidal hormones and lower K_{sw} for the other compound classes. The latter indicates that partitioning of these groups of organic compounds depends merely on the available h-DVB sorption sites.

The effect of environmental parameters on K_{sw} was investigated in a cost-effective manner using response surface modelling and Box-Behnken experimental designs. Here, temperature dependency of the partitioning process was confirmed (Log = 0.78 over 12° C units), while pH (Log = 0.15 over 3 pH units) and salinity (Log = 0.35 over 35 psu) had less pronounced effects on partitioning. More details can be found in Huysman (2019) and Vanryckeghem (2020).

4.3. Field results of monitoring campaigns.

4.3.1. Trace metals.

4.3.1.1. Trace metals in the dissolved fraction.

4.3.1.1.1. Total dissolved trace metals.

The range of dissolved trace metal concentrations investigated in our study is presented in Table IV.

Table IV. Seasonal and spatial variation of dissolved trace metal concentrations in the BCZ water column compared to EQS and BRC values (EU, 2008; Maycock et al., 2011).

Element	Station	min.–max. (μg L^{-1})	Average (μg L^{-1})	Median (μg L^{-1})	EQS[a] dissolved		BRCs[a] dissolved
					YA[a]	MAC[a]	
Cd	HO-1	0.08–0.19	0.11	0.09	0.2	0.45	0.004–0.009
	HO-2	0.09–0.16	0.11	0.10			
	HZ-2	0.10–0.15	0.11	0.11			
	HZ-1	0.10–0.14	0.12	0.12			
	OZ-MOW1	0.09–0.19	0.13	0.12			
Pb	HO-1	0.08–0.54	0.28	0.26	1.3	14	0.033
	HO-2	0.04–0.15	0.09	0.09			
	HZ-2	<0.011–0.015	0.01	0.01			
	HZ-1	<0.011–0.13	0.04	0.02			
	OZ-MOW1	0.02–0.53	0.19	0.10			
Co	HO-1	0.10–0.40	0.26	0.26	–	19	0.0035
	HO-2	0.06–0.29	0.17	0.16			
	HZ-2	0.05–0.13	0.09	0.09			
	HZ-1	0.06–0.13	0.09	0.09			
	OZ-MOW1	0.03–0.14	0.07	0.06			
Ni	HO-1	0.27–2.83	1.78	2.01	8.6	34	0.140
	HO-2	0.62–1.91	1.20	1.13			
	HZ-2	0.49–0.61	0.54	0.53			
	HZ-1	0.61–0.63	0.62	0.63			
	OZ-MOW1	0.61–1.01	0.77	0.73			
Cu	HO-1	1.40–2.18	1.64	1.49	–	10	0.070
	HO-2	0.67–1.04	0.88	0.90			
	HZ-2	0.60–1.60	0.87	0.65			
	HZ-1	0.44–1.02	0.83	0.94			
	OZ-MOW1	0.32–10.1	2.99	0.79			

[a] Environmental Quality Standard (EQS); yearly average (YA); maximum acceptable concentration (MAC); background/reference concentrations (BRCs).

Highest concentrations (average) of Pb, Co and Ni are recorded at HO-1 while those of Cd and Cu at OZ-MOW1. The two stations of Zeebrugge harbour show similar concentration ranges for all elements, while this is not the case for Ostend harbour. Higher Co and Ni concentrations are observed in Springtime than in Autumn at stations HO-1 and HO-2. At HZ-1, HZ-2 and OZ-MOW1, no particular trend is recorded over the year whatever the metal considered (for the graphs over time, see the Supplementary Information). Regarding dissolved Pb, higher concentrations are observed for the stations HZ-1 and OZ-MOW1 in October 2017, while they are more or less constant at the other stations for the rest of the year. At station HO-1 higher dissolved Pb concentrations occurred in October 2018 (see SI).

Regarding total dissolved levels in the BPNS, our results display a metal contamination which is higher than in the 80's for Cu and Cd, and in the same range for Pb (Baeyens et al., 1987). Total dissolved concentrations measured in our study are also higher than in 2010 for Cd and Cu, while the concentration levels are in the same range for Pb. This is in accordance with observations made by Gao et al. (2013) of increasing dissolved concentrations of trace metals in the BPNS and the Scheldt Estuary.

4.3.1.1.2. Labile trace metals.

Labile metal concentrations are presented in Table V. On average, highest labile concentrations are observed at the station OZ-MOW1 for all elements, except for Cu the average concentration of which is higher at HZ-2 reaching 0.41 µg L^{-1}. Labile trace metal concentrations at the harbour stations do not differ significantly (except Cu at HZ-2). Temporal trends are observed for Cd and Cu (see SI): for Cu, the concentrations are higher in Autumn at stations HZ-2 and HO-1 (respectively, 0.6 and 0.4 µg L^{-1} in Autumn, 0.2 and 0.1 µg L^{-1} in Spring), while for Cd it is the opposite (respectively, 0.012 and 0.010 µg L^{-1} in Autumn, 0.023 and 0.026 µg L^{-1} in Spring).

Table V. Seasonal and spatial variations of labile trace metal concentrations in the BCZ water column.

Element	Station	min.-max. (µg L^{-1})	Average (µg L^{-1})	Median (µg L^{-1})
Cd	HO-1	0.005–0.037	0.018	0.015
	HO-2	0.003–0.049	0.021	0.017
	HZ-2	0.010–0.028	0.018	0.016
	HZ-1	0.014–0.036	0.022	0.018
	OZ-MOW1[a]	0.027 - 0.029	0.028	0.028
Pb	HO-1	0.015–0.024	0.019	0.018
	HO-2	0.014–0.024	0.017	0.015
	HZ-2	<0.011–0.020	0.014	0.014
	HZ-1	0.019–0.024	0.021	0.021
	OZ-MOW1[a]	0.017–0.234	0.126	0.126
Co	HO-1	0.055–0.087	0.071	0.071
	HO-2	0.053–0.081	0.065	0.063
	HZ-2	0.045–0.100	0.067	0.062
	HZ-1	0.018–0.112	0.061	0.057
	OZ-MOW1[a]	0.028 - 0.221	0.125	0.125
Ni	HO-1	0.43–0.59	0.49	0.47
	HO-2	0.35–0.55	0.42	0.39
	HZ-2	0.27–0.45	0.36	0.35
	HZ-1	0.25–0.45	0.37	0.40
	OZ-MOW1[a]	0.40 - 0.64	0.52	0.52
Cu	HO-1	0.10–0.46	0.25	0.22
	HO-2	0.10–0.28	0.17	0.16
	HZ-2	0.21–0.60	0.41	0.42
	HZ-1	0.17–0.28	0.22	0.21
	OZ-MOW1[a]	0.09 - 0.26	0.17	0.17

[a] For OZ-MOW1, only the samples from April and October 2017 are taken into account.

No labile reference value exists yet. Moreover, no labile trace metal was previously measured using DGT in the BPNS. However, our labile Cd results are in the same order of magnitude as those measured in Mediterranean and Black Sea coastal areas (Schintu et al., 2008; Slaveykova et al., 2009), while labile Cu, Ni and Pb show higher values in the BPNS.

4.3.1.2. Trace metals in the particulate fraction.

Particulate trace metal values have been normalized to those of aluminium, as this element is a major component of fine-grained aluminosilicates and commonly used as a reference element when studying metal contents in marine SPM (Dehairs et al., 1989; Regnier and Wollast, 1993). This geochemical normalization balances the mineralogical and the natural granular variability of trace metal contents

in SPM (Loring, 1991). The range of particulate normalized ($x10^4$) concentrations is presented in Table VI. For information purposes only, the non-normalized values are given in the SI.

These broad ranges highlight spatially and temporally concentration differences. For particulate Cd, all stations follow the same trend: the concentrations increase from 2017 to 2018 (+ 0.2 offshore and +1.5 in the harbours), and values are higher for Ostend harbour stations. For the other elements, the temporal trends seem to be station and element dependent. Particulate Co concentrations remain steady over the whole year and at all stations, with average values of 2. SPM is most enriched in Cd, Cu, Ni, Pb, and Co at station HO-1 (Table VI), despite its low amount. Station OZ-MOW1 is situated further away from the coastline but is the second most contaminated in particulate trace metals: higher levels for Cd and Pb are only observed at station HO-2. Conversely, Zeebrugge harbour stations (HZ-1 and HZ-2) show the lowest values for all elements.

Table VI. Seasonal and spatial variations of particulate trace metal concentrations in the BCZ water column, normalized to Al $\times 10^4$.

Element	Station	min. - max.	Average	Median
Cd	HO-1	0.1–2.4	0.9	0.6
	HO-2	0.1–2.5	0.9	0.5
	HZ-2	0.2–2	0.7	0.3
	HZ-1	0.1–1.1	0.5	0.3
	OZ-MOW1	0.1–0.3	0.1	0.1
Pb	HO-1	11–217	66	18
	HO-2	6–17	10	9
	HZ-2	4–8	6	6
	HZ-1	4–8	6	6
	OZ-MOW1	4–12	7	5
Co	HO-1	2–3	2	2
	HO-2	1–2	2	2
	HZ-2	1–2	2	2
	HZ-1	1–2	2	2
	OZ-MOW1	2–3	2	2
Ni	HO-1	4–35	16	12
	HO-2	0.3–6	3	3
	HZ-2	<0.2–5	3	4
	HZ-1	2–13	6	4
	OZ-MOW1	4–15	8	6
Cu	HO-1	15–56	35	34
	HO-2	6–16	10	9
	HZ-2	10–15	13	12
	HZ-1	4–12	8	9
	OZ-MOW1	2–67	19	4

Particulate concentrations measured for Ni are above the EQS value of 4.3 mg kg^{-1}, except for stations HO-2 and HZ-2. The particulate concentrations of Cd, Cu and Pb are all above the Background/Reference Concentrations (BRCs; measured in the Earth's crust; Ronov et al., 1991) and those of Co and Ni are all below the BRCs, except for particulate Ni at HO-1.

In order to indicate if the particulate metals in the BCZ highly exceed the concentrations naturally found in the Earth's crust (i.e. to link the concentrations of particulate trace metals to the actual contamination level of SPM), an enrichment factor (EF) of suspended particles was calculated for each element, as follows (Eq. 20):

$$EF(Me) = \left(\frac{Me}{Al}\right)_{sample} \Big/ \left(\frac{Me}{Al}\right)_{background}$$

Eq. 20

where *EF* is the enrichment factor, Me/Al is the ratio of the particulate metal and Al concentration; the extension sample or background (natural median levels in earth's crust) are identifiers. EF values are ranked into five categories ranging from low (EF < 2) to high enrichment (EF > 40) (Barbieri, 2016) and are given in SI. Overall, SPM shows a wide range of enrichment for all trace metals and at all stations. EF values of Co and Ni are ≤ 2, which is equivalent to a minimal enrichment. The same is true for Cu, at the Zeebrugge harbour stations and HO-2. Moderate enrichments are observed for Cu (HO-1 and OZ-MOW1), and Pb (Zeebrugge harbour stations and OZ-MOW1). Finally, very high enrichments are observed for particulate Pb (Ostend harbour stations) and Cd (all stations). Regardless of the element, the highest enrichment is always at station HO-1, while the lowest ones are at HZ-1 for Pb and Cu, at HZ-2 for Ni and Co and at OZ-MOW1 for Cd. In average, particulate Cd displays the highest EF values.

4.3.1.3. Partitioning of trace metals between the solid and the liquid phases.

Three trace metal pools in seawater have been considered: dissolved labile metal, dissolved non-labile metal and particulate metals (Figure 20). Average values over one-year sampling at each station were used. Three metals show a clear pattern: for Cd, the dissolved non-labile fraction seems to be dominant while for Pb and Co (except at HO-1), the particulate one is dominant. For the other metals, there is no clear pattern: for Ni, the dissolved non-labile fraction seems to be more important at Ostend harbour, while the labile one dominates at Zeebrugge harbour and the particulate fraction is higher at the marine station OZ-MOW1. For Cu, the particulate fraction is dominant at OZ-MOW1, the dissolved non-labile fraction is slightly higher than the particulate one at Ostend harbour and HZ-1, while the three fractions are more or less equilibrated at station HZ-2. The concentrations of the three pools in the water column (dissolved labile, dissolved non-labile and particulate - Figure 20) were compared to other studies: in the BCZ, dissolved non-labile Cd is the largest pool of the total Cd content while particulate Pb dominates the total Pb content, as in the Northern Adriatic Sea (Illuminati et al., 2019) or as shown in a previous study on the BCZ and along the Scheldt Estuary (Baeyens et al., 1987). Cu content is dominated by the dissolved fraction as shown by Baeyens et al. (1987) and Illuminati et al. (2019) (except at OZ-MOW1 were the particulate fraction is dominant), but does not account for 100% of the total Cu content, opposite to observations in the Northern Adriatic Sea (Illuminati et al., 2019).

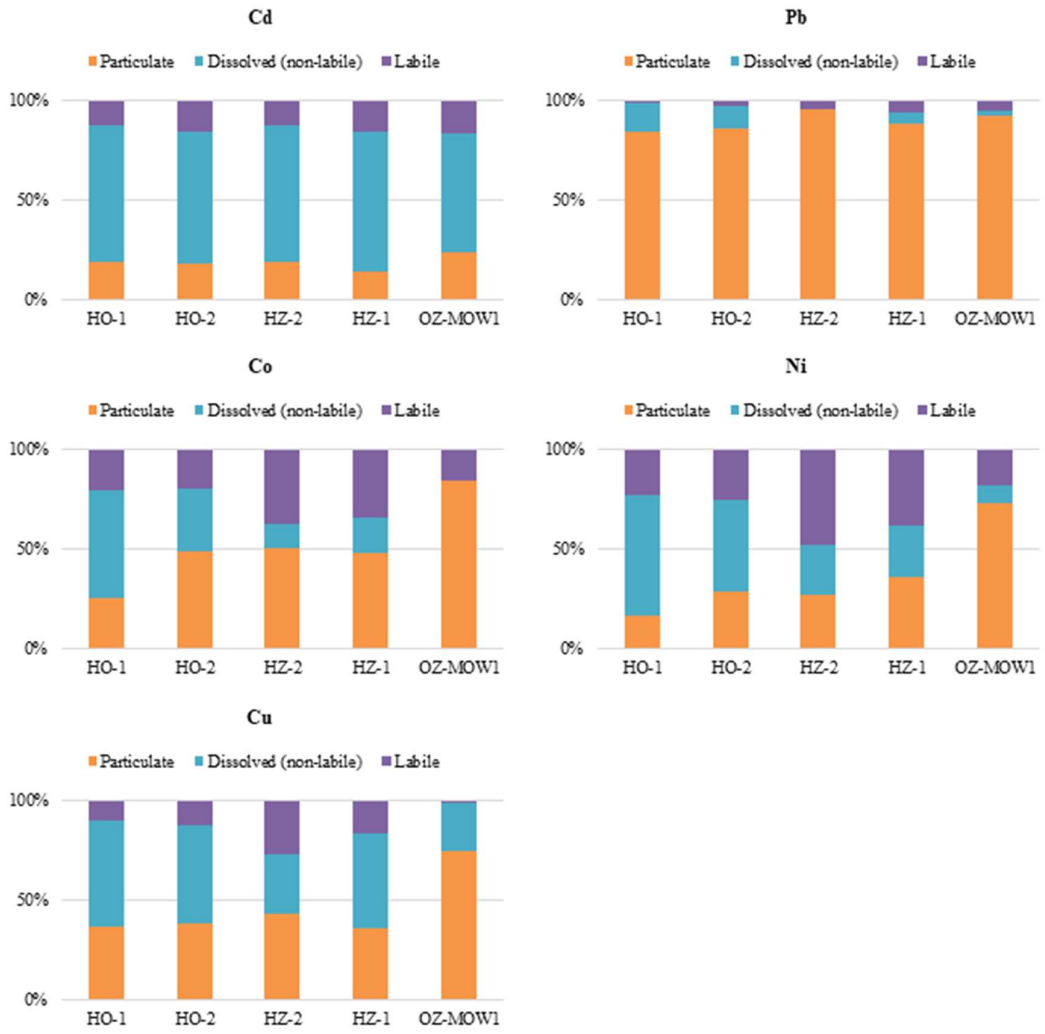

Figure 20. Trace metal distribution between particulate, dissolved and labile forms, in the BCZ water column.

Moreover, the ratio of labile to total dissolved concentrations was determined for each element according to the following formula (Eq. 21):

$$\text{Lability} = \frac{[\text{TM}]_{\text{labile}}}{[\text{TM}]_{\text{dissolved}}} \times 100$$

Eq. 21

Where [TM] is the trace metal concentration, either for the labile fraction or for the total dissolved amount (both in mg L^{-1}). The results are presented in Figure 21.

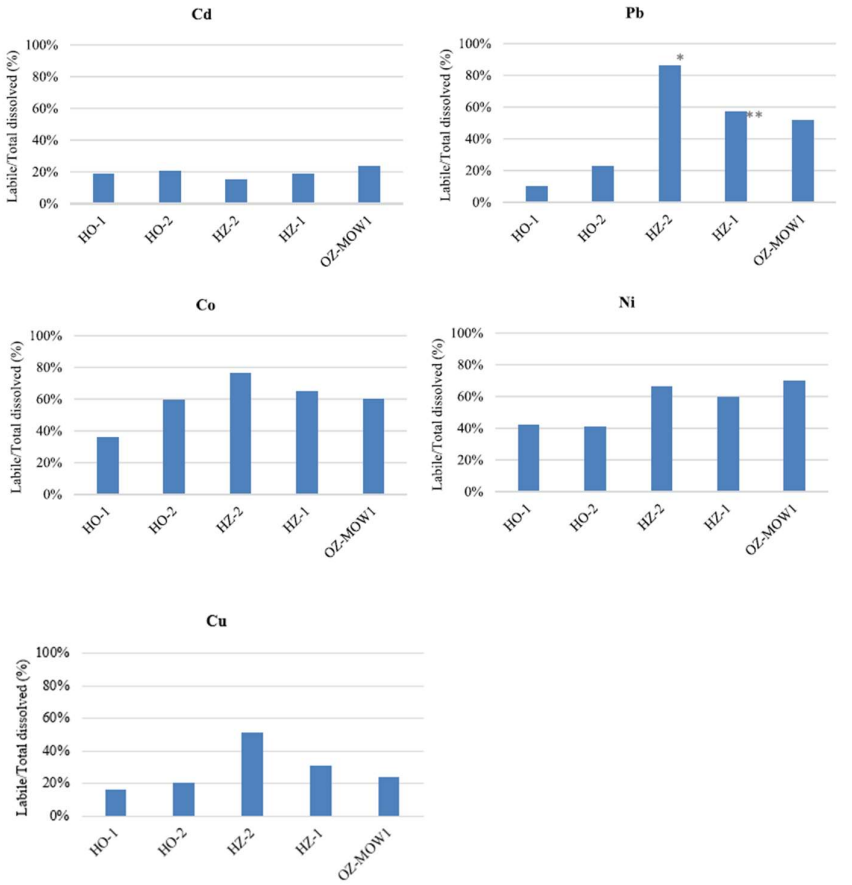

*for total dissolved and therefore labile Pb at HZ-2, 3 values out of 4 were below the LOD. The bar chart only represents the ratio measured in October 2017.
** for total dissolved and therefore labile Pb at HZ-1, 2 values out of 4 were below the LOD. The bar chart represents the average of the ratios measured in October 2017 and March 2018.

Figure 21. Trace metal lability, in the BCZ water column. The lability ratios result from an average of all the measurements.

The higher the labile fraction, the more the metal is bioavailable and the greater the risk for the marine ecosystem (Baeyens et al., 2018; Simpson et al., 2012). Based on Figure 21, the lability of Cd varies from 15 to 24%, showing the lowest lability values of all elements. Annual averages are similar at all stations, except that a slightly higher lability is observed at station OZ-MOW1. The maximum lability is observed in Springtime for Cd. The lability of Pb varies between 10 to 52% (the largest range of all metals), with the highest value observed at the marine station OZ-MOW1 and the lowest at HO-1. Cobalt displays the highest lability with values varying from 36 (HO-1) to 76% (HZ-2). The lability of Ni fluctuates from 41 to 70%, station HO-2 showing the minimum value and OZ-MOW1 the maximum one. Labile Cu varies from 16 to 52%. The highest average value for Cu is observed at station HZ-2 and the lowest at HO-1.

In the BCZ, Cd complexes are highly stable, while complexes of Co and Ni are mainly labile. The harbour station HO-1 shows the lowest lability for Pb, Co and Cu at their highest dissolved and particulate concentrations (i.e. the highest contamination level). On the other hand, Cd, Pb and Ni

form the weakest complexes at the marine station OZ-MOW1, while Co and Cu form the weakest ones at the harbour station HZ-2. A marina with a yacht refit and repair facility is located nearby station HZ-2. This infrastructure is used to take small boats out of the water and repair or restore them, using different kind of coatings and paints like copper-based antifouling paints. The latter could explain high labile Cu concentrations measured at this station.

Labile and total dissolved concentrations do not correlate well. Moreover, it seems that when dissolved Co and Ni concentrations are lower, the labile fraction is higher and vice versa. Considering the ratio of labile-total dissolved concentrations at each station, different rankings can be observed:

HO-1: Ni>Co>Cd>Cu>Pb

HO-2: Co>Ni>Pb>Cd>Cu

HZ-1: Co>Ni>(Pb>) Cu>Cd

HZ-2: (Pb>) Co>Ni>Cu >Cd

OZ-MOW1: Ni>Co>Pb>Cd=Cu

The ratio varies between stations, but both stations located in Zeebrugge harbour show the same ranking of metal lability, highlighting again similarities between these two stations. Considering all stations, Co and Ni show the highest lability capacity, indicating that their complexes are more labile than for the other elements. There is no clear trend for Pb, Cu and Cd, but they have a tendency to form complexes with lower lability. These lability ratios in the BCZ reflect less lability for Cd complexes than those recently measured by voltammetry in the Northern Adriatic Sea, while ratios for Cu and Pb are in the same range as those in the BCZ (Illuminati et al., 2019).

To estimate the affinity of each trace metal for the particulate phase, the partition coefficients K_D were calculated according to Eq. 22:

$$K_D = \frac{[TM]_{particulate}}{[TM]_{dissolved}} \qquad \text{Eq. 22}$$

Where [TM] is the total trace metal concentrations, either in its dissolved (in mg kg^{-1} water) or particulate phase (in mg kg^{-1} suspended matter). The logarithm of K_D is presented in Table VII.

Table VII. Partition coefficient K_D of trace metals observed in the BPNS water column over one year.

Element	Station	min. - max. *Log Kd*	Average *Log Kd*
Cd	HO-1	2.8 - 4.3	3.8
	HO-2	2.7 - 4.1	3.5
	HZ-2	2.8 - 4.2	3.6
	HZ-1	2.8 - 4.0	3.4
	OZ-MOW1	3.1 - 3.9	3.5
Pb	HO-1	5.0 - 5.5	5.2
	HO-2	4.7 - 5.4	5.0
	HZ-2	5.4 - 6.0	5.7
	HZ-1	4.6 – 5.9	5.4
	OZ-MOW1	4.7 - 5.9	5.2
Co	HO-1	3.9 - 4.3	4.1
	HO-2	3.5 - 4.4	4.0
	HZ-2	3.8 - 4.7	4.3
	HZ-1	4.1 - 4.6	4.3
	OZ-MOW1	4.6 - 5.3	4.9
Ni	HO-1	3.5 - 4.7	4.0
	HO-2	<2.4 - 4.2	3.5
	HZ-2	<2.5 - 4.2	4.0
	HZ-1	3.5 - 4.4	3.8
	OZ-MOW1	4.3 - 4.6	4.4
Cu	HO-1	4.1 - 4.6	4.4
	HO-2	3.7 - 4.3	3.9
	HZ-2	3.8 - 4.6	4.2
	HZ-1	3.4 - 4.5	4.0
	OZ-MOW1	4.0 - 4.4	4.2

Log $K_{D,Cd}$ and log K_D^{Co} respectively vary from 2.7 to 4.3 and from 3.5 to 5.3. Cd and Co have the largest K_D ranges, compared to the other elements. Log K_D^{Pb} varies from 4.6 to 6.0 and has, compared to the other elements, the highest K_D values. Log K_D^{Ni} fluctuates from < 2.4 to 4.7, with the maximum value at station HO-1. Looking at the annual average values, the differences between stations are small, except for Pb at HZ-2 and Co at OZ-MOW1 (see SI).

While total dissolved trace metals were not correlated to their labile fraction, more similarities are found with their particulate fraction. This highlights that high dissolved or particulate trace metal concentrations do not necessarily imply high labile concentrations. As for the dissolved fraction, our results exhibit an important particulate trace metal contamination, especially for Cd.

K_D values reveal the affinity of a trace metal for either the particulate or the dissolved phase in the water column and vary depending on the element, the season and the location. Overall, our K_D^{Cd} values are slightly lower than those reported in other studies in the BCZ (Baeyens, 1998; Parmentier, 2003; Valenta et al., 1986), revealing less affinity for Cd for the particulate phase than during the

last decades. For the other elements, their K_D's are within the range reported in other studies (Baeyens, 1998; Parmentier, 2003; Valenta et al., 1986). All trace metals, except Cd, show higher solubility at HO-2 than at other stations. In general, log K_D is highest for Pb, followed by Co, Cu, Ni and Cd:

$$\text{HO-1: } K_D^{Pb} > K_D^{Cu} > K_D^{Co} > K_D^{Ni} > K_D^{Cd}$$

$$\text{HO-2: } K_D^{Pb} > K_D^{Co} > K_D^{Cu} > K_D^{Cd} > K_D^{Ni}$$

$$\text{HZ-1: } K_D^{Pb} > K_D^{Co} > K_D^{Cu} > K_D^{Ni} > K_D^{Cd}$$

$$\text{HZ-2: } K_D^{Pb} > K_D^{Co} > K_D^{Cu} > K_D^{Cd} = K_D^{Ni}$$

$$\text{OZ-MOW1: } K_D^{Pb} > K_D^{Co} > K_D^{Ni} > K_D^{Cu} > K_D^{Cd}$$

These rankings are in good agreement with results obtained at the mouth of the Scheldt estuary (Baeyens, 1998 - Pb>Zn>Cu>Cd). The high K_D^{Pb} values are also in agreement with observations made by Valenta et al. (1986), Baeyens (1998) and Parmentier (2003) in the BCZ. Stations from Zeebrugge harbour and HO-2 show similar rankings of partition coefficients.

4.3.2. Estrogenic activity analysis using o-DGT coupled with ERE-CALUX bioassay.

At the Belgian Ostend Harbour and in the North Sea, triplicate of o-DGT samplers were deployed for 2 weeks, and for each site 1 L water samples were collected by grab sampling at 0 h and 14 days to prepare the mixed water sample. The water temperature was 12.6-15.9℃ at HO-1 in the Belgian Ostend Harbour, and 15.8-16.6℃ at station MOW1 in the North Sea. All DGT experiments were carried out at triplicate and the results were expressed as the mean ± standard deviation. Statistical analysis was performed with GraphPad Prism 7.0 software. Analysis of variance (ANOVA) was performed to detect results that were significantly different at a level of $\alpha = 0.05$. The DGT samplers are different from many other passive sampling techniques in that transport inside the sampler (filter and hydrogel) is diffusion-controlled. However, outside the DGT a zone exists where transport is also limited by molecular diffusion (the DBL) but the thickness of this zone, in contrast to those of filter and hydrogel, is not so well-defined. The DBL is a thin layer of viscous fluid close to a solid surface in contact with a moving stream in which the velocity varies from zero at the surface up to the boundary that corresponds to the free stream velocity (Guo et al., 2017).

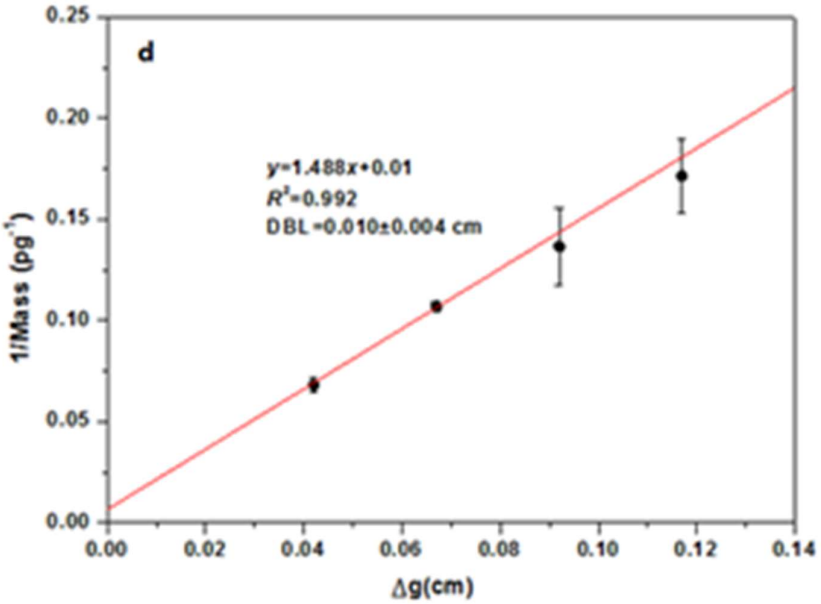

Figure 22. DGT deployments in HO-1. A plot is made of 1/mass of E2 on XAD18 resin gel (in pg^{-1}) versus the diffusive layer thickness (Δg, cm). The DBL is the thickness of the diffusive boundary layer obtained under laboratory conditions and during field sampling and is derived from the slope and intercept of the plot of 1/M versus Δg (see Guo et al., 2019 for the detailed equation and calculation).

In the field, mean DBL values of 0.010 cm were obtained at HO-1 (Figure 22). Therefore, ignoring the DBL thickness in our study would underestimate the estrogenic activities by ≈10%. In general, results from the mixed sea water samples (grab sampling) and results from the o-DGT samples correspond well (Figure 22) with no statistically significant difference (ANOVA, $p > 0.05$). Low estrogenic activities were observed at HO-1 with the value of 0.05 ± 0.01 ng E2-equivalents L^{-1} and at MOW1 with the value of 0.08 ± 0.003 ng E2-equivalents L^{-1}. These values seem to correspond well with the results obtained for targeted steroidal EDCs by active and passive sampling (below 10 ng L-1, at all stations; see 4.3.4).

4.3.3. Analysis of pharmaceuticals, personal care products and pesticides.

Out of the 89 investigated target compounds, 63 compounds with representatives of each investigated class were measured at least once in the BPNS using grab or passive sampling, at concentrations between 0.01 and 680 ng L^{-1}. A good precision - exemplified by low relative standard deviations (RSD; average < 30%) on triplicate samples - was achieved for both passive samplers and grab samples, demonstrating the applicability of both methods.

4.3.3.1. Pharmaceuticals.

A total of thirty-two PhACs were detected at least once in the BPNS using the grab or passive sampling approach. A large difference among PhACs was noticed as concentrations ranged from 0.01 up to 370 ng L^{-1}, with around 20% of the measured values above 10 ng L^{-1} (Table VIII). The most detected compound was venlafaxine with a detection frequency (DF) of 100% and median concentration of 5.5 ng L^{-1}, which can be related to its widespread use as antidepressant in *e.g.*

nursing homes (Annemans et al., 2014; Bourgeois et al., 2012). The anti-epilepticum carbamazepine was detected in most of the samples (DF > 90%) at concentrations varying from 1.4 to 54 ng L^{-1}. The β-blockers were, on average, the most frequently detected group of pharmaceuticals with atenolol (0.7 - 76 ng L^{-1}), bisoprolol (0.07 - 73 ng L^{-1}), metoprolol (0.2 - 34 ng L^{-1}), propranolol (0.1 - 19 ng L^{-1}) and sotalol (0.4 - 156 ng L^{-1}) detected in 54%, 94%, 98%, 73% and 54% of the samples. With respect to the antibiotics, the sulfonamide antibiotics sulfamethoxazole (0.7 - 35 ng L^{-1}) and trimethoprim (0.06 - 7 ng L^{-1}) were most prevailing, in line with their commonly combined use as the antibiotic co-trimoxazole (Wormser et al., 1982).

Table VIII. Overview of PhACs concentrations in the BPNS, divided per subclass (concentrations in ng L^{-1}).

Subclass	Location	min.-max.	Average	Median
Analgesic	OZ_MOW1	1.2 – 22.8	7.6	5.4
	HZ	2.9 – 119.8	23.7	25.6
	HO	2.5 – 39.2	12.5	13.4
	OO	5.6 – 22.3	13.1	9.8
Alkylating agent	OZ_MOW1	-	-	-
	HZ	-	-	-
	HO	0.3 – 0.4	0.3	0.3
	OO	-	-	-
Antidepressant	OZ_MOW1	1.3 – 11.8	3.9	2.3
	HZ	0.1 – 8.4	4.1	2.8
	HO	0.0 – 40.6	11.1	5.4
	OO	1.1 – 6.4	2.6	2.5
Anti-epilepticum	OZ_MOW1	2.3 – 12.2	6.8	6.8
	HZ	1.4 – 16.7	8.1	4.5
	HO	3.0 – 54.4	20.5	15.8
	OO	2.0 – 17.5	6.4	5.4
Anti(retro)viral	OZ_MOW1	0.4 – 13.7	3.9	2.8
	HZ	0.0 – 9.1	2.7	2.0
	HO	0.1 – 6.5	2.1	3.0
	OO	0.3 – 370.2	35.6	33.7
β-blocker	OZ_MOW1	0.3 – 16.7	2.9	1.6
	HZ	0.1 – 66.8	5.6	12.3
	HO	0.7 – 155.9	23.9	22.0
	OO	0.1 – 34.2	3.0	2.7
Lipid regulator	OZ_MOW1	0.7 – 23.7	7.6	5.6
	HZ	0.7 – 14.0	4.7	1.2
	HO	0.5 – 8.7	4.7	4.3
	OO	0.6 – 12.8	5.1	4.3
NSAIDs	OZ_MOW1	5.2 – 37.2	17.4	12.3
	HZ	0.1 – 53.7	16.5	15.5
	HO	0.8 – 103.6	35.8	23.8
	OO	-	24.1	24.1
Tranquilizer	OZ_MOW1	0.1 – 0.1	0.1	0.1
	HZ	0.1 – 0.2	0.2	0.1
	HO	0.1 – 0.2	0.2	0.1
	OO	-	-	-
Antibiotics	OZ_MOW1	0.1 – 35.1	3.8	2.7
	HZ	0.1 – 12.1	1.8	0.9
	HO	0.0 – 34.5	3.9	3.4
	OO	3.2 – 71.1	37.1	26.3

NSAIDs: non-steroidal anti-inflammatory drug; OZ_MOW1: offshore Zeebrugge; HZ: Harbor Zeebrugge; HO: Harbor Ostend; OO: Offshore Ostend

This study also revealed the presence of two pharmaceuticals included in the EU Watchlist for water monitoring (EU, 2018a); *i.e.* the macrolide antibiotics azithromycin (DF 10%) and clarithromycin (DF 33%) found at concentrations ranging from 0.2 to 24 ng L^{-1}. The non-steroidal anti-inflammatory drug diclofenac (DF 39%) - formerly included in the EU Watchlist (EU, 2015) - was found at concentrations up to 100 ng L^{-1} in the marine environment.

Finally, to the best of our knowledge, this study provides first-time measurement data for several pharmaceuticals in seawater, including the fluoroquinolone antibiotics flumequine and nalidixic acid and the antiviral drugs amantadine, efavirenz, nevirapine and rimantadine, detected in 2% to 85% of the samples, at concentrations up to 14 ng L^{-1}.

4.3.3.2. Personal care products.

Eight PCPs representing disinfectants, insect repellents, preservatives and UV filters were detected in the BPNS. Concentrations ranged predominantly (65% of the measurements) between 1 and 10 ng L^{-1} (Table IX) The most frequently detected PCP was the insect repellent DEET, at concentrations ranging from 1.4 to 25 ng L^{-1} (DF 98%), which corresponds well with previous research on the occurrence of DEET in the North Sea (Weigel et al., 2002). The widespread occurrence of DEET in harbour and open sea regions can be attributed to its broad use as repellent on clothing or skin to provide protection against mosquito bites and ticks, among others (Tanwar et al., 2015). Propylparaben was the second most detected PCP (DF 54%) whereas all other PCPs were detected in less than half of the samples. Due to their widespread use in cosmetic products, propylparaben and other parabens have been detected in different environmental matrices, including the marine environment, at similar concentrations (up to 20 ng L^{-1}) as reported for the BPNS (Tanwar et al., 2015; Jonkers et al., 2010).

Table IX. Overview of PCPs concentrations in the BPNS, divided per subclass (concentrations in ng L^{-1}).

Subclass	Location	min.-max.	Average	Median
Disinfectant	OZ_MOW1	-	-	-
	HZ	-	-	-
	HO	-	-	-
	OO	-	680	680
Insect repellent	OZ_MOW1	3.1 – 24.9	8.4	4.5
	HZ	0.9 – 10.8	4.5	4.2
	HO	2.2 – 16.1	9.6	10.2
	OO	1.9 – 7.8	4.4	4.0
Preservatives	OZ_MOW1	0.7 – 594	86.5	4.3
	HZ	0.1 – 10.3	2.4	1.0
	HO	0.1 – 8.1	1.9	0.9
	OO	0.4 – 9.1	3.0	1.8
UV filter	OZ_MOW1	-	-	-
	HZ	6.3 – 7.3	6.8	6.8
	HO	7.4 – 9.1	7.9	7.5
	OO	-	6.9	6.9

OZ_MOW1: offshore Zeebrugge; HZ: Harbor Zeebrugge; HO: Harbor Ostend; OO: Offshore Ostend

4.3.3.3. Pesticides.

Twenty-three pesticides were detected in at least one sample from the BPNS at concentrations ranging from 0.01 up to 70 ng L^{-1}, with more than 95% of the measured values below 10 ng L^{-1} (Table X). The herbicides atrazine (0.3 - 4.5 ng L^{-1}), chloridazon (0.2 - 41 ng L^{-1}), isoproturon (0.2 - 70 ng L^{-1}), simazine (0.3 - 4 ng L^{-1}) and terbuthylazine (0.3 - 19 ng L^{-1}) were the most frequently detected pesticides with overall DF > 90%. Moreover, atrazine, chloridazon and terbuthylazine were found during all sampling campaigns and in all locations using grab and passive sampling (DF = 100%). Especially the frequent detection of atrazine and isoproturon is remarkable, since they have been banned for application in the EU since 2004 and 2016, respectively (EU, 2009; EU, 2016). The ubiquitous presence of atrazine in marine water more than 10 years after its ban in EU countries provides evidence for its resistance to environmental degradation and/or lack in governmental control.

Five neonicotinoid insecticides that are included in the EU Watchlist (EU, 2018a) - *i.e.* acetamiprid, clothianidin, imidacloprid, thiacloprid and thiamethoxam - were also frequently found in the BPNS (DF ranging between 11 and 88%) at maximum concentrations of respectively 0.7, 5, 10, 65 and 54 ng L^{-1}. Neonicotinoids are a class of insecticides with (limited) evidence of adverse effects on humans (Han et al., 2018), yet toxic effects on pollinators and other insects (Carrasco-Navarro and Skaldina, 2019). Despite their occurrence in other matrices such as freshwater samples (Weston et al., 2015), to the best of our knowledge, this work is the first to report the regular occurrence of these hazardous chemicals in the marine environment.

Table X. Overview of pesticide concentrations in the BPNS, divided per subclass (concentrations in ng L^{-1}).

Subclass	Location	min.-max.	Average	Median
Fungicide	OZ_MOW1	0.04 – 0.33	0.2	0.1
	HZ	0.0 – 1.0	0.3	0.2
	HO	0.0 – 0.9	0.2	0.1
	OO	0.1 – 0.5	0.2	0.1
Herbicide	OZ_MOW1	0.4 – 46.4	3.4	2.5
	HZ	0.1 – 47.8	2.7	1.8
	HO	0.2 – 69.5	5.2	4.6
	OO	0.2 – 5.7	1.2	1.0
Carbamate insecticide	OZ_MOW1	0.1 – 0.5	0.2	0.1
	HZ	0.0 – 1.5	0.3	0.1
	HO	2.5 – 14.8	0.8	0.7
	OO	0.1 – 0.1	0.1	0.1
Neonicotinoid insecticide	OZ_MOW1	0.2 – 3.1	0.9	0.7
	HZ	0.0 – 10.3	1.1	0.6
	HO	0.0 – 64.6	4.5	1.3
	OO	0.1 – 1.6	0.6	0.5
Organochloride insecticide	OZ_MOW1	-	13.0	13.0
	HZ	12.3 – 18.7	14.6	13.2
	HO	10.6 – 13.2	11.5	11.4
	OO	-	10.6	10.6
Organophosphate insecticide	OZ_MOW1	-	-	-
	HZ	-	-	-
	HO	0.6 – 0.8	0.7	0.7
	OO	-	-	-

OZ_MOW1: offshore Zeebrugge; HZ: Harbor Zeebrugge; HO: Harbor Ostend; OO: Offshore Ostend

Moreover, expect for the work of Noppe et al. (2007) and Brumovsky et al. (2016), pesticide monitoring in the Belgian Part of the North Sea has not received much attention in recent years, signifying the importance of this work.

4.3.4. Analysis of steroidal EDCs, plasticizers and plastic additives.

The steroidal EDCs - i.e. androgens, oestrogens, progestogens and corticosteroids - and plasticizers - i.e. alkylphenols and phthalates - that were detected during the 4 sampling campaigns are summarized in Table XI. All analysed target classes were ubiquitously present in the BPNS. The steroidal EDCs were on average mainly observed below 10 ng L^{-1} (except for corticosteroids) while the plastics additives and plasticizers were detected on average at concentrations ranging between 10 and 1000 ng L^{-1}.

Table XI. Overview of steroidal hormones, alkylphenol and phthalate concentrations (in ng L^{-1}) on the BPNS, divided per subclass.

Subclass	Location	min.-max.	Average	Median
Androgens	OZ_MOW1	0.1 – 63.9	2.0	0.9
	HZ	0.1 – 37.3	2.9	0.9
	HO	0.1 – 83.2	3.8	1.3
	OO	0.2 – 168.8	4.5	1.3
Oestrogens	OZ_MOW1	0.2 – 85.0	3.1	4.9
	HZ	0.2 – 35.1	2.6	2.3
	HO	0.3 – 50.3	4.2	3.7
	OO	0.8 – 70.3	6.1	4.5
Progestagens	OZ_MOW1	0.1 – 11.2	1.6	0.9
	HZ	0.1 – 13.4	1.6	0.8
	HO	0.1 – 28.0	2.1	1.2
	OO	0.3 – 141.5	8.1	1.1
Corticosteroids	OZ_MOW1	0.1 – 229.3	29.6	5.1
	HZ	0.2 – 254.9	18.2	2.9
	HO	1.0 – 224.2	17.1	5.0
	OO	0.8 – 70.3	6.1	9.2
Alkylphenols	OZ_MOW1	16.7 – 2065	461.5	89.7
	HZ	7.2 – 2674	629.4	127.5
	HO	18.4 – 6503	650.3	114.8
	OO	32.0 – 2629	622.2	213.3
Phthalates	OZ_MOW1	0.5 – 5297	311.1	31.4
	HZ	0.3 – 3166	255.7	48.7
	HO	1.1 – 3773	285.6	56.9
	OO	2.3 – 6104	427.4	74.0

OZ_MOW1: offshore Zeebrugge; HZ: Harbor Zeebrugge; HO: Harbor Ostend; OO: Offshore Ostend

Besides the parent steroidal EDCs, different metabolites, transformation products, and or degradation products of testosterone, estradiol, and progesterone were quantified (i.e. dihydro,

methyl, acetate, propionate, and benzoate form). The most abundant class that was detected during the different sampling campaigns and at the different locations comprised the corticosteroids. The natural (i.e. cortisone, cortisol and tetrahydro-cortisone) and the synthetic corticosteroids (i.e. prednisone, prednisolone and dexamethasone) were the most prominently present. The unambiguous prevalence of these corticosteroids in the marine BPNS environment can be ascribed to their extensive use in human and veterinary medicine as therapeutic drugs for the treatment of various inflammatory and autoimmune diseases (Barnes, 1998). Different studies have observed that corticosteroids can be directly excreted or partially released in the aquatic environment following an incomplete elimination from wastewater treatment plants with removal efficiencies ranging between 73 and 99% (Wu et al., 2019; Fan et al., 2011., Chang et al., 2007) Nevertheless, until now the prevalence of corticosteroids had only been reported in fresh water environments (Wu et al., 2019). Therefore, this study is the first in its kind providing evidence that corticosteroids have already reached our marine environment.

The prevalence of plastics additives and phthalates was also clearly demonstrated in the BPNS. The analytes 4-ethylphenol, dibutyl phthalate (DBP) and di-ethyl-hexyl phthalate (DEHP) occurred at the highest concentrations in both active and passive samples, and this at every sampling location. The maximum detected concentrations for the above-mentioned plastics additives and phthalates amounted respectively 6.5, 5.3 and 0.7 µg L^{-1}. The occurrence of 4-ethylphenol can originate from wastewater treatment plant discharges and anthropogenic activities (Schmidt-Bäumler et al., 1999). The high concentrations measured for DBP and DEHP may be caused by extensive industrial activities at the harbours or major freshwater inputs from land inwards. In addition to the quantified parent phthalates, also mono-phthalates (i.e. primary phthalate metabolites) were ubiquitously detected at all sampling locations. This may be attributed to the metabolic transformation (and excretion) from aquatic species (Hu et al., 2016) or human excretion (Ramesh Kumar and Sivaperumal, 2016). Furthermore, despite its extensive use in products and applications and previous reports on its widespread occurrence in human biofluids (Fox et al., 2011), Bisphenol A was mainly not detected (below detection limits).

4.3.5. Results for HOC (CBs, BFRs, PAHs, chlorinated pesticides, musk fragrances).

4.3.5.1. Passive Sampling in water.

Monitoring of HOC in seawater using silicone sheets was in use since 2002 (Smedes F. 2007), and guidelines are available (Smedes and Booij, 2012). Obtained data during this project are listed in Annex 12. Figure 23 compares the dissolved concentrations (C_W in ng L^{-1}) for MOW1 and harbours of Ostend and Zeebrugge. The graph shows low C_W for substances of high K_{OW} that still could be measured due to their high accumulation in the passive samplers (like they do in organisms). To compare the C_W over the three locations on the left in Figure 23 the results are plotted relative to the mean. This indicated that C_W of hexachlorobenzene (HCB) and pentachlorobenzene (PeCB) were slightly higher at MOW1, and CBs slightly higher in the harbours, each having a different congener-distribution in comparison to MOW1. The PAHs show a lot of scatter in the compound patterns with

high levels for acenaphthene and acenaphthylene at MOW1. This pattern variability could be associated with riverine inputs (not only from Scheldt and IJzer, but also Rhine/Meuse, Thames and Seine) in combination with atmospheric contribution (e.g. PAHs). There is of course the impact of MOW1 being a dredged spoil disposal site.

The low turbulence in the harbours caused low sampling rates but still the C_Ws of BDE could be measured showing highest levels at ZB and obviously lowest at MOW1.

Of the chlorinated pesticides, the C_W of lindane, 4,4'-DDD and 4,4'-DDE were highest in the harbours.

Galaxolide and Tonalide are two musk fragrances that are used in huge quantities. As the Ostend harbour receives the effluent of a large WWTP, it is not surprising the highest values for C_W are encountered here (20 and 2.6 ng L^{-1} for respectively Galaxolide and Tonalide), approximately 5 times higher than in Zeebrugge harbour and MOW1. Equal C_W for the latter two indicates that the harbours themselves are not a major source.

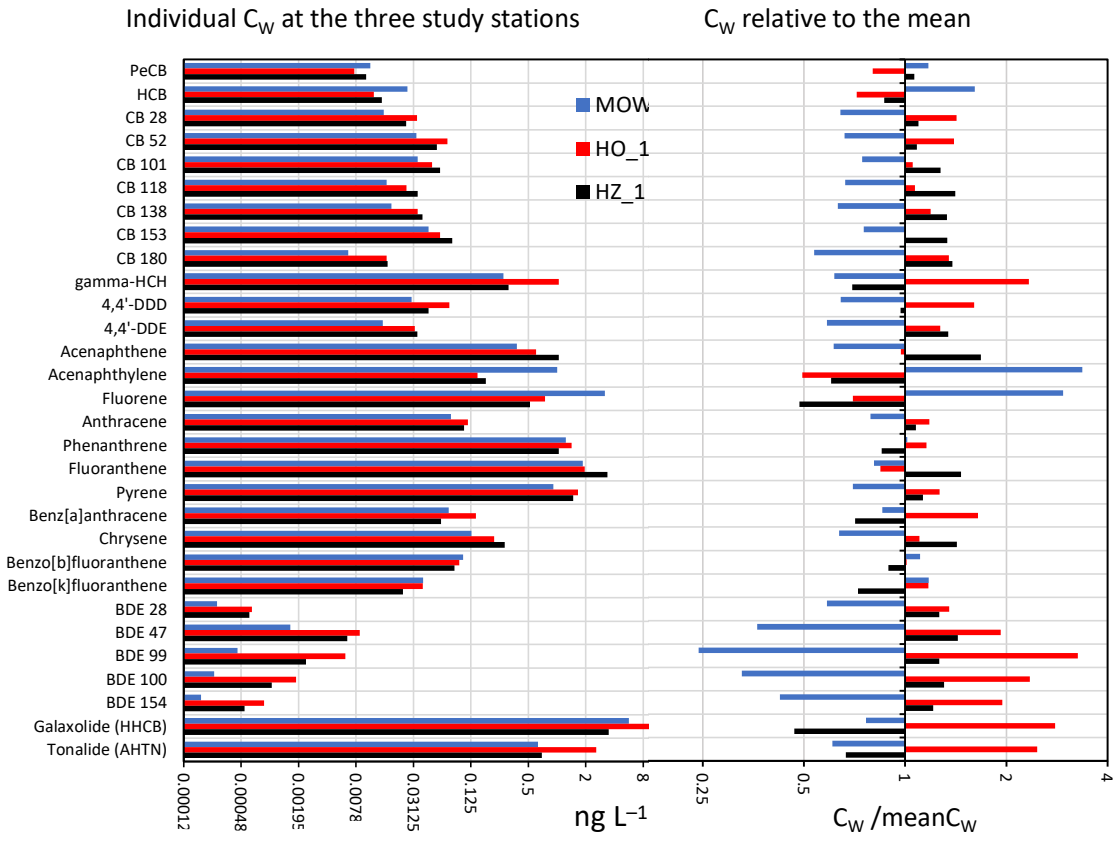

Figure 23. Overview of results from the deployment of SR in water in the harbours of Zeebrugge, Ostend and at MOW1 on C_W concentrations for CBs, BFRs, PAHs, chlorinated pesticides and musk fragrances. The right-hand section of the graph shows the difference of C_W at a station relative to the mean of all stations.

For PeCB, HCB, BDE, fluoranthene, benzo[a]pyrene and indeno[1,2,3-c,d]pyrene, WFD EQS exist which were exceeded for BDE levels by three orders of magnitude at all stations as depicted in Figure 24. Except for PeCB, both the PS results and the EQS were recalculated to concentrations on a lipid basis. Hereto the sampler equilibrium concentration was multiplied by the lipid—polymer partition coefficient (Smedes et al, 2020), while the EQS for HCB and BDEs, valid for fish with 5% lipid, were multiplied by 20, and EQS for PAH that apply to molluscs with 1% lipid, by 100. The extreme exceedance for BDEs may indicate that the EQS is set extremely precautious and stringent measure would be needed to meet it.

Evaluating the passive sampling process, improvements can be made by a more adequate set of PRC (Smedes and Booij, 2007) to accurately calibrate the sampler—water exchange. Also longer exposure times for sampling of very hydrophobic substances, e.g. a whole year are advantageous due to the larger accumulation. Extended exposure times would also bring passive sampling further in agreement with alternative monitoring matrices like sediment or biota that do not have a time-limited exposure.

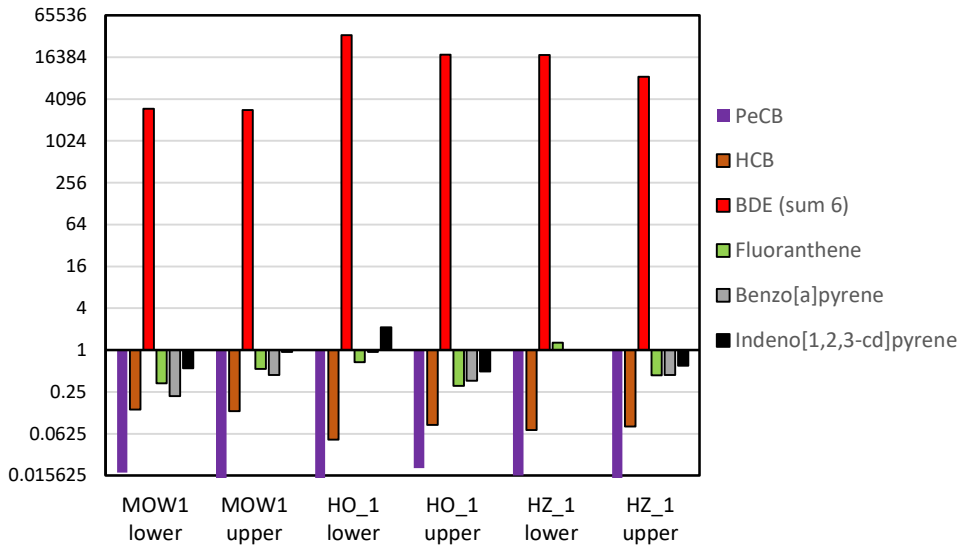

Figure 24. Ratios of passive sampling results in the water phase and the WFD—EQS after both being converted to concentrations on a lipid basis. For PeCB the C_W/EQS was given. "lower" and "upper" indicate placement of the sampler near the bottom and closer to the surface, respectively.

4.3.5.2. Results of the multi- ratio experiment on bioavailability of non-polar organic contaminants.

The method is described under 3.5.3.2. and data listed in Annex 12. Figure 25 shows the decrease in C_W as the sampler—sediment ratio increases and progressively exhaust the releasable HOCs from the sediment. The intercept of the regression line and the X—axis indicates the releasable or bioavailable concentration in the sediment or SPM, showing that only a limited portion of the HOCs in the sediment is readily exchangeable with the sampler and thus the water phase. The fraction between intercept and the total concentration (indicated by the arrow) is inaccessible or so strongly bound it releases very slowly and only when C_W is close to zero. Especially for HOCs, it is possible

to demonstrate this model. For PAHs that may, despite biocide addition, degrade during the long exposures required for equilibrium, it is more difficult to demonstrate they also follow this release model. Degradation can develop differently in the individual exposures giving random deviations of the regression line. PAHs may be trapped in soot or ash and randomly become available due to grinding, occurring during shaking. The method was demonstrated for assessing bioavailability of BDEs (Rusina et al, 2019), but the amount of SPM and sediments available in this project was too small to setup multi-ratio passive sampling with sufficient sampler mass to quantify absorbed BDE. Multi-ratio passive sampling is not suitable as a monitoring method, but is useful to determine the actual risk in case remediation measures would be necessary based on exceeding quality criteria by total levels measured in sediment.

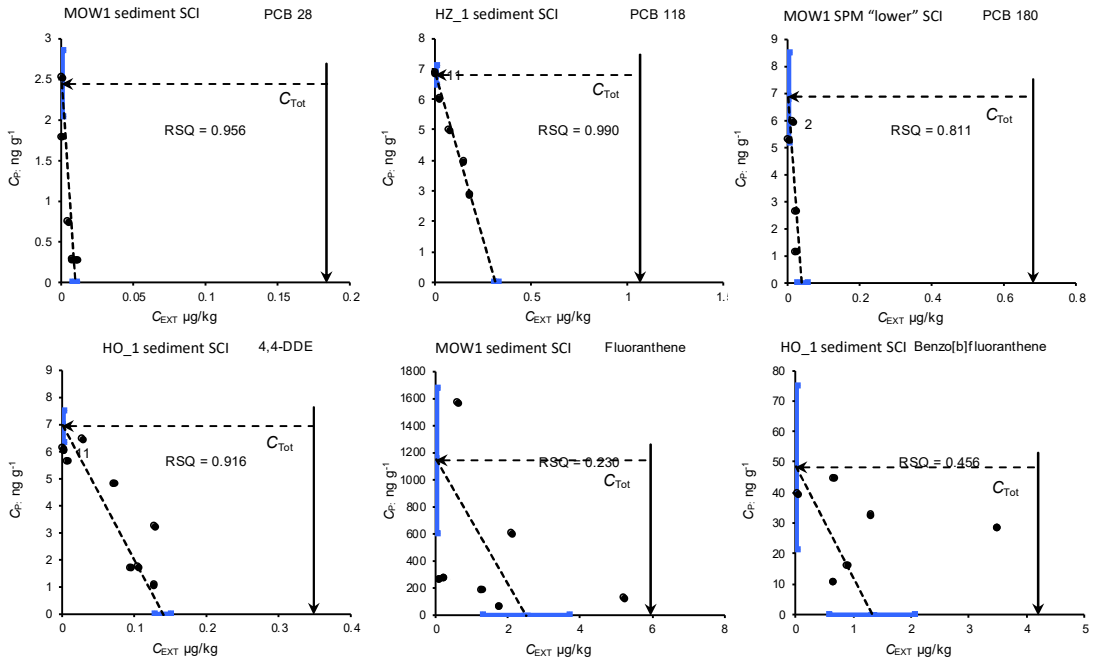

Figure 25. Some examples from multi-ratio passive sampling for differing hydrophobicity and HOC nature. The concentration in the sampler is plotted versus the concentration extracted from the sediment and extrapolated to sampler absence, where the intercept reveals the bioavailable concentration. The total concentration by exhaustive solvent extraction is indicated by the vertical arrow (C_{Tot}).

4.3.5.3. Results for the Equilibration of passive samplers with Suspended Particulate Matter collected from SPM traps.

Sediment traps are a simple, cheap and effective way to collect the SPM, acting as the vector of hydrophobic contaminants in seawater. The traps consist of a PVC tube, closed at top and bottom, with an odd number of small holes close to the upper lid. During the project, experiments have been running with several numbers and sizes of holes in order to obtain a maximum harvest of SPM. Water is passing through the holes, and once sediment starts moving down, it is trapped into the tube. After 1-2 months, the traps are collected and the content frozen and stored at -20° C until analysis. It is

important to have the trap settling at 4° C before freezing. In an upright position, the material gets more compact and water is lost. Otherwise, the remaining water in the SPM core creates crystals upon freezing, disturbing the patterns that can be observed otherwise. As modelling techniques (see section 4.5.) confirmed that the major source of HOCs is not the harbours, the applicability of SPM traps in harbours satisfies investigation purposes only, the impact on observed substances concentration is dominated by the output of the different estuaries influencing the BPNS.

In open sea stations, the problem is to attach the traps in a safe, stable and secure way. Apart from the permanently operated station at MOW1, the stations of aKust39, Obst14 and Buitenstroombank proved to be unreliable upon recovery of the tripods. Despite their deployment very close to navigation buoys, where ship traffic is forbidden, tripods were almost all the time either fished up, replaced or hardly accessible for Research Vessels.

A very instructive example of what level of detail SPM traps can offer is presented in Figure 26. A trap is split lengthwise, one half is available for sampling, another half for non-destructive analysis. Every single tidal cycle can be distinguished, and at neap tide, layers are much smaller than during spring tide, as the higher currents swipe up more coarse material, even fine sand (as indicated by the Si content).

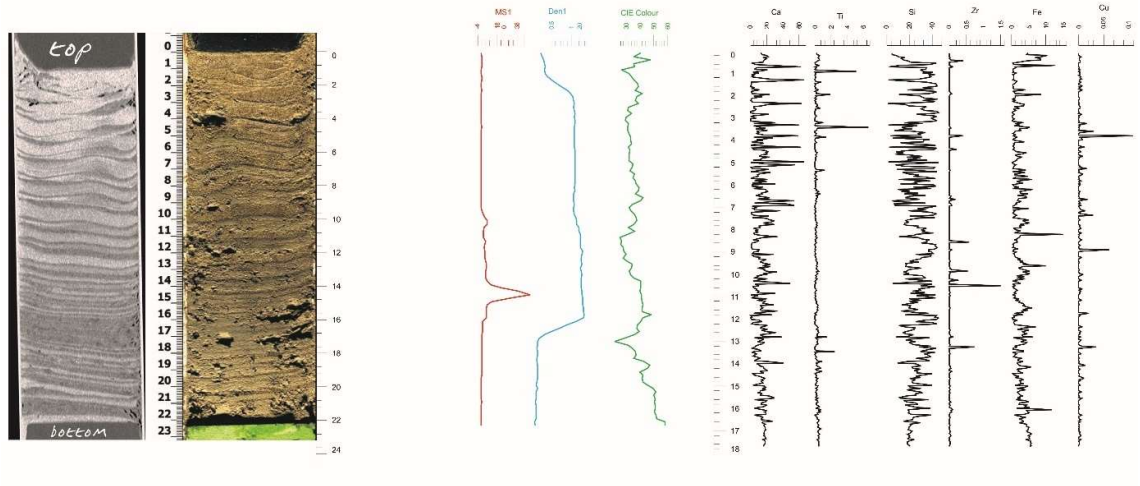

Figure 26. Results for the MOW1 core close to the bottom (under), SC1. From left to right: CT scan, photo magnetic susceptibility, density, colour and relative concentrations of diverse trace metals illustrating the difference in composition of different layers.

A complete overview of obtained results is presented in Annex 12. Some cores were disturbed, e.g. if too much water was present, the tripod tumbled or displaced by ship traffic, or strong currents.

The core with SPM was sliced in portions which were individually equilibrated with PS as described under 3.5.3.3. Application of passive sampling in sediments or SPM, provides equal results if those samples were in equilibrium with the same water, irrespective of the physical sediment composition. Consequently, in such case PS results are also not depending on OC%. In Figure 27, the OC% and

concentrations in PS equilibrated with SPM from the sedimentation traps is presented. For legacy compounds like CBs, little variability is noted between harbour and open sea stations, although higher concentrations typically reflect harbours (e.g. HO_2). This is in correspondence to measures, the ban of these substances decades ago and the high level of equilibrium established over the years, with only limited new input.

PAHs concentrations show slightly higher variability, which is associated with the ongoing input from burning of wood and fossil fuels, and oil pollution. Highest concentrations of musk fragrances were observed in Oostende (HO_2) related to the presence of a huge WWTP. Much lower concentrations were observed at open sea (Obst14), while at MOW1 they were still notably high. More graphs and underlying data can be found in Annex 12.

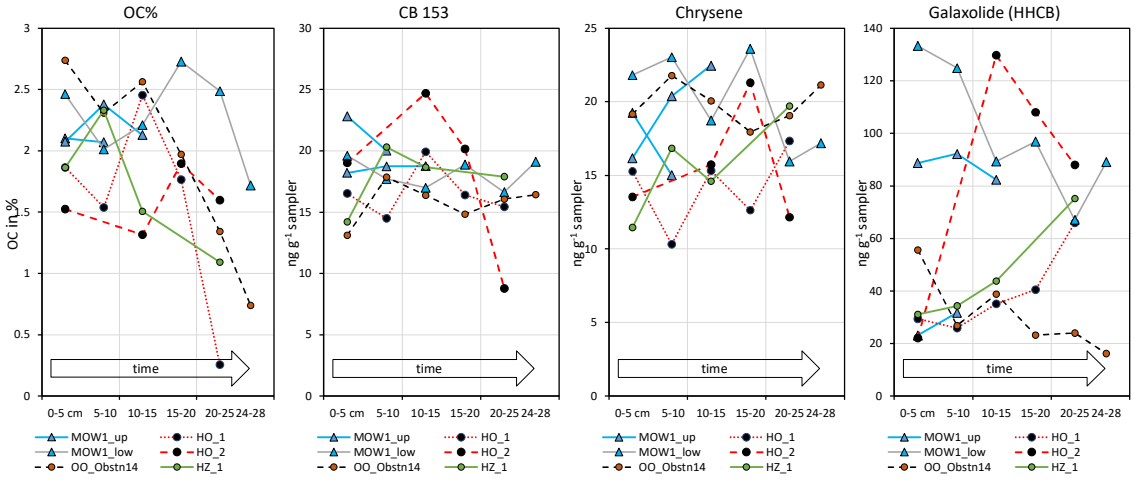

Figure 27. Organic carbon contents (OC in %) in SPM layers collected by the sediment traps at different positions in the study area (left panel). The three right-hand graphs show the levels in passive samplers equilibrated with same sediment layers for CB 153, chrysene and galaxolide.

4.3.6. Particulate Carbon concentrations and stable isotope ratios.

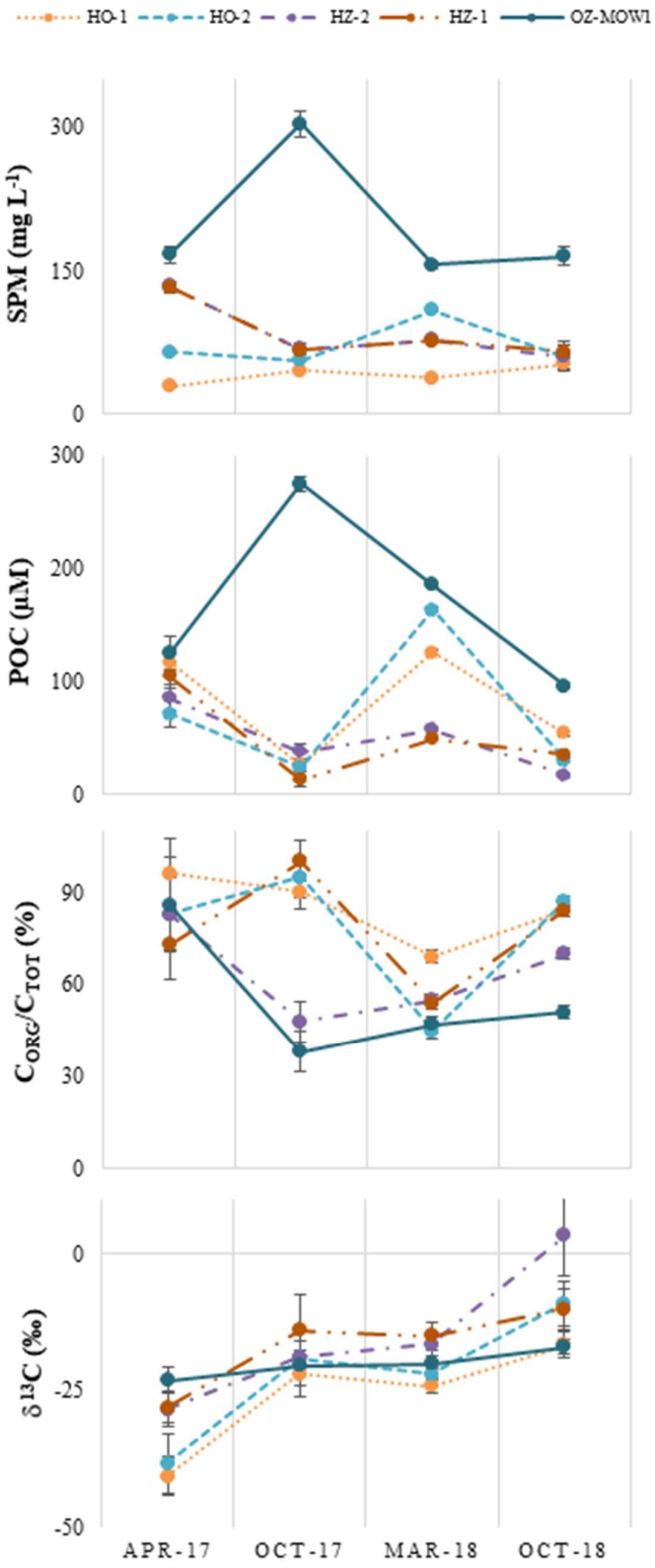

Figure 28. Seasonal variations of the SPM composition in the BCZ water column.

SPM amount at station OZ-MOW1 is much higher than at the harbour stations and reaches its highest peak in October 2017 (304 mg L^{-1}; Figure 28). Tidal currents at the offshore station are usually stronger than in the coastal harbours, causing much higher resuspension of bottom sediments and higher SPM concentrations. Conversely, station HO-1 shows the lowest amount of SPM in October 2017, below 50 mg L^{-1}. In most cases, the carbon content of SPM is dominated by C_{org} with percentages ranging between 45 and 100% of total C, but stations OZ-MOW1 and HZ-2 also show a high amount of inorganic C (respectively 44% and 36% of total C in average). No particular seasonal trend is noticed at our scale of monitoring. In terms of concentration, POC contents are higher at OZ-MOW1 than in the harbours reaching a maximum value of 275 µM in October 2017. At OZ-MOW1, the POC concentration varies around 1.5-3.6 mg L^{-1} of carbon. Compared to the 200-300 mg L^{-1} of SPM, the organic fraction is very small. This is typical for a shallow sea with sandy sediments and strong tidal currents. Conversely, the values are the lowest in Zeebrugge harbour; it varies from 14 to 106 µM at HZ-1 and from 17 to 85 µM at HZ-2. Moreover, POC contents in the harbour stations exhibit the highest values in Spring time, with the maximum concentration observed at HO-2 (164 µM). $\delta^{13}C$ isotopic ratios fluctuate over a wide range: between -41 and 3.4‰. At the harbour stations, $\delta^{13}C$ isotopic ratios increase from Spring to Autumn in both years (Figure 28). In contrast, $\delta^{13}C$ values remain stable at around -20‰, at the marine station OZ-MOW1.

The change of $\delta^{13}C$ values in the harbours stations indicates a change in the SPM origin. The results from April 2017 (-20 to -40‰) are in the harbours the lowest of the 4 campaigns and correspond to the range of $\delta^{13}C$ values observed in POC of the Scheldt estuary (De Brabandere et al., 2002). These results thus clearly indicate a dominance of allochthonous SPM in the harbours in April 2017, coming from terrestrial sources (especially for HO-1 and HO-2). In the 3 other sampling periods, the isotopic C signature of the POC ranges from -10 to -20‰ indicating its marine origin.

In October 2018 at the station HZ-2, $\delta^{13}C$ shows an exceptional high positive value, 3.4‰, which is even close to the inorganic carbon isotope values in shallow marine environments (Trumbore and Druffel, 1995). Although we follow the analytical procedures in a stringent way, it cannot be excluded that all carbonate material in the SPM of the HZ-2 sample was eliminated when $\delta^{13}C$ was determined in the organic matter. This could have led to the high $\delta^{13}C$ result we found. At marine station OZ-MOW1, the particulate carbon source seems to remain almost constant during the monitoring period. The range and average values of $\delta^{13}C$ suggest that autochthonous, marine organic matter prevailed in the SPM at this offshore station for all sampling periods. We can conclude that, in general, the POC in BCZ is of autochthonous origin even if the Scheldt Estuary constitutes one of the major freshwater sources. However, several factors influence its impact on the BCZ water composition such as the increase of salinity, dilution with the marine water mass and mixing processes with bottom sediments. Moreover, other smaller freshwater sources around or inside the harbours can also change the SPM composition and nature.

4.4. Ecotoxicological effects.

4.4.1. Ecotoxicity testing of individual contaminants of emerging concern.

4.4.1.1. Growth inhibition tests with the diatom Phaeodactylum tricornutum.

The 72h-EC_{10} and 72h-EC_{50} values for 20 substances are provided in Annex 13. The lowest 72h-EC_{10} and 72h-EC_{50} were observed for oxytetracycline (0.60 mg L^{-1}) and metoprolol (4.2 mg L^{-1}). Overall, these data suggest a low sensitivity of the diatom *P. tricornutum* to these substances. The 72h-EC_{50} values for atenolol, bezafibrate, and carbamazepine were in close correspondence with those reported by Claessens et al. (2013).

4 4.1.2. Acute toxicity tests with the copepod Nitocra spinipes.

Detailed results of the acute toxicity tests with 23 substances (pesticides, pharmaceuticals and personal care products) are provided in Annex 13. For substances other than the neonicotinoid insecticides, the lowest 96h-LC_{50} was observed for amantadine 4.8 mg L^{-1}. Therefore, these substances are of low toxicity to *N. spinipes*. The 96h-LC_{50}s of four neonicotinoids were between 18 µg L^{-1} (clothianidin) and 25 mg L^{-1} (imidacloprid) (Table XII). However, immobility was a 2.6 - 1000 fold more sensitive endpoint than mortality for neonicotinoids, with 96h-EC_{50} values between 6.9 µg L^{-1} (clothianidin) and 120 µg L^{-1} (thiamethoxam). This corresponds with reports for several freshwater crustaceans been reported before in several freshwater crustaceans (Sanchez-Bayo and Goka 2006; Arican et al. 2017). Sanchez-Bayo and Goka (2006) suggested that immobilization due to neonicotinoid exposure can endanger natural zooplankton populations because it could make them easy prey for their predators and/or it could cause starvation related to feeding inhibition. In addition, the 10% effective concentrations for both mortality and immobility were considerably lower than 50% effective concentrations, with 96h-EC_{10} values for immobilisation between 0.96 and 2.3 µg L^{-1} and 96h-LC_{10} values as low as 0.31 µg L^{-1} for clothianidin. Together our data suggest that neonicotinoids are acutely very toxic to *N. spinipes* and that they could negatively affect marine copepod populations at or slightly below µg L^{-1} concentrations, with clothianidin being the most acutely toxic one.

Table XII Acute 96h-EC_{10} and 96h-EC_{50} (in µg L^{-1}) values for four neonicotinoid insecticides to the copepod *Nitocra spinipes* and their 95% confidence intervals (in parentheses) for the two endpoints mortality and immobility.

	Mortality	Mortality	Immobility	Immobility
	96h-LC_{10}	96h-LC_{50}	96h-EC_{10}	96h-EC_{50}
Clothianidin	0.31	18	0.99	6.9
	(0.12 - 1.4)	(6 - 41)	(0.51 - 2.5)	(3.2-11)
Imidacloprid	270	25,000	0.96	25
	(31 - 840)	(20,000 - 55,000)	(0.43 - 1.5)	(18-31)
Thiacloprid	12	6,100	2.0	7.2
	(10 - 47)	(2,500 - 16,000)	(0.52 - 3.4)	(6.2-8.2)
Thiamethoxam	0.43	740	2.3	120
	(0.28 - 2.0)	(430 - 1,800)	(0.81 - 6.1)	(39-200)

4.4.1.3. Larval development toxicity of neonicotinoids to Nitocra spinipes.

Because the high acute toxicity of the four neonicotinoids to *N. spinipes* (see 4.4.1.2) we also investigated their effects on larval development. The 7-day effect concentrations are shown in Table XIII. Concentration-response data and more detailed discussion is available in Annex 13.

Thiamethoxam did not exhibit any toxicity to larval development up to 99 µg L^{-1}, but the other three neonicotinoids did, with 7d-NOEC values for larval development between 2.5 and 4.2 µg L^{-1}, and a reliable 7d-EC_{10} for thiacloprid of 1.1 µg L^{-1}. Differences in toxicity (both acute and chronic) between neonicotinoid insecticides, despite their common mode of action are most likely related to toxicokinetic and/or toxicodynamic variability (Focks et al. 2018). Interestingly, these NOEC and EC_{10} values (except for thiamethoxam) are in the same low µg L^{-1} range as the 96h-EC_{10}s for adult immobilization. The lower toxicity of thiamethoxam corresponds to observations with the freshwater crustacean *H. azteca* (Bartlett et al. 2019). Overall, considering both adult mortality and immobilisation (see 4.4.1.2) and larval development, the lowest EC_{10} (or NOEC) value is between 0.31 and 1.1 µg L^{-1} for all neonicotinoids, suggesting potential impact on copepod populations at or slightly below the µg L^{-1} range.

Table XIII. Effect concentrations of the 7-day larval development test with *Nitocra spinipes* (µg L^{-1}). Shown are the no-observed effect concentration (NOEC), the lowest-observed effect concentration (LOEC), and the effect concentration showing 10 % effect (EC_{10}) with its 95% confidence interval (95%-CI). See Annex 13 for concentration response data and model fits. Values in bold are recommended for use in PNEC derivation.

	NOEC	LOEC	EC_{10}	95%-CI	Model (as in drc package for R) [a]
Clothianidin	**2.5**	14	2.6[b]	0.62 - 4.5	CRS.4c (names = c("b", "d", "e", "f"))
Imidacloprid	**4.2**	13	0.18[c]	0.01 - 2.1	llogistic2 (fixed = c(NA,0,LDR_{CTL},NA,1))
Thiacloprid	2.7	8.6	**1.1**	0.4 - 3.2	llogistic2 (fixed = c(NA,0,LDR_{CTL},NA,1))
Thiamethoxam	>99	>99	>99	NA[d]	NA

[a] Concentration response model fitted to the data for the determination of the EC_{10}. The upper limit of the larval development ratio (LDR) was fixed to the average larval development ratio in the control treatments (LDR_{CTL}) for imidacloprid and thiacloprid. CRS.4c is a hormesis model (Cedergreen et al. 2005); llogistic2 is a log-logistic model.

[b] Uncertain model fit and EC_{10} value because only one tested concentration showed significant negative effect

[c] Uncertain EC_{10} value because extrapolated below lowest test concentration

[d] Not Applicable

4.4.2. Ecotoxicity testing of environmental samples collected with passive sampler.

4.4.2.1. Silicone rubber sheet approaches for non-polar contaminant mixtures.

4.4.2.1.1. Passive dosing experiments with larval Nitocra spinipes for testing of environmentally realistic contaminant concentrations.

No significant effects on *N. spinipes* larval development were observed in a passive dosing test with SR sheets that were deployed during SC1 (Annex 2, Mann-Whitney-U Test, $\alpha = 0.05$). Nonetheless, further exploration of the usefulness of passive dosing tests with *N. spinipes* in effects-based marine

monitoring is recommended. This could include enrichment of the ERCM to allow for MoS assessment (as explained in 3.7.3.1).

4.4.2.1.2. Proof of principle study for enrichment of environmentally realistic contaminant mixtures on silicone rubber sheets.

Based on the test with *N. spinipes* (see 4.4.2.1.1.) showing no effects on larval development and based on previous findings of Claessens et al. (2015) showing effects ranging from 49 ± 1 % growth stimulation to 100 % growth inhibition on *P. tricornutum* , it was decided to limit in this project further investigations on applications of SR sheet passive dosing to algae toxicity testing. Since passive dosing with SR sheets is typically limited to re-establishing the environmentally realistic concentration levels as they occur in the field, we investigated the possibility to test concentration series (enrichments) of the sampled ERCM's to investigate the possible feasibility for application in the MoS assessment approach. Detailed results of this experiment can be consulted in Annex 2. The main conclusion from this work is that the actual enrichment (of model PAH's) obtained by our method was less than theoretically expected, which was related to considerable loss of PAH's, especially the more volatile ones and increasingly so at high concentrations (likely due to capacity limits of the SR sheets). Yet, since concentrations in the field are low and since observed enrichments equivalent to REF = 10 were reasonably close to the theoretical one (within factor 2), we believe that our enrichment method could, with some further optimisation, become a valuable tool for ecotoxicity tests with passive dosing of SR sheets deployed in the field in the framework of a margin of safety approach. This is because in a regulatory context the lowest applied assessment factor to ecotoxicity data is usually 10, and therefore the observation of no effects at a REF ≥ 10 would lead to a classification of the sampled location as "not at risk". Toxicity of samples with REF < 10 on the other hand would be an indication for potential risks. Further optimisation and testing with SR sheets deployed in the field is recommended.

4.4.3. Speedisk extract testing approaches for ERCMs.

4.4.3.1. Toxicity Identification and Evaluation (TIE) approach.

Testing of fractionated Speedisk extracts from SC1 resulted in no statistically significant effects (Mann-Whitney-U Test, α = 0.05) on the larval development of *N. spinipes* (see Annex 3). Sample enrichment in this test was approximately REF ≈ 1 assuming a similar extraction efficiency of the individual solvents and the standard method using MeOH : ACN (1:1, v/v). The extraction procedure applied in this experiment did not lead to a sample enrichment. Thus, testing presumably occurred maximally at REF ≈ 1. Thus, we assume no toxicity of the sampled mixtures occurred at environmentally realistic concentration levels. In order to work with more enriched samples an adaptation of the extraction protocol was required (see 3.7.2.2.2).

4.4.3.2. Testing enriched ERCMs collected with Speedisk for MoS derivation.

Ecotoxicity testing with *P. tricornutum* of Speedisk extracts from SC1 with our initial method showed small but statistically significant growth stimulation for samples from inside and outside the harbour of Zeebrugge (Moeris et al., 2019). These effects occurred at summed concentrations (of 88

substances) that were within a 1.1- to 2.4-fold range of those observed in grab water samples taken during sampler deployment, but also at lower concentrations. These stimulatory effects were confirmed in two independent tests with extracts stored for <1 or 8 months that had undergone limited sample handling, whereas no effects were observed for extracts that had been stored for 16 months and that had undergone repeated handling (notably repeated freezing, thawing and exposure to light). Based on this difference, we strongly recommend to reduce sample handling while working with Speedisk extracts. This includes minimizing the amount of freezing and thawing of samples and reducing the exposure to light to a minimum. We were not able to identify one of the targeted substances as the cause of the stimulation, suggesting that non-targeted substances in extracts from SC1 may have contributed to the observed stimulatory effects (see Moeris et al., 2019, for detailed results and discussion). This growth stimulation was not confirmed in SC4 samples (performed with initial method), where no significant growth effects were found for a wide range of extract dilutions (see Annex 3), nor in SC2, SC3 or SC5 samples (performed with the final method, see further). Therefore, the small growth stimulation observed in SC1 extracts remains an unexplained once-only event.

Results of the toxicity testing with Speedisk extracts from SC2, SC3, and SC5 performed with our final method (i.e. solvent-free testing in multi-well plates combined with fluorescence measurements of algal growth) are presented in Figure 29. Enrichment factors up to 17 (SC2), 44 (SC3) and 19 (SC5) were obtained with our method. In general, the three to four highest concentration treatments represented enriched ERCMs (relative to the field situation), while the lower four to five treatments were dilutions of ERCM concentrations. The third or fourth highest concentration treatment approximately represented ERCM seawater levels (i.e., REF ≈ 1, vertical dashed line in Figure 29).

Across all samples, significant growth inhibition was observed between 3.2 to 44-fold concentration of ERCMs ($REF_{geomean}$ = 3.2 - 44) (Table XIV). This toxicity can likely not be explained by the target chemicals we measured because of their very low toxicities to *P. tricornutum* (see 4.4.1.1). For comparison, Shaw et al. (2009) reported significant inhibition of *P. tricornutum* at REF = 5 – 10 for a river mouth in the Great Barrier Reef, Queensland, Australia; Tousova et al. (2017) reported significant growth inhibition of the green algae *Raphidocelis subcapitata* at REF ≥ 17 for a range of European surface waters.

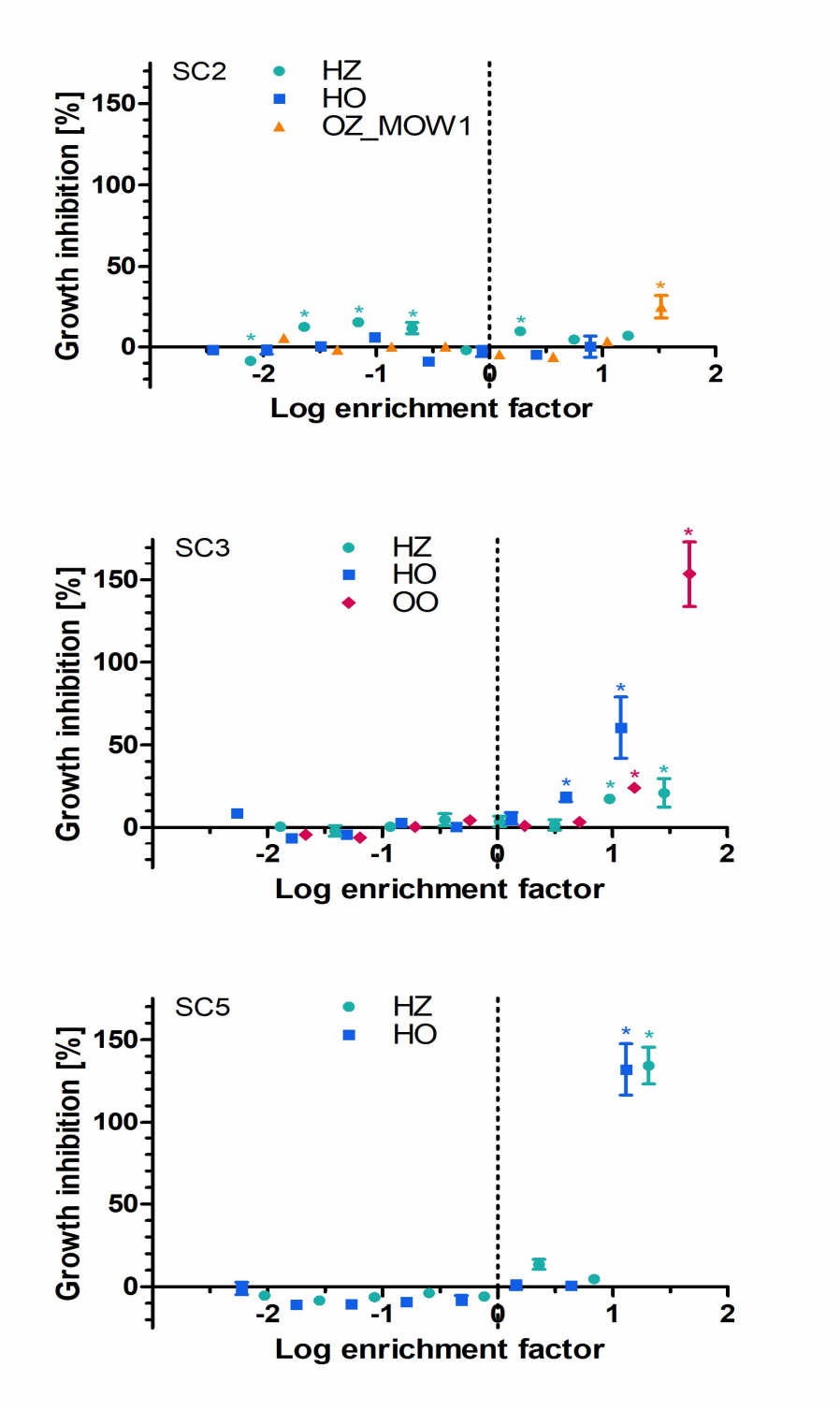

Figure 29. Summary of Speedisk extract testing for sampling campaign (SC) 2, 3 and 5. Shown are the percentage growth inhibition vs. the log relative enrichment factor (REF) of ERCMs collected with Speedisks HZ (Harbour Zeebrugge), HO (Harbour Ostend), OZ_MOW1 (Open Sea Zeebrugge) and OO (Open Sea Ostend). The vertical dashed line indicates REF = 1, i.e. representing the realistic field concentration of the

ERCMs. Data is presented as the average of triplicate Speedisks for each location. Error bars represent the standard error of the mean.

4.4.4. Integrated Environmental Risk Assessment.

4.4.4.1. Margin of Safety (MoS) approach for assessing risks through direct toxicity testing of ERCMs collected with Speedisks.

We successfully developed a Margin of Safety (MoS) as a novel method to assess risks of ERCMs using passive sampling with Speedisks. The MoS for a given species (here: the diatom *P. tricornutum*) is to be considered as the number of times the ERCM occurring in the field can be enriched (or concentrated) without resulting in significant toxicity. It is defined as the NOEC, expressed as REF (Eq. 15), i.e. $MOS_{diatom} = NOEC_{REF,diatom}$. Margins of safety (MoS) per sampling location and campaign are reported in Table XIV and their overall range was from 1.1 to 11.

There appears to be some differences between sampling campaigns, with MoS between ≥ 8.1 - 11 (SC2), between 1.1 - 4.9 (SC3), and between 4.3 - 6.5 (SC5). There is no obvious difference of the MoS in open sea locations (4.9 – 11) compared with harbour locations (1.1 - ≥ 8.1), but sample size is too small for a definitive conclusion. In addition, there is considerable uncertainty in the derived MoS, due to the fact that it is derived from a NOEC estimation from tests with a relatively large spacing factor between two concentration treatments (approx. factor 3). Indeed, a REF > 13 always resulted in growth inhibition, while a REF ≤ 2.8 never resulted in growth inhibition, but REF values in-between were associated with cases of both growth inhibition ($LOEC_{REF}$) and no growth inhibition ($NOEC_{REF}$). To decrease this uncertainty in MoS in the future, we recommend to focus on testing dilution series of Speedisk extracts with REF > 1, and with a spacing factor <2. In addition, with more dilutions being tested over a narrower range of REF, it could be considered to derive an EC_{10} expressed as REF using dose-response analysis and defining the MoS = $EC_{10,REF}$. These optimizations could make this approach be more efficient, less resource-demanding, and generate more reliable assessments.

Table XIV. Summary of algae growth inhibition testing of Speedisk extracts and link to environmental concentrations. Shown are the highest relative enrichment factors (REF) resulting in no statistically significant effect ($NOEC_{REF}$) and the lowest REF resulting in a statistically significant effect on the growth of *Phaeodactylum tricornutum* ($LOEC_{REF}$). The margin of safety (MoS) is defined as equal to the $NOEC_{REF}$.

Sampling campaign (SC) & location	MoS = $NOEC_{REF}$ (% growth inhibition)	Sum analyte C at $NOEC_{REF}$ (µg L^{-1})	$LOEC_{REF}$ (% growth inhibition)	Sum analyte C at $LOEC_{REF}$ (µg L^{-1})
SC2 HZ	ND[a]	ND	ND	ND
SC2 HO	≥ 8.1 (0.2)	4.7	> 8.1 (0.2)	NA[b]
SC2 OZ MOW1	11 (3.7)	1.5	33 (25)	4.4
SC3 HZ	2.8 (1.5)	0.22	8.3 (17)	0.67
SC3 HO	1.1 (5.6)	0.21	3.2 (19)	0.63
SC3 OO	4.9 (3.3)	0.26	15 (24)	0.78
SC5 HZ	6.5 (4.7)	0.60	19 (134)	1.8
SC5 HO	4.3 (0.5)	2.2	13 (132)	6.7

[a] Not determined: no reliable NOEC or LOEC could be determined because concentration-response relationship was highly non-monotonous; [b] Not applicable: highest tested REF did not result in significant growth inhibition.

Speedisk passive samplers have been shown to sample a broad polarity range of contaminants (see section 4.1.1) and reconstitution of the extracts in HPLC water after solvent extraction is a promising approach to be combined with ecotoxicity testing, as it allows higher REF to be tested (>10). This is important because it allows to align the MoS approach with conventional risk assessment approaches in most regulatory frameworks. When doing so, the results reported here for a single species, would already result in a risk conclusion for all sampling locations but OZ_MOW1 in at least one sampling campaign. This is because 5 out of 8 MoS_{diatom} values were found to be <10, which is below the lowest possible assessment factor that is applied to the most sensitive ecotoxicity value (among all species tested) in PNEC derivation (Eq. 23). Some caution is warranted here because of the above-mentioned uncertainty in MoS derivation, but for 2 samples (SC3 HZ and SC3 HO) the conclusion of risk would remain, because even the $LOEC_{REF}$ was <10 (Table SM12).

In conclusion, we have taken a first important step in the development of a ready-to-use method for effect-based monitoring and risk assessment of ERCMs, which we here explored with the marine diatom *P. tricornutum* as test species. However, in order to make this methodology fully compliant with conventional risk assessment it would be required to extend the ecotoxicity test battery. We would recommend the adaptation of the method to at least one chronic test with a marine crustacean such as e.g. the larval development test with *N. spinipes* and one (sub)chronic test with fish such as e.g. the fish early-life stage toxicity test with *Cyprinodon variegatus*. In that case, and if it can be argued that (sub)chronic testing with 3 sensitive species from three trophic levels is sufficient to allow for an assessment factor (AF) = 10, the MoS values could be translated into a conventional risk characterization ratio (RCR) of the ERCM, as follows:

$$RCR = 10 / \text{Minimum}\ (MoS_{algae}, MoS_{crustacean}, MoS_{fish}) \qquad \text{Eq. 23}$$

Optionally, the use of in-vitro assays such as the CALUX (Chemical Activated LUciferase gene eXpression) assay (see 3.3) could help classifying the mode of action of the sampled ERCM to identifying mixture toxicity driving chemicals or groups of chemicals within the ERCM.

4.4.4.2. Risk characterisation for substances with existing EQS or PNEC values.

Probability distributions of risk quotients for 7 WFD priority substances, 7 WFD watch list substances, and 18 antibiotics across all monitoring stations and campaigns, and for both grab samples (median of deployment and retrieval) and passive samples are presented in Figure 30. The PNECs used for all substances considered here are available in Annex 4. Summaries of RQ values per substance are available in Annex 4.

Among the 6 WFD priority substances, none showed RQ > 1 for grab samples, with median RQ > 0.1 only for DEHP, cybutryne and terbutryn. For passive samples, none of the WFD priority substances showed RQ > 1, with median RQ > 0.1 only for terbutryn.

Among the 7 WFD watchlist substances, 2 showed RQ > 1 for grab samples, i.e. 17-alpha-ethinyl-estradiol (EE2)(median RQ = 36) and 17-beta-estradiol (E2) (median RQ = 19), and 1 showed RQ >0.1, i.e. Estrone (E1). For passive samples, 2 WFD watchlist substances showed RQ > 1, i.e. EE2 (median RQ = 11) and E2 (median RQ = 88) and 1 showed RQ > 0.1, i.e. azithromycin.

Among the 15 antibiotics, none showed RQ > 0.1 for grab samples. For passive samples 1 antibiotic showed RQ > 0.1, i.e. azithromycin, and all others showed RQ < 0.01.

Overall, Figure 30 suggests higher RQs based on grab samples than based on passive samples, with the difference being more pronounced for WFD priority and WFD watchlist substances, and with no obvious difference for antibiotics.

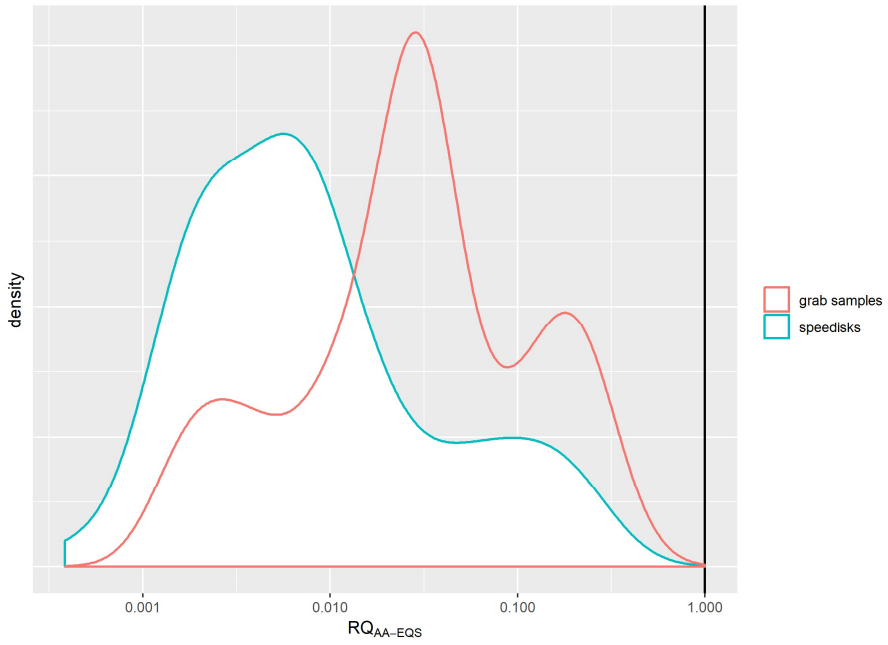

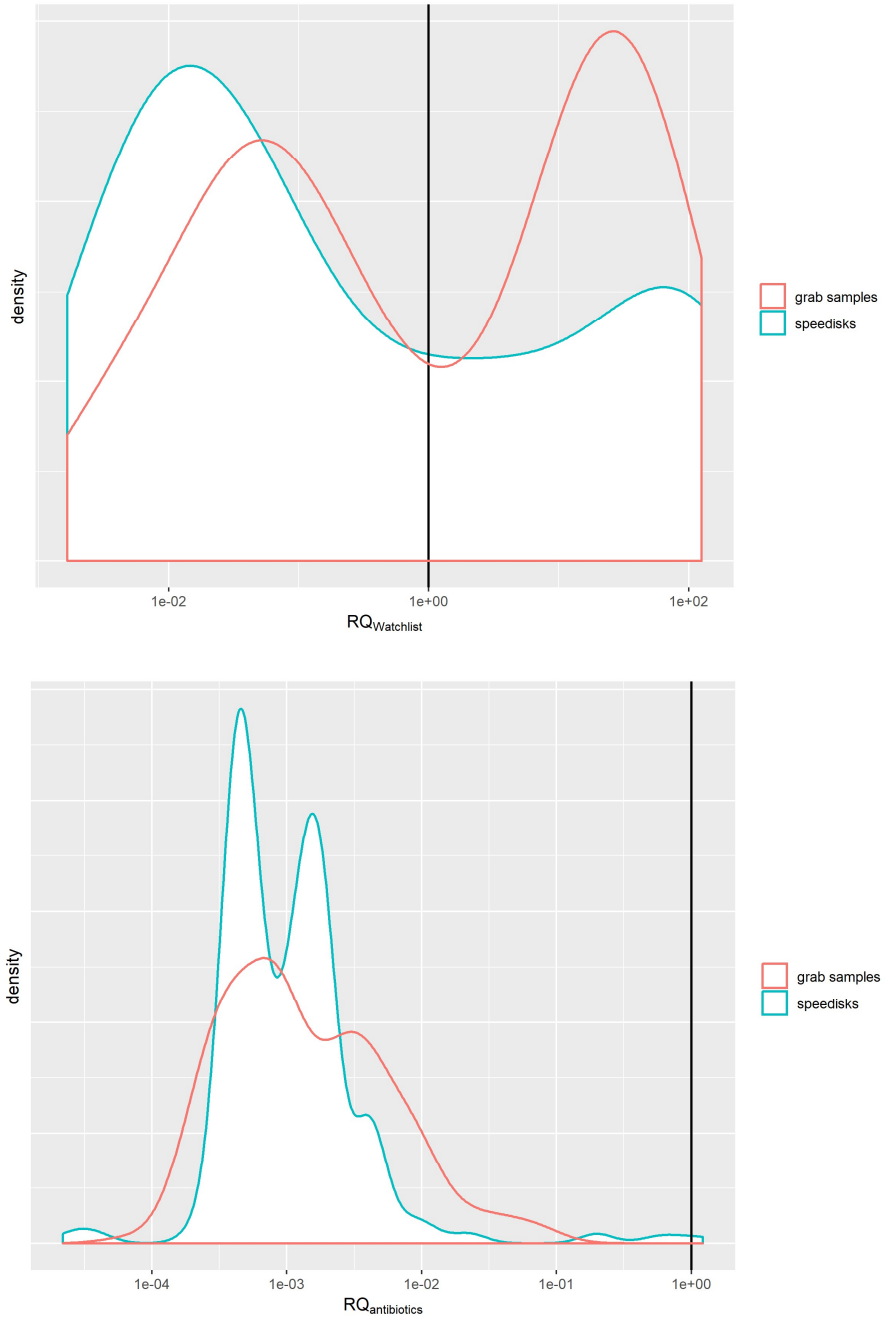

Figure 30. Probability distributions of risk quotients for 6 WFD priority substances (RQ_{AA-EQS}), 7 WFD watchlist substances ($RQ_{watchlist}$), and 15 antibiotics ($RQ_{antiobiotics}$) across all monitoring stations and campaigns for grab samples.

4.4.4.3. Marine PNECs and risk assessment for neonicotinoids and their mixtures.

Since the watch list PNECs for neonicotinoids are not specifically derived for marine waters, and given the relatively high sensitivity of *N. spinipes* (see 4.4.1.2 and 4.4.1.3) we derived specific marine PNECs for four neonicotinoids, following the marine EQS derivation guidance (EU, 2011; see 3.7.3.3). An overview of these PNEC values (toxicity data used for their derivation and applied assessment

factors (AFs)) is shown in Table XV. The derived marine PNECs ranged between 8.3 and 42 ng L^{-1} and were 2 – 4 times lower than the WFD watch list PNECs, which is probably related to the higher AFs used in marine risk assessment. Insects were the most sensitive for imidacloprid, thiacloprid, and thiamethoxam.

Table XV. Derived marine predicted no-effect concentrations (PNECs) for four neonicotinoid insecticides (by dividing the lowest toxicity value by the AF as reported in this table); all values in µg L^{-1}.

Substance	Total nr. of species	Most sensitive species	Test duration [d]	Most sensitive endpoint	Lowest NOEC or EC_{10}	AF	Marine PNEC	WFD Watch list PNEC
Clothianidin	8	*Nitocra spinipes*[a,c]	6	Larval development	2.5	50	0.05	0.13
Imidacloprid	8	*Epeorus sp.*[b]	20	Length	0.1	50	0.002	0.0083
Thiacloprid	7	*Cloeon dipterum*[b]	7	Mortality	0.24	50	0.0048	0.01
Thiamethoxam	6	*Cloeon dipterum*[b]	28	Mortality	0.81	50	0.016	0.042

[a] copepods; [b] insects; [c] our data

The high sensitivity of insects to neonicotinoids has been documented in several studies (Anderson et al. 2015; Morrissey et al. 2015; Raby et al. 2018b). However, our larval development tests with the marine copepod *N. spinipes* resulted in the lowest EC_{10} value for clothianidin (see 4.4.1.3), among all other chronic toxicity values available in databases.

Overall, the risk characterization based on toxic units (TUs) for neonicotinoid insecticides showed that most risks were observed for imidacloprid and the harbour of Ostend (Figure 31). The TU_{mix} was mainly driven by imidacloprid and to a minor extent by thiacloprid or thiamethoxam. Specific mixture risks (i.e. $TU_{mix}>1$ when no single neonicotinoid by itself had TU>1) were not observed with one exception, i.e. the passive sample from HZ in SC2. In general, we observed TUs>1 only with grab sample-based data, with the exception for SC2. The exceedance of PNECs at two harbour sites suggests the presence of ecological risks due to neonicotinoids in the harbours of the BPNS. The TU_{mix} at the open sea locations consistently being ≥ 0.1 indicate a relatively limited margin of safety for neonicotinoid risks in the BPNS. The important contribution of the non-banned TCP to the TU_{mix} suggests that replacement of banned or restricted-use neonicotinoids like clothianidin, imidacloprid and thiamethoxam with thiacloprid could be regrettable and would likely not help reducing risks.

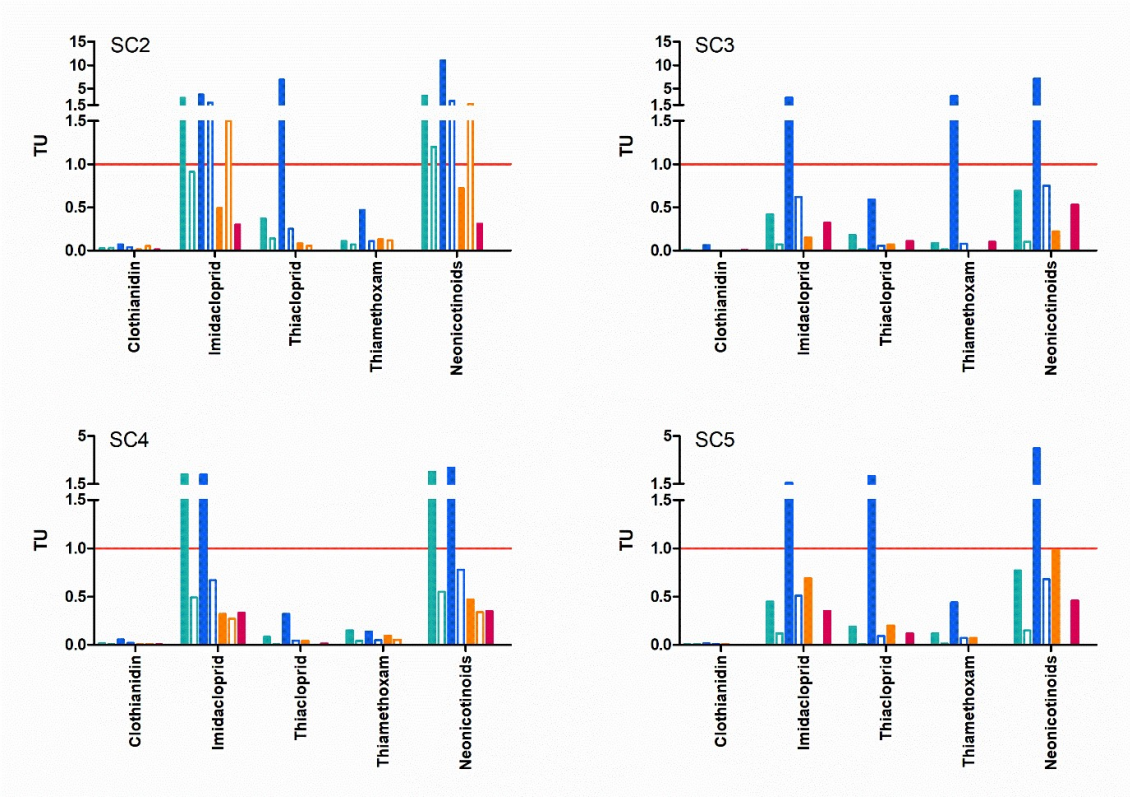

Figure 31. Risk quotients (RQ) for sampling campaigns 2–5 in the Belgian part of the North Sea based on grab sampling (filled bars) and passive sampling data (empty bars) and derived PNECs. Shown are the toxic units (TU) for four neonicotinoid insecticides and their mixture (Neonicotinoids) for the four sampling locations HZ (green), HO (blue), OZ_MOW1 (orange) and OO (pink). Bars show the TU calculated based on the average measured concentration.

4.4.4.4. Screening-level marine PNECs and screening-level risk characterisation for CECs.

We developed an automated calculation algorithm that estimates screening-level marine PNECs and applied it to data from the US EPA ecotox database (see 3.7.3.4. and Annex 6 for methods) to estimate PNECs for 97 CEC's. These PNEC's (and RQ's derived from it) should not be considered definitive, as they have been estimated using a simplified (and easily automatable) set of rules compared to the marine EQS derivation guidance under the WFD (EC, 2011) (see 3.7.3.4. for details). Rather they should be used to provide an overall picture and to prioritize certain sampling locations, certain chemicals or certain classes of chemicals for closer inspection and detailed refinement of PNEC and RQ calculations (such as performed under 4.4.3.2 for neonicotinoids). The latter was, however, not within the scope of the current project. Details about the quantity and type of ecotoxicity data available and used for PNEC derivation can be found in Annex 6.

Figure 32 provides probability distributions of risk quotients for each sampling location across all campaigns, for both grab samples (mean of deployment and retrieval) and passive samples. There appears to be no obvious difference of RQ distributions between sampling locations or sampling methods. RQs > 1 (and even >10 or >100) are found at all locations and with both sampling methods.

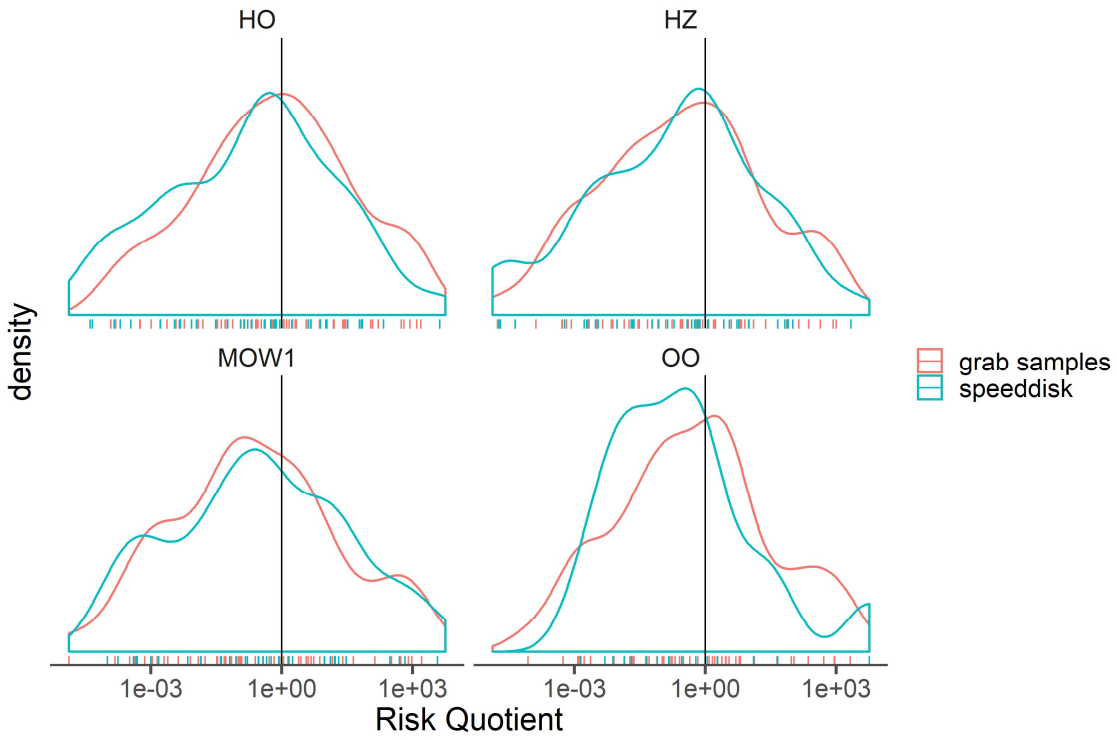

Figure 32. Probability distribution of RQs for CECs in grab samples and passive samples (taken with Speedisks) across sampling locations and SC2 to SC5.

Figure 33 provides probability distributions of risk quotients grouped per chemical class across all locations and sampling campaigns, and for both grab samples (mean of deployment and retrieval) and passive samples. Based on grab samples, the widest distribution of RQ appears to be for steroids, spanning > 6 orders of magnitude. All substance classes contain many cases with RQ > 1, with most RQs for PCPs and pharmaceuticals and phthalates < 10, but with pesticides, phenols and steroids even cases > 100. The distribution of grab sample and Speedisk derived RQs are comparable with each other for pesticides and pharmaceuticals, but for phenols, phthalates and steroids the grab sample-based RQs are higher than the Speedisk-based RQs, while for PCPs the Speedisk-based RQs show a higher density around RQ = 1.

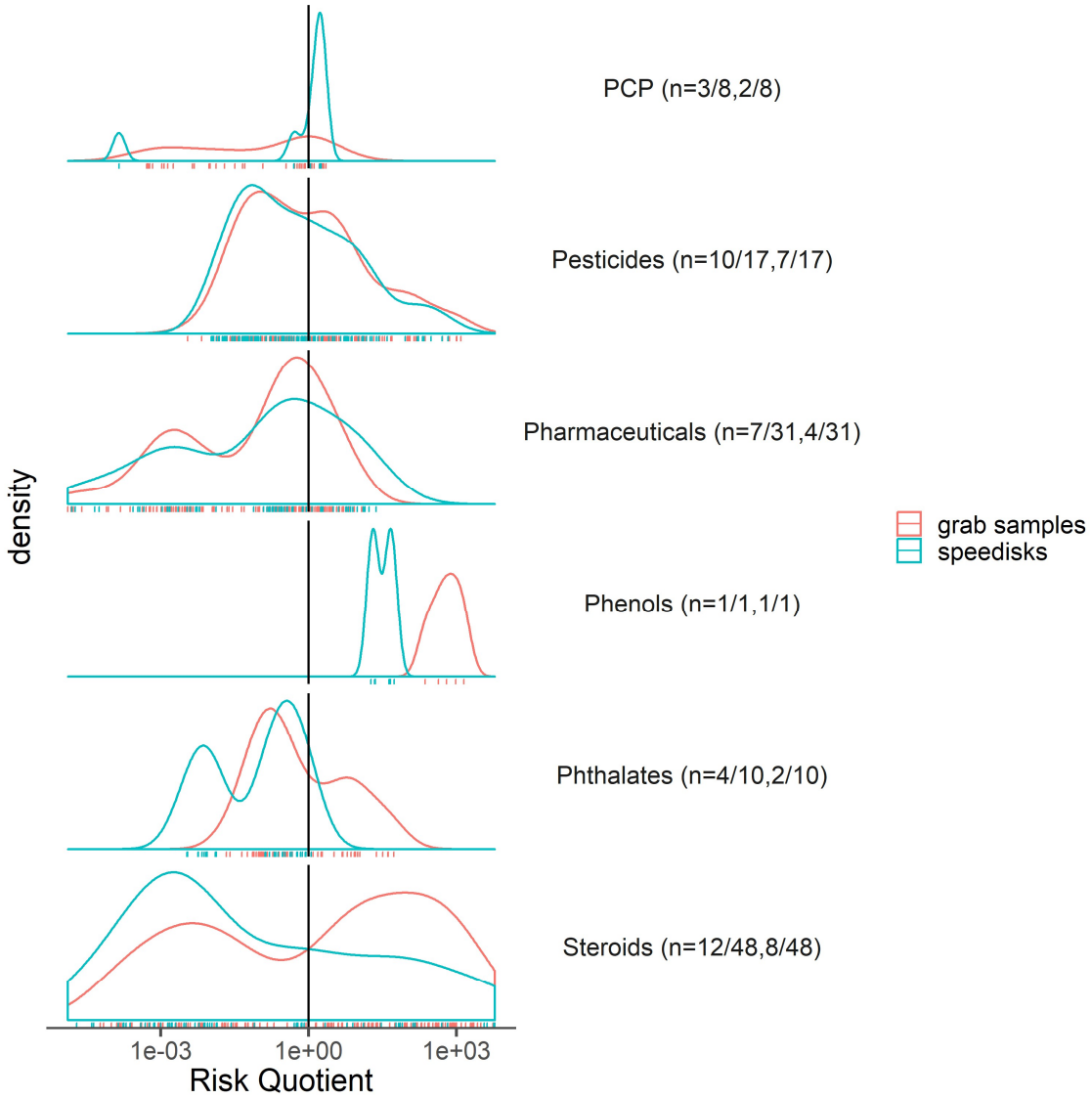

Figure 33. Probability distribution of screening level risk quotients for CECs in grab samples and Speedisk samples across sampling campaigns 2-5, per chemical class. n describes the amount of substances per compound class with an RQ >1 for grab samples and Speedisk samples, respectively.

Based on RQ size, this screening-level marine risk assessment suggests to prioritize in future work Bisphenol A, certain pesticides and steroids for further ecotoxicological testing and/or refined PNEC calculation, but specific substances in the PCP, phthalate or pharmaceuticals class should also not be neglected (see Annex 6 with RQ overview per substance). This should initially occur on a substance-per-substance basis, since with so many RQ's>1 for individual substances performing mixtures assessment with measured targeted substances is not necessarily meaningful.

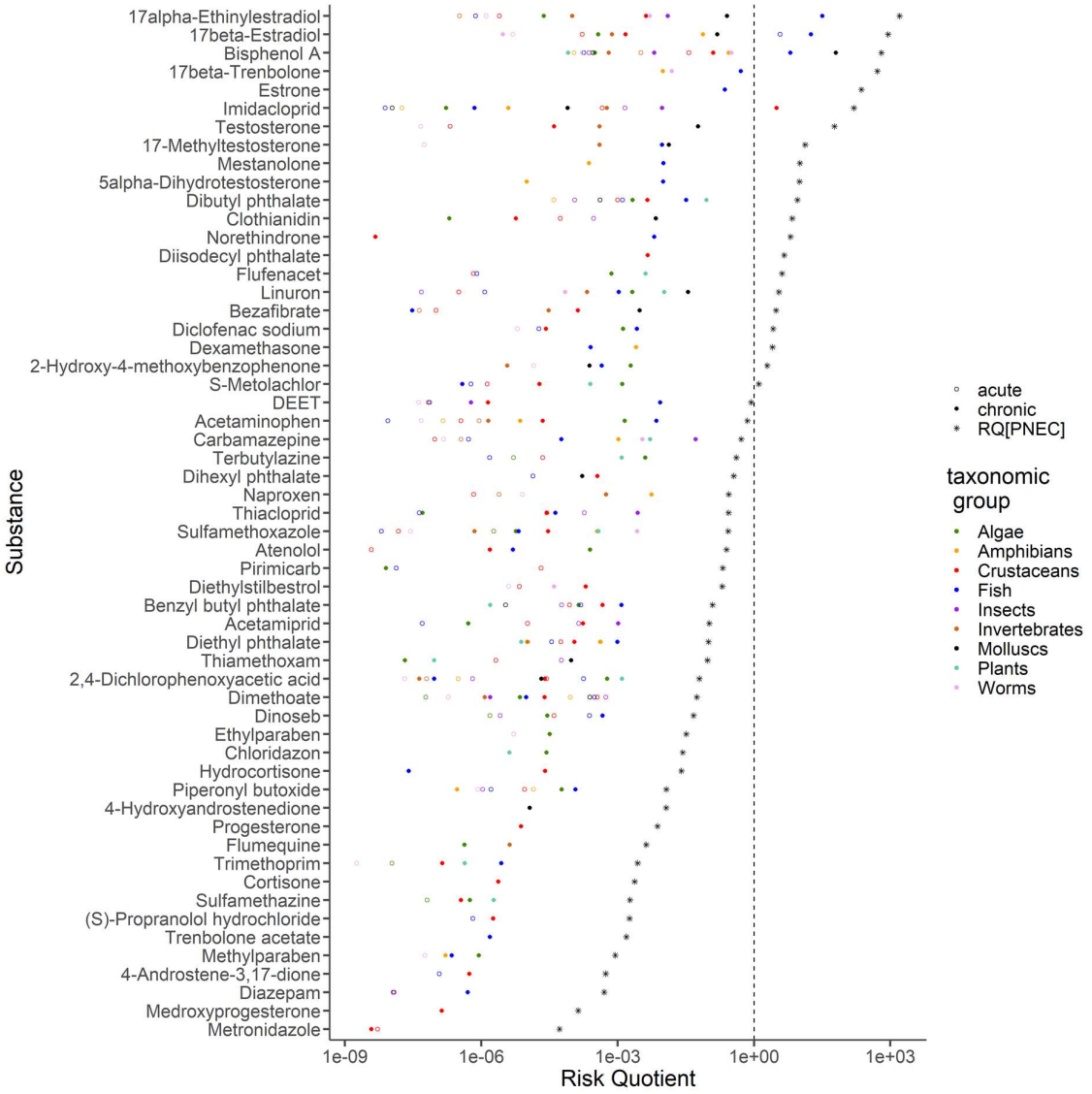

Figure 34. Overview of the risk quotients (RQ) against either the screening-level PNEC as effect measurement, or against the lowest acute LC50 or EC50 or chronic NOEC or EC10 per taxonomic group for which ecotoxicity data were available, based on grab samples.

In order to shed some further light on the substances with RQ > 1, we calculated median RQ values against the PNEC for grab samples (Figure 34). WFD priority substances were not included in this analysis, but WFD watchlist substances were. We identified 21 substances with median RQ > 1. Among those, only 6 belong to the WFD watchlist substances, i.e. 17-alpha-Ethinylestradiol, 17-beta-Estradiol, estrone, imidacloprid, clothianidin and diclofenac. Among those 21 substances, we found 10 steroids, 5 pesticides (2 neonicotinoid insecticides and 3 herbicides), 2 pharmaceuticals, 2 phthalates, 1 PCP and Bisphenol A. Overall, this suggests that there are several substances of emerging concern for the marine environment that are currently not on the WFD watchlist.

Finally, we also calculated RQ values at taxonomic level, with e.g. chronic RQ_{fish} = median concentration in grab sample / lowest chronic NOEC or EC10 for a fish species (Figure SM54), in order to gain some additional insights into taxonomic group sensitivity. For 4 substances we observed the measured environmental concentration to exceed the chronic NOEC or EC_{10} ($RQ_{taxonomic\ group} > 1$) of at least one species namely for 17-alpha-Ethinylestradiol (fish), 17-beta-Estradiol (fish), Bisphenol A (fish and mollusc) and imidacloprid (crustacean). Further, it is shown that most PNECs are derived based on long-term data. In addition, it appears that especially for substances with higher RQ's (including for many steroids), fish are often the most sensitive taxonomic group. However, among all substances with RQ > 1, various taxonomic group appear the most sensitive (Figure 34). The information presented here, can be used to prioritize certain substances and further testing with sensitive taxonomic groups on a substance-by-substance or on a chemical class basis (e.g. steroids for fish).

4.5. Exposure modelling of pollutants: case study and recommendations for further work.

In this section, we demonstrate some applications of chemical exposure modelling in the Belgian part of the North Sea (BPNS) and the harbour of Zeebrugge (ZB). To this end, we used the pollutant exposure model developed in this project as described in Annex 7. Briefly, the model is based on the hydrodynamic model COHERENS. It allows to consider advection, diffusion, adsorption/desorption to suspended and bed sediment and degradation of pollutants. In this chapter, we demonstrate some applications using an organic emerging pollutant (i.e., the neonicotinoid insecticide clothianidin) and considering degradation but not sorption (4.4.1). Modelling sorption for organic pollutants is possible, but this will require (new) data on sorption/desorption kinetics, whereas usually only equilibrium partitioning constants are available for sediments or suspended solids. Although the exposure model can be used for addressing many research and policy questions, we only address a few here to provide a proof-of-principle of their usefulness.

4.5.1. Exposure modelling of clothianidin in the BPNS (open sea): influence of sources and degradation.

Here we addressed, for a hypothetical scenario, the question: "What is the relative contribution of different riverine inputs to the dissolved concentration of the emerging organic pollutant clothianidin at the location MOW1?".

The area covered by the model is illustrated in Figure 5. The model has a uniform grid resolution of 250 m with 345 × 350 grid cells and 10 vertical σ-levels (see Annex 7 for more info). The bathymetry was obtained from the European Marine Observation and Data Network (EMODnet). The wind forcing is extracted from 6-hourly wind and atmospheric pressure fields from the analysed/forecast data of the UK Meteorological Office with a resolution of 0.125° . Figure 5 shows the positions of the riverine inputs of the Scheldt, Rhine (Hoek van Holland), and Meuse (Haringvlietsluis). They were obtained on a daily basis for the year 2010 and interpolated to match the model 3D timestep of 60 s. The daily river discharge data for the Rhine and Meuse are provided

by the "Ministerie van Infrastructuur en Milieu, Rijkswaterstaat", for the Scheldt by the Hydrological Information Centre (Flanders). At the river boundaries a condition of zero vertical gradient of current is applied. The salinity of the Rhine, the most Northern river, is modelled through the open boundary conditions. At the open sea boundaries the time series of cross-boundary transport (vertically-integrated current) and surface elevation are applied using data from a nested model chain of the North Sea continental shelf based on COHERENS (Luyten, 2011). The model starting this chain is a 2D model, driven by sea elevations at the open sea boundaries and wind. The elevation at the open boundaries is governed by four semi-diurnal (M 2, S 2, N 2, K 2) and four diurnal (0 1, K 1, P 1, Q 1) harmonic constituents.

We assumed equal concentrations of clothianidin at the mouths of the three rivers (see Figure for positions). Based on information about environmental fate in the PubChem(R) database (https://pubchem.ncbi.nlm.nih.gov/), clothianidin does not readily sorb to particles (and is thus expected to be mainly in the dissolved phase) and photolysis (degradation under influence of light) is the predominant degradation process. Hence, the results of the simulations presented here for clothianidin are also representative for other organic chemicals with similar low sorption and mostly photodegradation (and limited biodegradation and hydrolysis).

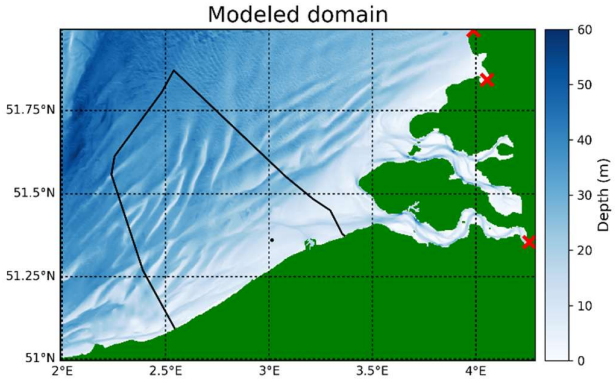

Figure 35. Overview of the modelled domain with bathymetry (blue shades), river input positions (red crosses with from North to South the Rhine, Meuse and Scheldt), measurement station MOW1 (black dot) and the Belgian Part of the North Sea (BNPS, black line).

Degradation of clothianidin via photolysis has been shown to occur with a half-life of 1 day or lower in lab experiments (PubChem). Lab experiments, however, usually take place at high light intensities (high incoming radiation and/or very low volumes/test vessel depths). In the field (i.e. the BPNS or harbour of ZB), average light intensity in the water column is likely much lower. Exact calculations of spatiotemporal light intensity dynamics are outside the scope of the current study. Future work should concentrate on making this half-life dependent on light intensity explicitly in the program code (i.e. considering local incoming solar radiation and light attenuation in the water column), for instance as in Oldenkamp et al. (2018). Here, in order to consider the uncertainty related to

(photo)degradation in the field, we performed simulations for assumed half-lives of clothianidin in the BPNS of 1, 10 and 100 days. This enabled us to evaluate the importance of degradation in the establishment of exposure concentrations in the BPNS. The simulations were run by setting concentrations at each of the three rivers' mouths at 33 ng L^{-1} (=95th percentile of concentrations measured in Europe (Loos et al., 2018)). Hourly absolute concentrations at each location and each depth were calculated for the BPNS. It is important to note that, at least when there is no sorption, there is a linear relation between absolute concentration at any time and location with the assumed input concentration at the river mouths. Hence, results and conclusions about relative concentrations are not dependent on the assumed input concentration at river mouths in this scenario. The MOW1 location was used as our focal point and the upper 10% of the water depth was considered (surface layer) for reporting summary results and conclusions.

Figure 36 provides maps of the predicted absolute exposure concentrations in the North Sea, including the BPNS, for the 3 degradation half-lives and for each river separately and all rivers combined. We see that the pollutant with a half-life of 1 day does not reach the MOW1 station (concentrations remain below 0.1 pg L^{-1}). At this station field measurements in the order of 0.5 ng L^{-1} of clothianidin are available (see section 4.3.3.3.). This means that a scenario where clothianidin has the same photodegradation half-life in the field as measured under lab condition is not likely. The half-life under environmental conditions is more likely to be between 10 and 100 days.

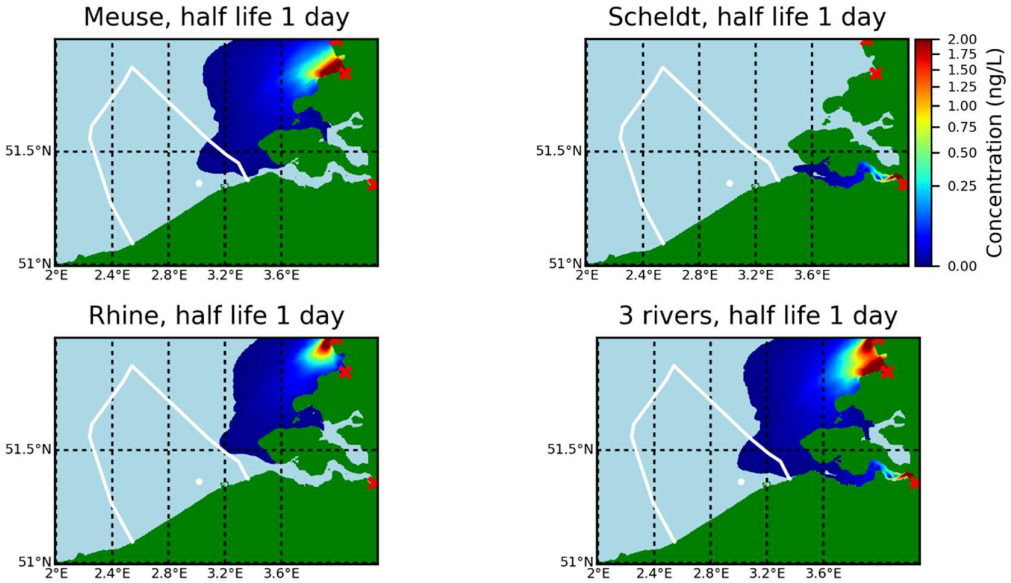

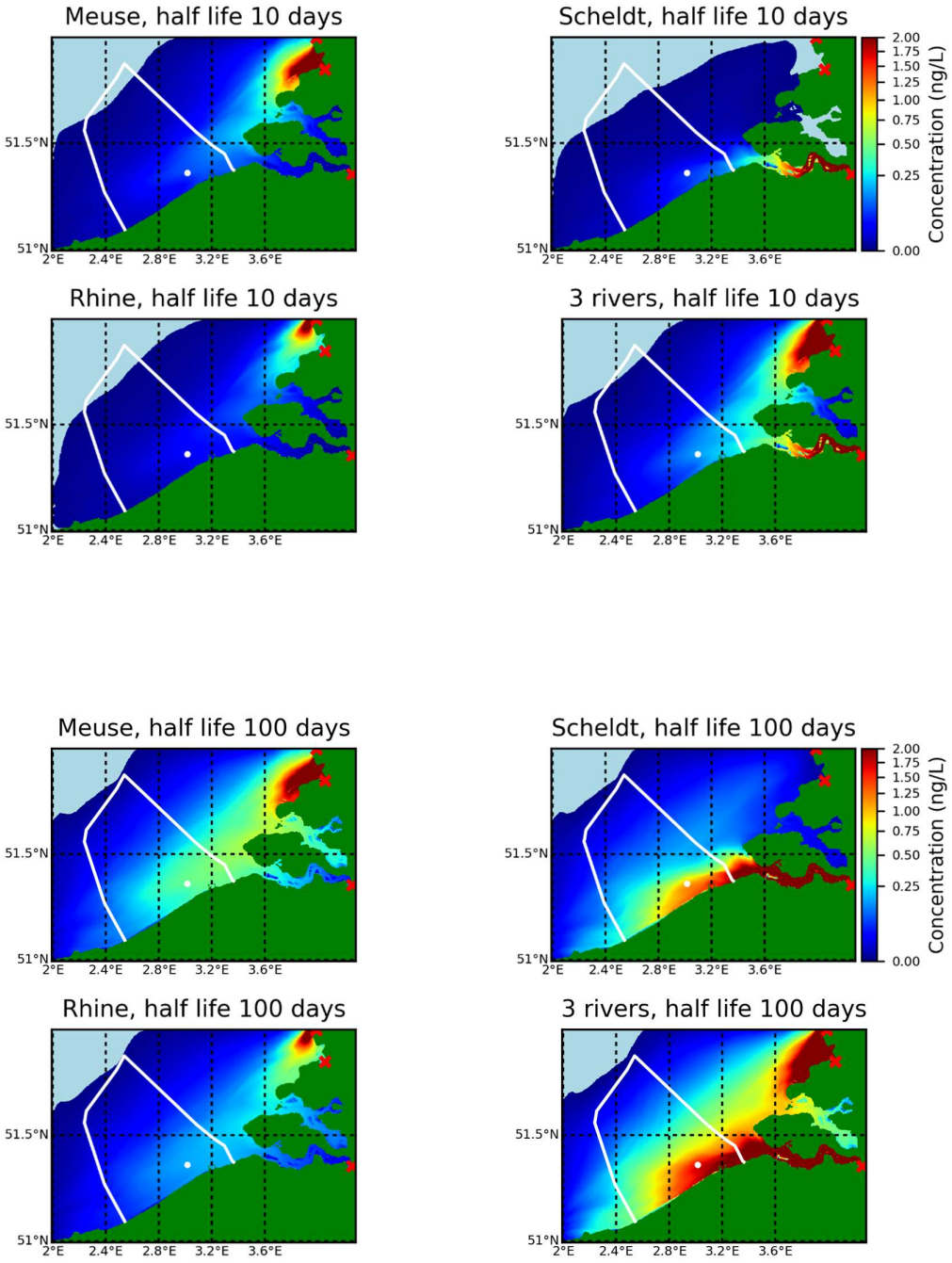

Figure 36. Year-average (2010) of the absolute exposure concentrations (ng L^{-1}) in upper surface layer with constant inflow concentrations of 33 ng L^{-1} at the mouth of Scheldt, Meuse and Rhine. The light blue colour equals concentrations lower than 1 pg L^{-1}. The Belgian part of the North Sea is defined by the white line, the white dot denotes the position of station MOW1, the red crosses the river mouths.

Figure 27 shows the relative contribution of each river to the pollutant exposure. The relative impact changes drastically with a different half-life. From this information it becomes clear that the degradation processes of pollutants need to be carefully considered when developing an exposure fate model for degrading substances. We also see in this picture that none of the modelled river

inputs can be ignored. With a changing degradation rate, the area and orientation of the area the three rivers cover seems to change. With a half-life of 10 days, the Scheldt water, the Rhine water and the Meuse water spread to the South (coastal zone), the north and the middle of the modelled domain respectively. With a half-life of 100 days the Scheldt water spreads up to the Western area, whereas the Rhine water reaches the Eastern and the Meuse water the middle. Further on at station MOW1 the three rivers contribute to the modelled pollution no matter what the degradation rate.

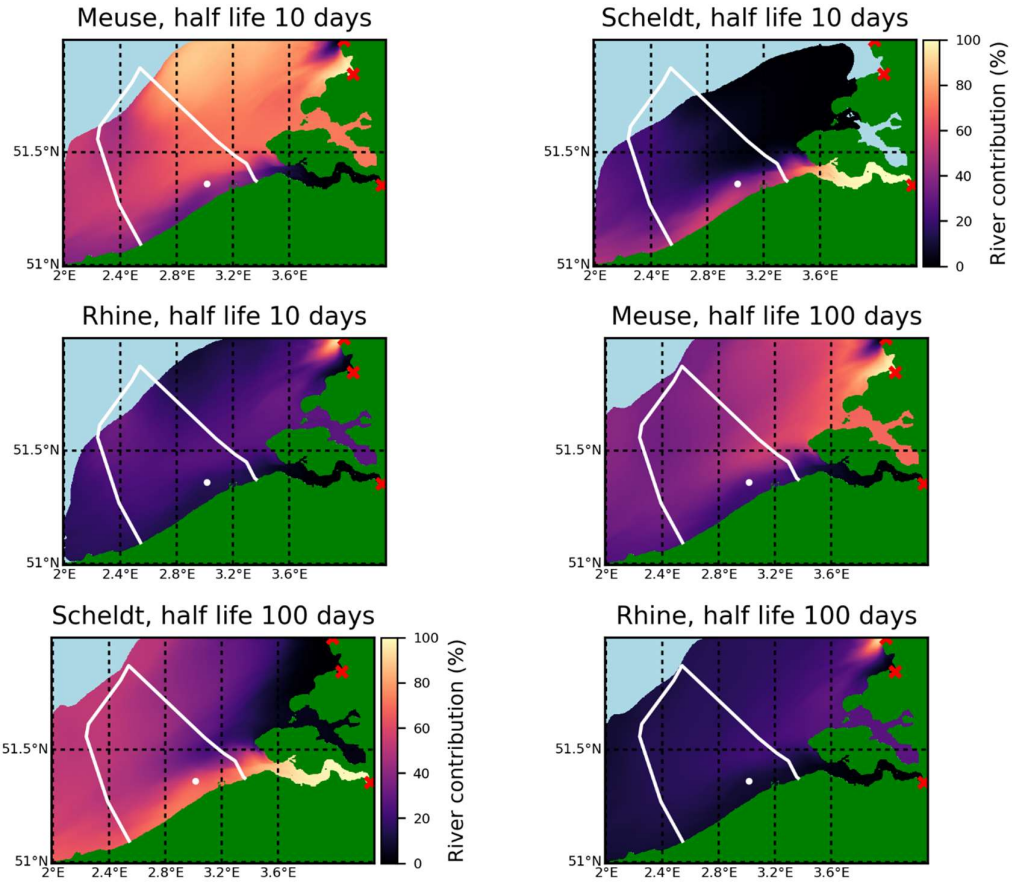

Figure 27. Relative contribution of three river systems (Scheldt, Rhine, Meuse) to the average annual concentration of clothianidin (%). The Belgian part of the North See is defined by the white line, the white dot denotes the station MOW1, the red crosses the river mouths.

The relative contribution of each river to the pollutant concentration in MOW1 (Figure) fluctuates considerably over a year. Each river contributes the most at a different period of the year. While Meuse and Scheldt contributions fluctuate between 0% and (almost) 100%, Rhine contribution fluctuates between 0% and 60%. This suggests that in exposure modelling of the BPNS, none of these rivers should be neglected. We also see that, even though the clothianidin originating from the Rhine is the highest contributor only during a limited amount of time, the amounts discharged during that period are so high that they result in relatively high yearly averaged concentration of clothianidin. This confirms the suggestion that all three rivers should be considered when interpreting the clothianidin concentrations measured at MOW1. Here as well, we see a clear influence of the

degradation rate on the relative contributions. Slower degradation rates result in higher clothianidin concentrations in MOW1. At low degradation rates, the Scheldt contribution becomes less important to the total exposure concentration. The Scheldt typically has a high residence time. Hence, when pollutants with a low half-life finally arrive at MOW1, big parts are already degraded. This is less obvious for the pollutants originating from the Meuse and the Rhine.

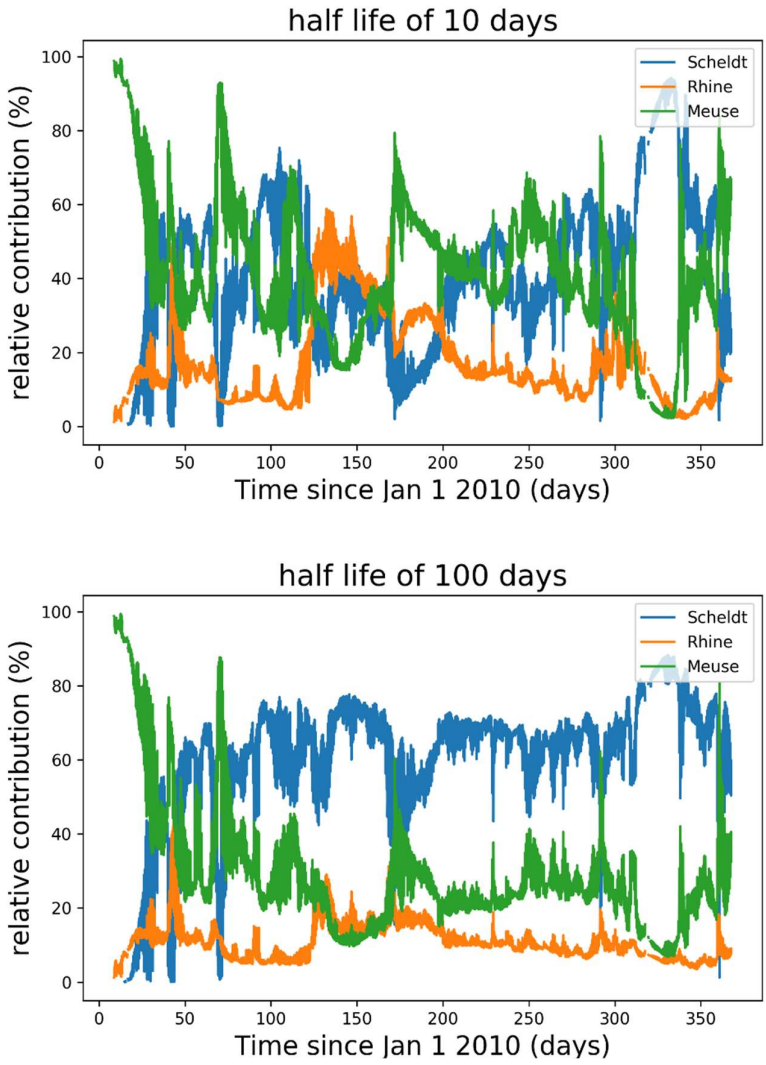

Figure 38. Relative contribution of each river to concentration of clothianidin at MOW1, with equal input concentrations at the three river mouths. (see Figure 5 for position of MOW1).

Table and Figure 39 provide simulated average annual concentrations at MOW1 for the 3 degradation scenarios. Half-lives between 10 and 100 days generate predicted annual average concentrations of 0.155 and 1.63 ng L^{-1} respectively, which is within 3-fold of the measured average value for MOW1 of 0.5 ng L^{-1}, if the contribution of all three rivers is considered. The figure shows an approximate log-linear relation between annual average concentration and degradation time, based on the mathematical description given in Delhez et al. (2003). This mathematical relation can be useful when

we want to make the pollutant exposure model available to users to perform their own model simulations and when calculation times need to be reduced as much as possible.

Table XVI. Modelled average yearly concentrations of clothianidin at station MOW1 at the surface (see Figure 5 for position of MOW1).

Half-life:	10 days	100 days	10 days	100 days
Origin	Average concentration (ng L-1)		Maximum concentration (ng L-1)	
Scheldt	5.71E-02	1.03	3.02E-01	2.71
Rhine	2.51E-02	1.66E-01	1.65E-01	3.68E-01
Meuse	7.29E-02	4.31E-01	6.52E-01	1.62
Total	1.55E-01	1.63	7.32E-01	3.40

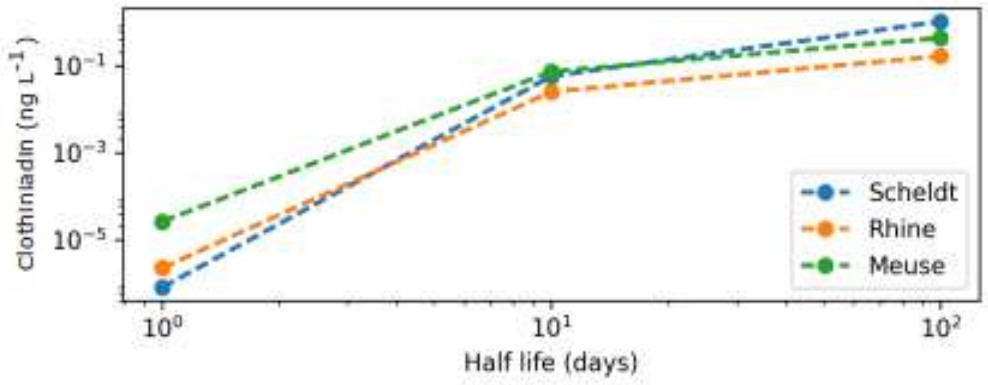

Figure 39. Modelled average yearly concentrations of clothianidin at station MOW1 (see Figure 5 for position of MOW1).

4.5.2. Conclusions and further recommended work.

The take-home message of this case study is that degradation rate has a huge effect on the total pollutant concentration and the distribution of the relative river contributions. Hence, it is highly recommended to improve the implementation of degradation in our model in order to achieve more realistic results. Degradation rates are important in all sorts of processes (such as bacterial models), so we can benefit from the expertise of these models to develop a more generic degradation model.

Assuming relatively high clothianidin concentrations of 33 ng L^{-1} at the river mouths of Scheldt, Meuse and Rhine of 33 ng L^{-1} (95^{th} percentile of samples in European surface water in the watch list report of the WFD (Loos et al., 2018)) and half-lives of 10-100 days provided concentration predictions for MOW1 within up to 3-fold of those measured during the sampling campaigns of this

project. This is encouraging but further research is needed to perform better validation by means of actually measured concentrations at the river mouths and coupling with a riverine pollutant exposure model, together with refinement of the photodegradation component. In addition, for substances that do sorb to suspended matter and/or degrade via other mechanisms, additional components have to be added to the model.

Moreover, the year-to-year variability can explain differences between modelled concentrations (here representative of the year 2010) and observations (measurements realized in year 2018-2019). Lacroix et al. (2004) showed that the interannual variability of the relative contribution of rivers can be important in the southern North Sea. Interannual variability should be assessed by considering simulations over about 10 years, which is the period representative of the timescale of the North Atlantic Oscillations (NAO), which trigger the relative contribution of rivers and water originating from the Atlantic to the water masses in the North Sea (Lacroix et al., 2004).

The main future applications of the model are:

- an assessment tool to predict the impact of policy measures on pollutant exposure in the BPNS.
- a tool to locate strategic positions to install passive samplers for pollutant monitoring, since these are most helpful in locations where the fluctuations of concentrations are the highest (in contrast to grab samplers).

4.6. A novel and integrated passive sampler-based approach for chemical exposure and biological effect assessment.

In this project, we have developed a wide suite of novel methods and innovative approaches to evaluate the Good Environmental Status (GES) of marine waters, more specifically related to Descriptor 8 of the Marine Strategy Framework Directive, which is about chemical pollution. We have applied these methods in the Belgian Part of the North Sea (BPNS), through monitoring and modelling, and this has yielded new insights into exposure, effects and ecological risks of contaminants of emerging concern (CECs), legacy organic compounds and metals. Below, we briefly summarize our key achievements, both related to developed methods and key findings on the current state of the BPNS, and we also summarize our key recommendations for future work.

Several **new (passive) sampling and analytical methodologies** were successfully developed and validated:

- The novel passive sampling technique of Diffusive Gradients in Thin-Films (DGT) was for the first time applied in the BPNS and therefore the first database about labile metal concentrations was obtained in this coastal area.

- A passive sampling method employing o-DGT samplers, followed by in vitro testing of the extract with ERA-CALUX, was used to measure **estrogenic activity** of marine waters.

- **Speedisk® extractions followed by SPE-UHPLC-Q-Orbitrap** analytical methods allowed (ultra)-trace measurement of a broad range of CECs in the marine environment, including pharmaceuticals, personal care products, pesticides, steroidal EDCs, plasticizers and plastic additives. Lower method detection limits (< 1 ng L^{-1}) were obtained in comparison with commonly applied methods using Oasis HLB based extractions.

- **Hydrophilic divinylbenzene (h-DVB) sorbent**, which was physico-chemically characterized in detail for the first time, is a novel and highly promising sorbent for passive sampling of CECs with a broad range of physicochemical properties (e.g., Log K_{ow} from 0.6 to 8.5).

- A novel **Simple Teabag Equilibrium Passive Sampler (STEPS) for polar CECs** was developed, and data obtained in a static exposure batch set-up showed fast uptake rates (R_s from 0.3 to 12 L d^{-1}, with a median value of 1.5 L d^{-1}) and high sampler-water equilibrium partitioning coefficients (Log K_{sw} between 4.1 and 6.5). The simple and cost-efficient design of STEPS and its versatility (ease of incorporating various sorbent materials) to capture a wide range of compounds offer great potential to holistic monitoring of (marine) CECs, although more in-depth in situ calibration is recommended to fully understand the underlying uptake mechanisms under field conditions.

- A new **multi-ratio method to estimate bioavailability** of non-polar (legacy) compounds was developed and works well for chlorinated biphenyls (CBs) and pesticides. For PAHs results were less precise, possibly due to degradation during the long shaking required to attain equilibrium. For BDE larger amounts of sampler and sediment are required to obtain sufficient sensitivity. Further, for especially the most hydrophobic HOCs, equilibrium time may become impractically long.

- We were able to demonstrate that most **legacy pollutants**, mainly consisting of non-polar compounds, **are in or close to equilibrium in the different environmental compartments** (water, SPM, sediment). Basically, this means that any environmental compartment can be selected for monitoring, offering information on all others.

We successfully developed a **new effect-based monitoring approach for environmental risk assessment**, linking passive sampling with Speedisk® and marine sample enrichment with ecotoxicity testing. We demonstrated a strong correspondence of the relative CEC composition between original field samples and enriched test media. Our method reaches Enrichment Factors (EF) of up to 44 in a microplate ecotoxicity test with the diatom *Phaeodactylum tricornutum*, enabling full concentration-response testing of environmentally realistic contaminant mixtures (ERCMs). We further propose that, if effects are measured below an EF of 10, this translates to the occurrence of ecological risk, considering the currently applied minimum safety factor of 10 to the most sensitive ecotoxicity data according to marine risk assessment guidance. This method could easily be extended to other organisms with small volume ecotoxicity test systems in the future. An analogous approach with silicone rubber (SR) sheets for non-polar substances showed some promise, but further optimisation and validation is needed.

We successfully developed and technically verified an initial high-resolution 3D **chemical fate and exposure model** for the BPNS. To this end, we have added components to model degradation and adsorption to suspended matter and sediment to the "COupled Hydrodynamic Ecological model for REgioNal Shelf seas (COHERENS)". The model was successfully tested for correct implementation under several set-up testing conditions to check for mass conservation. This model requires further development in the future – notably in terms of refined riverine chemical inputs into the BPNS and refined degradation and adsorption components – and thorough validation against chemical monitoring datasets.

We developed an **automated algorithm** and R code to compute **marine-specific predicted no effect concentrations (PNECs) of chemicals**. This algorithm uses extracted ecotoxicity data from publicly available and regularly updated US EPA online ecotoxicity database as input, and then applies EU guidance on deriving a marine PNEC based on the type and amount of data available for each substance. **This algorithm allows fast screening-level ecological risk assessment for any chemical of interest and allows straight-forward and rapid updates of PNECs with every updated of the US EPA database.**

In conjunction with already existing methods and laboratory experiments, all new methods and approaches mentioned above were applied, across 5 monitoring campaigns at 4 locations in the BPNS, i.e. two coastal sites and two harbour sites. Following **key results** were obtained:

- Maximum dissolved **trace metal concentrations** were 0.40 µg Co L^{-1},10.1 µg Cu L^{-1}, 2.83 µg Ni L^{-1}, 0.19 µg Cd L^{-1}, and 0.54 µg Pb L^{-1}. Measured dissolved concentrations of Ni, Pb, and Cd were all below AA-EQS (Annual Average Environmental Quality Standards). Labile metal concentrations were lower and ranged up to 0.22 µg Co L^{-1}, 0.60 µg Cu L^{-1}, 0.64 µg Ni L^{-1}, 0.049 µg Cd L^{-1}, and 0.23 µg Pb L^{-1}.

- **Trace metal species** show both seasonal and spatial variation in the BPNS. The labile trace metal concentration, measured with DGT passive samplers, are time averaged concentrations and they are different from the total, dissolved or particulate metal concentrations measured by spot sampling technique. Since the labile trace metal concentration is likely an indication of metal bioavailability much more than these other fractions, marine risk assessment of metals based on total or dissolved metal analysis may not be appropriate. For the future, we **recommended to monitor DGT-labile metal as complementary data** to total, dissolved and particulate metals, and to derive environmental quality standards expressed as labile metal concentrations to compare with.

- Particulate Organic Carbon in the open sea ranged from 1.5-3.6 mg L^{-1}. The $\delta^{13}C$ signatures were used to trace the origin of suspended organic matter. These indicated that both terrestrial and marine sources contribute to suspended organic matter in the BPNS, albeit the **organic matter in the BPNS is mostly from autochthonous, marine origin**. This is important to consider for the improvement of the marine fate and exposure model.

- We report **CEC occurrence data** for 63 PhACs, PCPs and pesticides and 97 steroidal EDCs and plastics additives and plasticizers in the BPNS, with concentrations ranging up to 680 ng L^{-1} for the pharmaceuticals, personal care products and pesticides group, up to 104 ng L^{-1} for the steroidal EDCs, and up to 6.5 µg L^{-1} for the plastics additives and plasticizers. Many of these CECs were detected for the first time in the marine environment.

- **Ecotoxicity testing of CECs** for which no marine toxicity data was available in scientific literature or databases revealed low toxicity for most substances to the diatom *P. tricornutum* (n=20, 72h-EC50 ≥0.6 mg L^{-1}) and the copepod *N. spinipes* (n=23, 48h-LC50 ≥4.8 mg L^{-1}), with the exception of **4 neonicotinoids**, which showed **high toxicity to copepods**, with NOECs between 0.31 and 1.1 µg L^{-1}, considering mobility, survival or reproduction of *N. spinipes*. **Mixtures risk assessment revealed ecological risk of neonicotinoids, mainly in harbour sites** .

- We found no evidence of toxicity of environmentally relevant contaminant mixtures to the copepod *N. spinipes* at concentrations approximating those actually occurring in the BPNS (neither for polar or non-polar compounds). Our **effects-based monitoring approach** with the diatom *P. tricornutum*, however, revealed significant growth inhibition at Relative Enrichment Factors (REF) between 3.2 and 33 and a Margin of Safety between only 1.1 and 11 across 8 marine samples. Using conventional risk assessment approaches, these data suggest **ecological risks due to realistic mixtures of CECs in the BPNS, both in harbours and open sea.** It was not possible, however to link the toxicity with the targeted CECs that we measured in this project. Effect Directed Analysis coupled untargeted compound analyses

and identification could help to disentangle the complex mixtures in the BPNS and indicate the causative compounds.

- Comparison of analytical data of CECs from passive and grab samples with existing EQS or PNECs, revealed **no EQS exceedance** for any of the 7 WFD priority substances, **exceedance of the PNEC for 2 out of 18 EU watchlist substances** (both steroidal EDCs, i.e. EE2 and E2), and **no exceedance of 15 PNECs for antibiotics** established to avoid antibiotic resistance. However, some substances showed risk quotients (RQ) > 0.1, pointing to their potential importance when considering mixtures risks.

- Application of our automated algorithm and code allowed to calculate screening-level **PNECs for 97 substances**. Comparing these with analytical data of CECs revealed no obvious difference of RQ distributions between sampling locations or sampling method (grab vs. passive). We found **21 substances that may present an ecological risk to the BPNS**, i.e. with median RQ > 1. Among those 21 substances, we found 10 steroids, 5 pesticides (2 neonicotinoid insecticides and 3 herbicides), 2 pharmaceuticals, 2 phthalates, 1 PCP and Bisphenol A. Fifteen of those are currently not part of the EU watchlist, are at risk to escape regulatory action, and thus require specific attention. For substances with the highest RQ's (including for many steroids), fish are often the most sensitive taxonomic group. Our screening-level risk assessment results can help delineating priorities for refined assessment or risk reduction in the future.

- Ou**r marine fate and exposure model** was applied to a case study of the neonicotinoid clothianidin. We showed that the degradation rate has a very strong impact on predicted concentrations in the BPNS, as well as on the relative contribution of each riverine input to it. We also showed that both the Scheldt, Rhine and Meuse rivers can significantly influence exposure in the BPNS. Our **initial model validation is encouraging**, but more extensive validation is needed in future work, together with the refinement of the degradation and adsorption components. This is needed to **evaluate the effectiveness of policy measures** proposed to reduce CEC exposure and risks in the BPNS.

5. DISSEMINATION AND VALORISATION.

5.1. Oral Presentations.

5.1.1. 2016.

Huysman, S., Vanryckeghem, F., Demeestere, K., Vanhaecke, L. (2016). Is the divinylbenzene passive sampler a useful tool for measuring hydrophylic endocrine disrupting compounds in the marine environment? The 8th International Passive Sampling workshop and symposium (IPSW 2016), September 7-10, Prague, Czech Republic.

Adamopoulou, A.; Baeye, M.; Monteyne, E.; Fettweis, M.; Neyts, M.; Parmentier, K.; Van Langenhove, H. (2016). Integrated monitoring of nonpolar compounds with the use of Passive Samplers, in: Degraer, S. et al. (Ed.) North Sea Open Science Conference 7-10/11/2016. Abstract Booklet. pp. 61

Huysman, S., Vanryckeghem, F., Van Langenhove, H., Demeestere, K., Vanhaecke, L. (2016). Is our North Sea contaminated with endocrine disrupting compounds? The North Sea Open Science Conference, November 7-10, Ostend, Belgium.

5.1.2. 2017.

Huysman, S., Vanryckeghem, F., Van Langenhove, H., Demeestere, K., Vanhaecke, L. (2017). Environmental forensics in seawater by coupling a divinylbenzene passive sampling device and high resolution mass spectrometry for the screening of organic micropollutants. The 27th SETAC Europe Annual Meeting: environmental quality through transdisciplinary collaboration, May 7-11, Brussels, Belgium.

Huysman, S., Vanryckeghem, F., Van Langenhove, H., Demeestere, K., Vanhaecke, L. (2017). Environmental screening of organic micropollutants in seawater by coupling a divinylbenzene passive sampling device and high resolution mass spectrometry. The VLIZ Science Symposium: The ocean and human health, September 6, Ostend, Belgium.

5.1.3. 2018.

Huysman, S., Van Meulebroeck, L., Vanryckeghem, F., Van Langenhove, H., Demeestere, K., Vanhaecke, L. (2018). UHPLC-HRMS based targeted and untargeted screening of plasticizers in the marine environment. 23th National Symposium for Applied Biological Sciences, Brussels, Belgium, 8 February 2018.

Vanryckeghem, F., Huysman, S., Van Langenhove, H., Vanhaecke, L. and Demeestere K. (2018). Screening of the Belgian Part of the North Sea towards emerging organic micropollutants - comparison of two SPE-techniques prior to UHPLC-Orbitrap-HRMS analysis. 23th National Symposium for Applied Biological Sciences, Brussels, Belgium, 8 February 2018.

Gaulier C., Superville P-J., Guo W., Baeyens W., Billon G. & Gao Y. (2018). Insight into the suspended particulate matter behaviour in a tidal environment. Book of abstracts - ChemCYS 2018. Blankenberge, Belgium, 21-23 February 2018.

Gaulier C., Superville P-J., Guo W., Baeyens W., Billon G. & Gao Y. (2018). The Geochemical behaviour of particulate trace metals in the Belgian Coastal Zone: Insight into the suspended particulate matter behaviour in a tidal environment. Book of abstracts - VLIZ Marine Science Day 2018. Bredene, Belgium, 21 March 2018. Vol. 80. p. 13-13.

Huysman, S., Van Meulebroeck, L., Vanryckeghem, F., Van Langenhove, H., Demeestere, K., Vanhaecke, L. (2018). Have plasticizers already reached our marine environment? The VLIZ Marine Science Day, March 21, Bredene. Belgium.

Moeris S., Vanryckeghem F., Huysman S., Demeestere K., Vanhaecke L., Van Langenhove H., Janssen C., De Schamphelaere K. (2018). Ecotoxicity testing of environmentally realistic contaminant mixtures using passive samplers: what can we learn from repeating toxicity tests over an extended period of time? Book of abstracts - VLIZ Marine Science Day 2018. Bredene, Belgium, 21 March 2018. Vol. 81. p. 22-22.

Huysman, S., Vanryckeghem, F., Smedes, F., Van Langenhove, H., Demeestere, K., Vanhaecke, L. (2018). Divinylbenzene samplers as surrogate tool for biological monitoring of (micro)pollutants in the marine environment. The 10th annual International Passive Sampling Workshop and Symposium, May 9-11, Dublin, Ireland.

Moeris S., Vanryckeghem F., Huysman S., Demeestere K., Vanhaecke L., Van Langenhove H., Janssen C., De Schamphelaere K. (2018). Using no observed effects to identify main contributing micropollutants in mixture toxicity assessment. SETAC Europe 28th Annual Meeting, Rome, Italy, 13-17 May 2018.

Vanryckeghem, F., Huysman, S., Van Langenhove, H., Vanhaecke, L. and Demeestere K. (2018). Ultra-trace analysis of pharmaceuticals and hormones in marine water by using UHPLC-Orbitrap-HRMS. Eighth International Symposium on Hormone and Veterinary Drug Residue Analysis, Ghent, Belgium, 22-25 May 2018.

Gaulier C., Superville P-J., Guo W., Baeyens W., Billon G. & Gao Y. (2018). The geochemical behaviour of trace metals along the Belgian coasts: what can we learn from the use of DGT? Book of Abstracts - Goldschmidt 2018. Boston, USA, 12-18 Aug 2018. p. 799-799 1 p.

Huysman, S., Vanryckeghem, F., Demeestere, K., Vanhaecke, L. (2018). A metabolomics approach towards identification of unknown emerging pollutants in marine waters. The Benelux Metabolomics Days, September 19-20, Rotterdam, The Netherlands.

5.1.4. 2019.

Vanryckeghem, F., Huysman, S., Van Langenhove, H., Vanhaecke, L. and Demeestere K. (2019). High-resolution Orbitrap mass spectrometry screening of pesticide residues in the Belgian Part of the North Sea. IUPAC International Congress, Ghent, Belgium, 19-24 May 2019.

Gaulier C., Leermakers M., Billon G. & Gao Y. (2018). The geochemical behaviour of trace metals in the Eastern Gotland Basin: a speciation study in oxic and anoxic waters. DGT Conference 2019. Vienna, Austria, 18-20 Sep 2019.

Moeris, S., Vanryckeghem F., Huysman S., Demeestere K., Vanhaecke L., De Schamphelaere K. (2019). Combining chemical and ecotoxicological monitoring of emerging polar micropollutants: towards an integrated environmental risk assessment approach. SETAC North America 40th Annual Meeting, Toronto, Canada, 3-7 November 2019.

5.2. Poster presentations.

5.2.1. 2016.

Huysman, S., Vanryckeghem, F., Van Langenhove, H., Demeestere, K., Vanhaecke, L. (2017). Passive samplers, as surrogates for biological monitoring, to measure emerging (micro)pollutants in the marine environment. The 8th Euroresidue Conference, May 23-25, Egmond aan Zee, The Netherlands.

5.2.2. 2017.

Gaulier C., Superville P-J., Guo W., Baeyens W., Billon G. and Gao Y. (2017). Study of the geochemical behaviour of pollutants in the Belgian coastal environment. Book of Abstracts - VLIZ Marine Science Day 2017. Brugge, Belgium, 03 March 2017. Vol. 79. p. 37-37 1 p.

Moeris S., Vanryckeghem F., Demeestere K., Van Langenhove H., Janssen C., De Schamphelaere K. (2017). Single substance and mixture toxicity of emerging polar micropollutants detected in the marine environment. SETAC Europe 27th Annual Meeting, Brussels, Belgium, 7-11 May 2017.

Huysman, S., Vanryckeghem, F., Van Langenhove, H., Demeestere, K., Vanhaecke, L. (2017). How far have plasticizers and additives penetrated our aquatic environment? The 27th SETAC Europe Annual Meeting: environmental quality through transdisciplinary collaboration, May 7-11, Brussels, Belgium.

Vanryckeghem, F., Huysman, S., Van Langenhove, H., Vanhaecke, L. and Demeestere K. (2017). Measuring emerging organic micropollutants in the North Sea using high-resolution Orbitrap mass spectrometry: method validation and occurrence in harbor and open sea. SETAC Europe 27th Annual Meeting, Brussels, Belgium, 7-11 May 2017.

Gaulier C., Superville P-J., Guo W., Baeyens W., Billon G. and Gao Y. (2017). The geochemical behavior of trace metals in the water column of the Belgian Coastal Zone. Book of Abstracts - Goldschmidt 2017. Paris, France, 11-17 Aug 2017.

Huysman, S., Vanryckeghem, F., Van Meulebroek, L., De Paepe, E., Van Langenhove, H., Demeestere, K., Vanhaecke, L. (2017). Targeted, suspected and non-targeted screening with high resolution mass spectrometry in the marine environment: ready to go? The Belgian Metabolomics day, September 29, Melle, Belgium.

5.2.3. 2018.

Vanryckeghem, F., Huysman, S., Van Langenhove, H., Vanhaecke, L. and Demeestere K. (2018). Targeted screening by Orbitrap HRMS reveals the occurrence of pharmaceuticals, personal care products and pesticides in the Belgian Part of the North Sea. VLIZ Marine Science Day, Bredene, Belgium, 21 March 2018.

Moeris S., Koch J., De Schamphelaere K. (2018). Testing of realistic contaminant mixtures with the harpacticoid copepod species *Nitocra spinipes* using passive sampler extracts. SETAC Europe 28th Annual Meeting, Rome, Italy, 13-17 May 2018.

Huysman, S., Vanryckeghem, F., Smedes, F., Van Langenhove, H., Demeestere, K., Vanhaecke, L. (2018). Divinylbenzene samplers as surrogate tool for biological monitoring of (micro)pollutants in the marine environment. The ASSET2018 Summit on Global Food Integrity, May 28-31, Belfast, Ireland.

Gaulier C., Superville P-J., Guo W., Baeyens W., Billon G. & Gao Y. (2018). Insight into the suspended particulate matter behaviour in a tidal environment. Book of abstracts - JNOEJC 2018. Lille, France, 06-08 June 2018.

5.2.4. 2019.

Moeris S., Vanryckeghem F., Demeestere K., De Schamphelaere K. (2019). Severe effects of neonicotinoid insecticides on *Nitocra spinipes* under different exposure conditions. SETAC Europe 29th Annual Meeting, Helsinki, Finland, 26-30 May 2019.

Moeris S., Vanryckeghem F., Demeestere K., De Schamphelaere K. (2019). Environmental risk assessment of emerging polar micropollutants in the Belgian part of the North Sea. SETAC Europe 29th Annual Meeting, Helsinki, Finland, 26-30 May 2019.

Huysman, S., Vanryckeghem, F., Demeestere, K., Vanhaecke, L. (2019). An omics approach towards identification of unknown emerging pollutants in marine waters. The 15th International Conference of the Metabolomics Society (Metabolomics 2019), June 23-27, The Hague, The Netherlands.

5.3. Website, Annexes and raw data archive.

The website of the NewSTHEPS Belspo BRAIN Project is to be found at:

http://www.newstheps.be/

Raw data from sampling campaigns and experimental work, as well as Annexes will become publicly available 2 years after the final project report (1 November 2022) in the VLIZ Marine Data Archive. Anyone who is interested in any annex or raw data file prior to that date can contact the authors.

After the project, VLIZ assures that data stay available through IMIS.

http://www.vliz.be/en/imis?module=dataset&dasid=5596

6. PUBLICATIONS.

6.1. Peer-reviewed publications.

6.1.1. 2017.

Guo, W., van Langenhove, K., Denison, M. S., Baeyens, W., Elskens, M., Gao, Y. (2017). Estrogenic Activity Measurements in Water Using Diffusive Gradients in Thin-Film Coupled with an Estrogen Bioassay. Analytical Chemistry. 89, 13357—13364. https://doi.org/10.1021/acs.analchem.7b03537

Huysman, S., Van Meulebroeck, L., Vanryckeghem, F., Van Langenhove, H., Demeestere, K., Vanhaecke, L. (2017). Development and validation of an ultra-high performance liquid chromatographic high resolution Q-Orbitrap mass spectrometric method for the simultaneous determination of steroidal endocrine disruption compounds in aquatic matrices. Analytica Chimica Acta, 984, 140-150.

6.1.2. 2019.

Gao, Y., Zhou, C., Gaulier, C., Bratkič, A., Galceran, J., Puy, J., Zhang, H., Leermakers, M., Baeyens, W. (2019). Labile trace metal concentration measurements in marine environments: From coastal to open ocean areas. Trends in Analytical Chemistry 116, 92-101. https://doi.org/10.1016/j.trac.2019.04.027

Guo, W., Van Langenhove, K., Vandermarken, T., Denison, M. S., Elskens, M., Baeyens, W., Gao, Y. (2019). In situ measurement of estrogenic activity in various aquatic systems using organic diffusive gradients in thin-film coupled with ERE-CALUX bioassay. Environment International 127, 13-20. https://doi.org/10.1016/j.envint.2019.03.027

Gaulier, C., Zhou, C., Guo, W., Bratkic, A., Superville, P.-J., Billon, G., Baeyens, W., Gao, Y. (2019). Trace metal speciation in North Sea coastal waters. Science of the Total Environment 692, 701-712. https://doi.org/10.1016/j.scitotenv.2019.07.314

Vanryckeghem, F., Huysman, S., Van Langenhove, H., Vanhaecke, L., Demeestere, K. (2019). Multi-residue quantification and screening of emerging organic micropollutants in the Belgian Part of the North Sea by use of Speedisk extraction and Q-Orbitrap HRMS. Mar. Pollut. Bull. 142, 350-360.

Moeris S., Vanryckeghem F., Huysman S., Demeestere K., Vanhaecke L., De Schamphelaere K. (2019). Growth stimulation effects of environmentally realistic contaminant mixtures on a marine diatom. Environmental Toxicology and Chemistry 38(6), 1313-1322. https://doi.org/10.1002/etc.4431

Huysman S, Van Meulebroek L, Janssens O, Vanryckeghem F, Van Langenhove H, Demeestere K, Vanhaecke L. (2019). "Targeted Quantification and Untargeted Screening of Alkylphenols, Bisphenol A and Phthalates in Aquatic Matrices Using Ultra-high-performance Liquid Chromatography Coupled to Hybrid Q-Orbitrap Mass Spectrometry." Anal. Chim. Acta 1049: 141-151.

Huysman S, Vanryckeghem F, De Paepe E, Smedes F, Haughey SA, Elliott, CT, Demeestere K, Vanhaecke L. (2019). Hydrophilic divinylbenzene for equilibrium sorption of emerging organic contaminants in aquatic matrices. Environmental Science and Technology, 53(18), 10803-10812.

6.1.3. 2020.

Adamopoulou A, Baeye M, Belháčová-Minaříková M, Parmentier K, Fettweis M. (in prep). The chemical and sedimentological characterization of suspended particulate matter collected in coastal marine ecosystems using sediment traps. Water.

Moeris S., Vanryckeghem F., Demeestere K., De Schamphelaere K. (2020) A margin of safety approach for the assessment of environmentally realistic chemical mixtures in the marine environment based on combined passive sampling and ecotoxicity testing. Science of the Total Environment (in press, https://doi.org/10.1016/j.scitotenv.2020.142748).

Gaulier, C., Ma, T. H., Gao, Y., Zhou, C. Y., Guo, W., Reichstädter, M., Baeyens, W., Billon, G. 2020. Investigation on trace metal speciation and distribution in the Scheldt estuary. STOTEN. In press. https://doi.org/10.1016/j.scitotenv.2020.143827

Zhou, C. Y., Gao, Y., Gaulier, C., Luo, M. Y., Zhang, X. H., Bratkic, A., Davison, W., Baeyens, W. 2020. Advances in understanding mobilization processes of trace metals in marine sediments. Environment Science and Technology. In press. https://doi.org/10.1021/acs.est.0c05954

Zhou, C. Y., Gaulier, C., Luo, M. Y., Guo, W., Baeyens, W., Gao, Y. 2020. Fine scale measurements in Belgian coastal sediments reveal different mobilization mechanisms for cationic trace metals and oxyanions. Environmental International. 145, 106140. https://doi.org/10.1016/j.envint.2020.106140

Reichstädter, M., Gao, Y., Diviš, P., Ma, T. H., Gaulier, C., Leermakers, M. 2020. Cysteine-modified silica resin in DGT samplers for mercury and trace metals assessment. Chemosphere. 263, 128320. https://doi.org/10.1016/j.chemosphere.2020.128320

6.2. Other publications.

6.2.1. 2018.

Vanryckeghem, F., Huysman, S., Van Langenhove, H., Vanhaecke, L. and Demeestere K. (2018). Screening of the Belgian Part of the North Sea towards emerging organic micropollutants - comparison of two SPE-techniques prior to UHPLC-Orbitrap-HRMS analysis. Extended abstract in Comm. Appl. Biol. Sci, Ghent University, 83/1, 41-45.

Luederwald S., Newton K., Heye K., Bitter K., Moeris S., Benner L., Boehm P., Koch J., Feckler A., Castro M., Eriksson A. (2018). SETAC GLB and SETAC Europe SAC: a liaison promoting the next generation of ecotoxicologists and environmental chemists. Environmental Sciences Europe. 30.

6.2.2. 2019.

Huysman, S. (2019). Development and validation of high-resolution mass spectrometry-based approaches for active and passive sampling of emerging organic micropollutants in the marine environment. PhD Thesis, Ghent University, Ghent, Belgium.

6.2.3. 2020.

Gaulier, C. (2020). Trace metals in estuarine and coastal waters: dynamics, speciation and bioavailability under various environmental conditions. Joint-PhD Thesis, Vrije Universiteit Brussel (Brussels, Belgium) and University of Lille (Lille, France).

Moeris, S. (2020). An Effect-Based Monitoring Approach for Environmental Risk Assessment of Chemicals of Emerging Concern and Complex Chemical Mixtures in the Marine Environment. PhD Thesis, Ghent University, Ghent, Belgium.

Vanryckeghem, F. (2020). Novel active and passive sampling based monitoring for contaminants of emerging concern in the marine environment. PhD Thesis, Ghent University, Ghent, Belgium.

7. ACKNOWLEDGEMENTS.

The NewSTHEPS project was funded by the Belgian Science Policy Office (BELSPO).

Field data were acquired during numerous campaigns on RV Belgica and RV Simon Stevin. For Belgian waters, shiptime was granted by Belspo / RBINS ODNature and Flanders Marine Institute. Brigitte Lauwaert (Royal Belgian Institute of Natural Sciences, Directorate Natural Environment, Management Unit of the Mathematical Models North Sea and Scheldt Estuary) supplied ships of opportunity to pick up samplers and tripods when R.V.s were not available or when the shallow coastal waters did not allow their safe operation.

Data and metadata are stored in and made available through national data repositories: the Belgian Marine Data Centre (www.bmdc.be) and Flanders Marine Institute (www.vliz.be). Special thanks to Annelies Goffin, Carolien Knockaert and Elien Dewitte (Flanders Marine Institute). The project partners thank VLIZ for keeping data and results permanently available after finishing the project, and for hosting the NewSTHEPS website.

The Marine Rescue and Control Centre of the Flemish Shipping Assistance Division granted locations to deploy tripods with samplers in the Marine Environment.

The Belgian Navy granted access to their docks to deploy Passive Samplers in the harbour of Zeebrugge.

We also want to thank the Follow-Up Committee members for their constructive collaboration:

David Cox (Belgian Science Policy), Phillippe Bersuder (CEFAS, UK), Gabriel Billon (University if Lille, France), Adrian Covaci (University if Antwerp), Gert Verreet (Department Economy, Science & Innovation, Division Research), Joachim Scheerlinck (Food Safety Centre), Lieve Jorens (Directorate-General Environment), Joris Van Loco (Scientific Institute of Public Health), Luc André (Royal Museum for Central Africa), Krien Hansen (Natuurpunt), Ruth Lagring (Royal Belgian Institute of Natural Sciences, Directorate Natural Environment);

The financial support from the Hercules Foundation (Flemish Government; AUGE/11/016) and from the Ghent University Special Research Fund (01B07512) is acknowledged for the UHPLC-Q-ExactiveTM and the automated SPE equipment, respectively.

8. REFERENCES.

Adamopoulou A, Baeye M, Belháčová-Minaříková M, Parmentier K, Fettweis M. (in prep). The chemical and sedimentological characterization of suspended particulate matter collected in coastal marine ecosystems using sediment traps. Water.

Annemans L., Brignone M., Druais S., De Pauw A., Gauthier A., Demyttenaere K. (2014). Cost-effectiveness analysis of pharmaceutical treatment options in the first-line management of major depressive disorder in Belgium, Pharmacoeconomics. 32 479-493. https://doi.org/10.1007/s40273-014-0138-x

Arican, C., Traunspurger W., and Spann N. (2017). The influence of thiacloprid on the feeding behaviour of the copepod, Diacyclops bicuspidatus, preying on nematodes. Nematology 19(10): p. 1201-1215.

ASTM International (2003). Standard for the Preparation of Substitute Ocean Water. D1141-98. pp. 98-100. https://doi.org/10.1520/D1141-98R13

Bade, R., Oh, S., Shin, W.S. (2012). Diffusive gradients in thin films (DGT) for the prediction of bioavailability of heavy metals in contaminated soils to earthworm (Eisenia foetida) and oral bioavailable concentrations. Science of The Total Environment 416, 127-136.

Baeyens, W. (1998). Trace metals in the WesterScheldt estuary: A case-study of a polluted, partially anoxic estuary. Developments in Hydrobiology, 128. Dordrecht ; Boston: Kluwer Academic Publishers. 167p.

Baeyens, W., Gillain, G., Decadt, G., Elskens, I. (1987). Trace metals in the eastern part of the North Sea. I : Analyses and short-term distributions. Oceanologica Acta 10, 169-179.

Baeyens, W., Elskens, M., Van Ryssen, R., Leermakers, M. (1998). The impact of the Scheldt input on the trace metal distribution in the Belgian Coastal area (results of 1981-1983 and 1995-1996). Hydrobiologia 366, 91-108.

Baeyens, W., Bowie, A.R., Buesseler, K., Elskens, M., Gao, Y., Lamborg, C., Leermakers, M., Remenyi, T., Zhang, H. (2011). Size-fractionated labile trace elements in the Northwest Pacific and Southern Oceans. Marine Chemistry 126, 108-113.

Baeyens, W., Gao, Y., Davison, W., Galceran, J., Leermakers, M., Puy, J., Superville, P.-J., Beguery, L. (2018). In situ measurements of micronutrient dynamics in open seawater show that complex dissociation rates may limit diatom growth. Nature Scientific Reports 8(1): 16125.

Barbieri, M. (2016). The Importance of Enrichment Factor (EF) and Geoaccumulation Index (Igeo) to Evaluate the Soil Contamination. Geology & Geophysics 5, 237.

Barnes, P. J. (1998). Anti-Inflammatory Actions of Glucocorticoids: Molecular Mechanisms. Clin. Sci. 94 (6), 557-572. https://doi.org/10.1042/cs0940557

Bartlett AJ, Hedges AM, Intini KD, Brown LR, Maisonneuve FJ, Robinson SA, Gilliss PL, de Solla SR. (2019). Acute and chronic toxicity of neonicotinoid and butenolide insecticides to the freshwater amphipod, hyalella azteca. Ecotoxicology and Environmental Safety. 175:215–223.

Belles A., Pardon P., Budzinski H. (2014). Development of an adapted version of polar organic chemical integrative samplers (POCIS-Nylon), Anal. Bioanal. Chem. 406 1099-1110. https://doi.org/10.1007/s00216-013-7286-2

Bourgeois J., Elseviers M.M., Van Bortel L., Petrovic M., Vander Stichele R.H. (2012). The use of antidepressants in Belgian nursing homes: Focus on indications and dosages in the PHEBE study, Drugs and Aging. 29 759-769. https://doi.org/10.1007/s40266-012-0003-6

Brumovský M., Be J., Thomas H., Petersen W., Sørensen K., Nizzetto, L. (2016). Exploring the occurrence and distribution of contaminants of emerging concern through unmanned sampling from ships of opportunity in the North Sea, J. Mar. Syst. 162 (2016) 47-56. https://doi.org/10.1016/j.jmarsys.2016.03.004

Carrasco-Navarro V., and O. Skaldina O. (2019). Contamination links between terrestrial and aquatic ecosystems: the neonicotinoid case, in: K.K. Kesari (Ed.), Netw. Mutagen. Environ. Toxicol.: pp. 145-158. Doi: https://doi.org/10.1007/978-3-319-96511-6_8

Cedergreen N., Ritz C., Streibig J.C. (2005). Improved empirical models describing hormesis. Environ Toxicol Chem.;24(12):3166-72. https://doi.org/10.1897/05-014r.1

Chang, H., Hu, J., Shao, B. (2007). Occurrence of Natural and Synthetic Glucocorticoids in Sewage Treatment Plants and Receiving River Waters. Environ. Sci. Technol., 41 (10), 3462-3468. https://doi.org/10.1021/es062746o

Chen, W., Huang, H., Chen, C. E., Qi, S., Price, O. R., Zhang, H., Jones, K. C., Sweetman, A. J. (2016). Simultaneous Determination of 20 Trace Organic Chemicals in Waters by Solid-Phase Extraction (SPE) with Triple-Quadrupole Mass Spectrometer (QqQ-MS) and Hybrid Quadrupole Orbitrap High Resolution MS (Q-Orbitrap-HRMS). Chemosphere, 163, 99-107. https://doi.org/10.1016/j.chemosphere.2016.07.080

Choi, Y., Cho, Y.M., Luthy, R.G. (2013). Polyethylene-water partitioning coefficients for parent- and alkylated-polycyclic aromatic hydrocarbons and polychlorinated biphenyls, Environ. Sci. Technol., 47, 6943-6950. https://doi.org/10.1021/es304566v

Claessens M., Vanhaecke L., Wille K., Janssen C.R. (2013). Emerging contaminants in Belgian marine waters: Single toxicant and mixture risks of pharmaceuticals. Marine Pollution Bulletin 71, 41-50.

Claessens, M., Monteyne, E., Wille, K., Vanhaecke, L., Roose, P., Janssen, C.R. (2015). Passive sampling reversed: Coupling passive field sampling with passive lab dosing to assess the ecotoxicity of mixtures present in the marine environment. Marine Pollution Bulletin, 2015. 93(1-2): p. 9-19. https://doi.org/10.1016/j.marpolbul.2015.02.028

Cnudde, V., Boone, M.N. (2013). High-resolution X-ray computed tomography in geosciences: A review of the current technology and applications. Earth-Science Rev., 123, 1-17. https://doi.org/10.1016/j.earscirev.2013.04.003

Davison, W. (2016). Diffusive Gradients in Thin-Films for Environmental Measurements Cambridge Environmental Chemistry Series. Cambridge: Cambridge University Press. 297p.

De Brabandere, L., Dehairs, F., Van Damme, S., Brion, N., Meire, P., Daro, N. (2002). δ 15N and δ 13C dynamics of suspended organic matter in freshwater and brackish waters of the Scheldt estuary. Journal of Sea Research 48, 1-15. https://doi.org/10.1016/S1385-1101(02)00132-6

Dehairs, F., Baeyens, W., Van Gansbeke, D. (1989). Tight coupling between enrichment of iron and manganese in North Sea suspended matter and sedimentary redox processes: Evidence for seasonal variability. Estuarine, Coastal and Shelf Science 29, 457-471.

Delhez, É. J., Deleersnijder, É., Mouchet, A.,Beckers, J. M. (2003). A note on the age of radioactive tracers. Journal of marine systems, 38(3-4), 277-286.

Ditoro, D.M., Zarba, C.S., Hansen, D.J., Berry, W.J., Swartz, R.C., Cowan, C.E., Pavlou, S.P., Allen, H.E., Thomas, N.A., Paquin, P.R. (1991). Technical Basis for Establishing Sediment Quality Criteria for Nonionic Organic-Chemicals Using Equilibrium Partitioning. Environ. Toxicol. Chem. 10, 1541-1583.

Esteve, C., Herrero, L., Gómara, B., Quintanilla-lópez, Talanta J. E. (2016). Fast and Simultaneous Determination of Endocrine Disrupting Compounds by Ultra-High Performance Liquid Chromatography - Tandem Mass Spectrometry. Talanta, 146, 326-334. https://doi.org/10.1016/j.talanta.2015.08.064

EU (2000). European Commission Directive 2000/60/EC of the European Parliament and of the Council of 23 October 2000 establishing a framework for community action in the field of water policy (Water Framework Directive). https://eur-lex.europa.eu/eli/dir/2000/60/oj

EU (2002). Commission Decision 2002/657/EC Implementing Council Directive 96/23/EC Concerning the Performance of Analytical Methods and the Interpretation of Results; Vol. L221, pp 8-36.

EU (2004). Commission Decision Concerning the non-inclusion of atrazine in Annex I to Council Directive 91/414/EEC and the withdrawal of authorisations for plant protection products containing this active substance, Off. J. Eur. Union. 53-55.

EU (2008). European Commission Directive 2008/56/EC of the European Parliament and of the Council of 17 June 2008 establishing a framework for community action in the field of marine environmental policy (Marine Strategy Framework Directive). http://eur-lex.europa.eu/LexUriServ/LexUriServ.do?uri=CELEX:32008L0056:en:NOT

EU (2009). European Commission Directive 2009/90/EC Laying down, Pursuant to Directive 2000/60/EC of the European Parliament and of the Council, Technical Specifications for Chemical Analysis and Monitoring of Water Status. Off. J. Eur. Union, 8 (3), 36-38.

EU (2011). European Commission, Technical guidance document for deriving Environmental Quality Standards.

EU (2013). European Commission Directive 2013/39/EU of the European Parliament and of the Council of 12 august 2013 amending Directives 2000/60/ec and 2008/105/ec as regards priority substances in the field of water policy. Official Journal of the European Union. European Commission. p. 17.

EU (2015). European Commission implementing Decision 2015/495 establishing a watch list of substances for Union-wide monitoring in the field of water policy pursuant to Directive 2008/105/EC of the European Parliament and of the Council, Off. J. Eur. Union. L78. doi:http://eur-lex.europa.eu/pri/en/oj/dat/2003/l_285/l_28520031101en00330037.pdf

EU (2016). European Commission Implementing Regulation 2016/872 concerning the non-renewal of approval of the active substance isoproturon, in accordance with Regulation (EC) No 1107/2009 of the European Parliamant and of the Council concerning the placin, Off. J. Eur. Union. L145 7-9. https://doi.org/10.2903/j.efsa.2015.4206

EU (2018a). European Commission implementing Decision (EU) 2018/840 establishing a watch list of substances for Union-wide monitoring in the field of water policy pursuant to Directive 2008/105/EC of the European Parliament and of the Council and repealing Commission Implemen, Off. J. Eur. Union. L 141.

EU (2018b). Review of the 1st watch list under the water framework directive and recommendations for the 2nd watch list. Joint Research Center.

Eurachem (2016). In: V. Barwick (Ed), Eurachem/CITAC Guide: Guide to Quality in Analytical Chemistry: An Aid to Accreditation (3rd ed. 2016). ISBN 978-0-948926-32-7. Available from www.eurachem.org

Fan, Z., Wu, S., Chang, H., Hu, J. (2011). Behaviors of Glucocorticoids, Androgens and Progestogens in a Municipal Sewage Treatment Plant: Comparison to Estrogens. Environ. Sci. Technol., 45 (7), 2725-2733. https://doi.org/10.1021/es103429c

Focks A, Belgers D, Boerwinkel MC, Buijse L, Roessink I, Van den Brink PJ. (2018). Calibration and validation of toxicokinetic–toxicodynamic models for three neonicotinoids and some aquatic macroinvertebrates. Ecotoxicology. 27(7):992–1007.

Fox, S. D., Falk, R. T., Veenstra, T. D., Issaq, H. J. (2011). Quantitation of Free and Total Bisphenol A in Human Urine Using Liquid Chromatography–Tandem Mass Spectrometry. J. Sep. Sci., 34 (11), 1268-1274. https://doi.org/10.1002/jssc.201100087

Frost, T.K. (2002). Calculation of PNEC values applied in environmental risk management of produced water discharges (Trondheim: Statoil).

Gao, Y., de Brauwere, A., Elskens, M., Croes, K., Baeyens, W., Leermakers, M. (2013). Evolution of trace metal and organic pollutant concentrations in the Scheldt River Basin and the Belgian Coastal Zone over the last three decades. Journal of Marine Systems 128, 52-61.

Goh, S. X. L., Duarah, A., Zhang, L., Snyder, S. A., Lee, H. K. (2016). Online Solid Phase Extraction with Liquid Chromatography-Tandem Mass Spectrometry for Determination of Estrogens and Glucocorticoids in Water. J. Chromatogr. A, 1465, 9-19. https://doi.org/10.1016/j.chroma.2016.08.040

Grandy, J.J., Singh, V., Lashgari, M., Gauthier, M., Pawliszyn, J. (2018). Development of a Hydrophilic Lipophilic Balanced Thin Film Solid Phase Microextraction Device for Balanced Determination of Volatile Organic Compounds, Anal. Chem. 90 14072-14080. https://doi.org/10.1021/acs.analchem.8b04544

Gros, M., Petrovic, M., Barcelo, D. (2009). Tracing pharmaceutical residues of different therapeutic classes in environmental waters by using liquid chromatography/quadrupole- linear ion trap mass spectrometry and automated library searching. Anal. Chem. 81, 898-912. https://doi.org/10.1021/ac801358e

Guo, W., Van Langenhove, K., Denison, M.S., Baeyens, W., Elskens, M., Gao, Y. (2017). Estrogenic Activity Measurements in Water Using Diffusive Gradients in Thin-Film Coupled with an Estrogen Bioassay. Anal. Chem. 89, 13357-13364. https://doi.org/10.1021/acs.analchem.7b03537

Guo, X., Liu, L., Wu, J., Fan, J., Wu, Y. (2018). Qualitatively and Quantitatively Characterizing Water Adsorption of a Cellulose Nanofiber Film Using Micro-FTIR Spectroscopy. RSC Adv., 8 (8), 4214-4220. https://doi.org/10.1039/c7ra09894d

Guo, W., Van Langenhove, K., Vandermarken, T., Denison, M.S., Elskens, M., Baeyens, W., Gao, Y. (2019). In situ measurement of estrogenic activity in various aquatic systems using organic diffusive gradients in thin-film coupled with ERE-CALUX bioassay. Environment International 127, 13-20. https://doi.org/10.1016/j.envint.2019.03.027

Hamers T., Legradi J., Zwart N., Smedes F., de Weert J., van den Brandhof E., van de Meent D., de Zwart D. (2018). Time-integrative passive sampling combined with TOxicity Profiling (TIPTOP): an effect-based strategy for cost-effective chemical water quality assessment. Environmental Toxicology and Pharmacology 64, 48-59. https://doi.org/10.1016/j.etap.2018.09.005

Han W., Tian Y., Shen X. (2018). Human exposure to neonicotinoid insecticides and the evaluation of their potential toxicity: An overview, Chemosphere. 192 59-65. https://doi.org/10.1016/j.chemosphere.2017.10.149

Holthaus, K.I.E., Kaag, N.H.B.M., Smit, M.G.D., Jak, R.G. (2004). Update and evaluation of PNEC values for produced water according to the revised EU-TGD. TNO-report R 2004, 79p.

Hu, X., Gu, Y., Huang, W., Yin, D. (2016). Phthalate Monoesters as Markers of Phthalate Contamination in Wild Marine Organisms. Environ. Pollut., 218, 410-418. https://doi.org/10.1016/j.envpol.2016.07.020

Huysman, S. (2019). Development and validation of high-resolution mass spectrometry-based approaches for active and passive sampling of emerging organic micropollutants in the marine environment. PhD Thesis, Ghent University, Ghent, Belgium.

Illuminati, S., Annibaldi, A., Truzzi, C., Tercier-Waeber, M.-L., Nöel, S., Braungardt, C.B., Achterberg, E.P., Howell, K.A., Turner, D., Marini, M., et al. (2019). In-situ trace metal (Cd, Pb, Cu) speciation along the Po River plume (Northern Adriatic Sea) using submersible systems. Marine Chemistry 212, 47-63.

Jahnke, A., McLachlan, M.S., Mayer, P. (2008). Equilibrium sampling: Partitioning of organochlorine compounds from lipids into polydimethylsiloxane. Chemosphere 73, 1575-1581.

Jeong, Y., Schäffer, A., Smith, K. (2017). Equilibrium partitioning of organic compounds to OASIS HLB®as a function of compound concentration, pH, temperature and salinity. Chemosphere, 174, 297-305. https://doi.org/10.1016/j.chemosphere.2017.01.116

Jia, A., Wan, Y., Xiao, Y., Hu, J. (2012). Occurrence and fate of quinolone and fluoroquinolone antibiotics in a municipal sewage treatment plant. Water Res. 46,387-394. https://doi.org/10.1016/j.watres.2011.10.055

Jonkers N., Sousa A., Galante-Oliveira S., Barroso C.M., Kohler H.P.E., Giger W. (2010). Occurrence and sources of selected phenolic endocrine disruptors in Ria de Aveiro, Portugal, Environ. Sci. Pollut. Res. 17 834-843. https://doi.org/10.1007/s11356-009-0275-5

Karickhoff, S.W., Brown, D.S., Scott, T.A. (1979). Sorption of hydrophobic pollutants on natural sediments. Water Res. 13, 241-248

Kermani, F.R., Tugulea, A.M., Hnatiw, J., Niri, V.H., Pawliszyn, J. (2013). Application of automated solid-phase microextraction to determine haloacetonitriles, haloketones, and chloropicrin in Canadian drinking water, Water Qual. Res. J. Canada. 48, 85-98. https://doi.org/10.2166/wqrjc.2013.012

Kim Tiam S., Morin S., Pesce S., Feurtet-Mazel A., Moreira A., Gonzalez P., Mazzella N. (2014). Environmental effects of realistic pesticide mixtures on natural biofilm communities with different exposure histories. Science of the Total Environment. 473:496-506.

Kizil, R., Irudayaraj, J., Seetharaman, K. (2002). Characterization of Irradiated Starches by Using FT-Raman and FTIR Spectroscopy. J. Agric. Food Chem., 50 (14), 3912-3918. https://doi.org/10.1021/jf011652p

Kruve, A., Rebane, R., Kipper, K., Oldekop, M.-L., Evard, H., Herodes, K., Ravio, P., Leito, I. (2015a). Tutorial Review on Validation of Liquid Chromatography-Mass Spectrometry Methods: Part I. Anal. Chim. Acta, 870, 29-44. https://doi.org/10.1016/j.aca.2015.02.017

Kruve, A., Rebane, R., Kipper, K., Oldekop, M.-L., Evard, H., Herodes, K., Ravio, P., Leito, I. (2015b). Tutorial Review on Validation of Liquid Chromatography-Mass Spectrometry Methods: Part II. Anal. Chim. Acta, 870, 8-28. https://doi.org/10.1016/j.aca.2015.02.016

Kudlak, B., Szczepanska, N., Owczarek, K., Mazerska, Z., Namiesnik, J. (2015). Revision of biological methods for determination of EDC presence and their endocrine potential. J. Crit. Rev. Anal.Chem., 45,191-200.

Lacroix G., Ruddick K., Ozer J., Lancelot C. (2004). Modelling the impact of the Scheldt and Rhine/Meuse plumes on the salinity distribution in Belgian waters (Southern North Sea). Journal of Sea Research, 52: 149-163. https://doi.org/10.1016/j.seares.2004.01.003

Liu, H., Wei, M., Yang, X., Yin, C., He, X. (2017). Development of TLSER model and QSAR model for predicting partition coefficients of hydrophobic organic chemicals between low density polyethylene film and water, Sci. Total Environ. 574 1371-1378. https://doi.org/10.1016/J.SCITOTENV.2016.08.051

Loos, R., Marinov, D., Sanseverino, I., Napierska, D., Lettieri, T. (2018). Review of the 1st Watch List under the Water Framework Directive and recommendations for the 2nd Watch List. Publications Office of the European Union, Luxemburg.

Loring, D.H. (1991). Normalization of heavy-metal data from estuarine and coastal sediments. Journal of Marine Sciences 48, 101-115.

Luyten P. (2011). COHERENS — A coupled Hydrodynamical-Ecological Model for Regional and Shelf Seas: User Documentation. Version 2.0. RBINS-MUMM Report, Royal Belgian Institute of the Natural Sciences, 1192 pp.

Magnusson, B., and Örnemark, U. (2014). Eurachem Guide: The Fitness for Purpose of Analytical Methods - A Laboratory Guide to Method Validation and Related Topics. https://doi.org/978-91-87461-59-0

Matuszewski, B.K., Constanzer, M.L., Chavez-Eng, C.M. (2003). Strategies for the assessment of matrix effect in quantitative bioanalytical methods based on HPLC - MS/MS. Anal. Chem. 75, 3019-3030. https://doi.org/10.1021/ac020361s

Maycock, D., Merrington, G., Peters, A. (2011). Proposed EQS for Water Framework Directive Annex VIII substances: copper (saltwater) (For consultation). SC080021/8n. Water Framework Directive - United Kingdom Technical Advisory Group. 88p.

Mizuguchi, M., Nara, M., Kawano, K., Nitta, K. (1997). FT-XR Study of the Ca2+-Binding to Bovine α-Lactalbumin. Relationships between the Type of Coordination and Characteristics of the Bands Due to the Asp COO-Groups in the Ca2+-Binding Site. FEBS Lett., 417 (1), 153-156. https://doi.org/10.1016/S0014-5793(97)01274-X

Morrison, S. A. and Belden, J. B. (2016). Calibration of nylon organic chemical integrative samplers and sentinel samplers for quantitative measurement of pulsed aquatic exposures. J. Chromatogr. A 1449, 109-117.

Noppe H., Verslycke T., De Wulf E., Verheyden K., Monteyne E., Van Caeter P., Janssen C.R., De brabander H.F. (2007). Occurrence of estrogens in the Scheldt estuary: A 2-year survey, Ecotoxicol. Environ. Saf. 66 1-8. https://doi.org/10.1016/j.ecoenv.2006.04.005

Oldenkamp, R., Hoeks, S., Čengić, M., Barbarossa, V., Burns, E. E., Boxall, A. B., & Ragas, A. M. (2018). A high-resolution spatial model to predict exposure to pharmaceuticals in European surface waters: EPiE. Environmental science & technology, 52(21), 12494-12503.

OSPAR (2008). Co-ordinated Environmental Monitoring Programme Assessment Manual for contaminants in sediment and biota. OSPAR Commission.

Parmentier, K. (2003). Biogeochemical behaviour of trace metals in the Scheldt estuary and the Southern Bight of the North Sea. Doctoral thesis. Vrije Universiteit Brussel. 271p.

Periañez, R., Casas-Ruíz, M., & Bolívar, J. P. (2013). Tidal circulation, sediment and pollutant transport in Cádiz Bay (SW Spain): a modelling study. Ocean engineering, 69, 60-69.

Ramesh Kumar A. and Sivaperumal P. (2016). Analytical Methods for the Determination of Biomarkers of Exposure to Phthalates in Human Urine Samples. TrAC - Trends in Analytical Chemistry. Elsevier January 1, pp 151-161. https://doi.org/10.1016/j.trac.2015.06.008

Raymond, P.A., and Bauer, J.E. (2001). Use of 14 C and 13 C natural abundances for evaluating riverine, estuarine, and coastal DOC and POC sources and cycling: a review and synthesis. Organic Geochemistry 32, 469-485.

Regnier, P., and Wollast, R. (1993). Distribution of trace metals in suspended matter of the Scheldt estuary. Marine Chemistry 43, 3-19.

Reichenberg F. and Mayer P. (2006). Two complementary sides of bioavailability: Accessibility and chemical activity of organic contaminants in sediments and soils. Environ. Toxicol. Chem. 25, 1239-1245.

Ritz C, Baty F, Streibig JC, Gerhard D (2015). Dose-Response Analysis Using R. PLoS ONE 10(12): e0146021.

Roig, N., Nadal, M., Sierra, J., Ginebreda, A., Schuhmacher, M., and Domingo, J.L. (2011). Novel approach for assessing heavy metal pollution and ecotoxicological status of rivers by means of passive sampling methods. Environment International 37, 671-677.

Ronan, J. M. and McHugh, B. A (2013). Sensitive Liquid Chromatography/Tandem Mass Spectrometry Method for the Determination of Natural and Synthetic Steroid Estrogens in Seawater and Marine Biota, with a Focus on Proposed Water Framework Directive Environmental Quality Standards. Rapid Commun. Mass Spectrom., 27 (7), 738-746. https://doi.org/10.1002/rcm.6505

Ronov, A.B., Yaroshevskiy, A.A., Migdisov, A.A. (1991). Chemical Consitution Of The Earth's Crust And Geochemical Balance Of The Major Elements (Part II) International Geology Review 33, 1049-1097. https://doi.org/10.1080/00206819109465737

Rusina, T.P.; Smedes, F.; Brborić, M.; Vrana, B. (2019). Investigating levels of organic contaminants in Danube River sediments in Serbia by multi-ratio equilibrium passive sampling. Sci. Total Environ., 696, 133935. https://doi.org/10.1016/j.scitotenv.2019.133935

Sanchez-Bayo, F. and K. Goka (2006). Influence of light in acute toxicity bioassays of imidacloprid and zinc pyrithione to zooplankton crustaceans. Aquatic Toxicology 78(3): p. 262-271.

Schintu, M., Durante, L., Maccioni, A., Meloni, P., Degetto, S., and Contu, A. (2008). Measurement of environmental trace-metal levels in Mediterranean coastal areas with transplanted mussels and DGT techniques. Marine Pollution Bulletin 57, 832-837.

Schmidt-Bäumler, K., Heberer, T., Stan, H. J. (1999). Occurrence and Distribution of Organic Contaminants in the Aquatic System in Berlin. Part II: Substituted Phenols in Berlin Surface Water. Acta Hydrochim. Hydrobiol., 27 (3), 143-149. https://doi.org/10.1002/(SICI)1521-401X(199905)27:3<143::AID-AHEH143>3.0.CO;2-9

Shaw M, Negri A, Fabricius K, Mueller JF (2009). Predicting water toxicity: Pairing passive sampling with bioassays on the Great Barrier Reef. Aquatic toxicology 95(2): p. 108-116.

Sierra, J., Roig, N., Giménez Papiol, G., Pérez-Gallego, E., and Schuhmacher, M. (2017). Prediction of the bioavailability of potentially toxic elements in freshwaters. Comparison between speciation models and passive samplers. Science of The Total Environment 605-606, 211-218.

Simpson, S.L., Yverneau, H., Cremazy, A., Jarolimek, C.V., Price, H.L., and Jolley, D.F. (2012). DGT-Induced Copper Flux Predicts Bioaccumulation and Toxicity to Bivalves in Sediments with Varying Properties. Environmental Science & Technology 46, 9038-9046.

Slaveykova, V.I., Karadjova, I.B., Karadjov, M., and Tsalev, D.L. (2009). Trace metal speciation and bioavailability in surface waters of the Black Sea coastal area evaluated by HF-PLM and DGT. Environ. Sci. Technol. 43, 1798-1803.

Smedes F. (2007). Monitoring of chlorinated biphenyls and polycyclic aromatic hydrocarbons by passive sampling in concert with deployed mussels. In: Greenwood R., Mills G., Vrana B. (Ed.): Comprehensive Analytical Chemistry Vol 48: Passive sampling Techniques in Environmental Monitoring. ISSN: 0166-526X https://DOI.org/10.1016/S0166-526X(06)48019-3

Smedes F., Geertsma R.W., Van der Zande T., Booij K. (2009). Polymer-Water Partition Coefficients of Hydrophobic Compounds for Passive Sampling: Application of Cosolvent Models for Validation. Environ. Sci. Technol., 43, 7047-7054.

Smedes F. and Booij K. (2012). Guidelines for passive sampling of hydrophobic contaminants in water using silicone rubber samplers. ICES Techniques in Marine Environmental Sciences. No. 52 (20pp); https://DOI.org/10.17895/ices.pub.5077

Smedes, F., van Vliet, L.A., Booij, K. (2013). Multi-Ratio equilibrium passive sampling method to estimate accessible and pore water concentrations of polycyclic aromatic hydrocarbons and polychlorinated biphenyls in sediment. Environ. Sci. Technol. 47, 510-517.

Smedes, F., Rusina, T.P., Beeltje, H., Mayer, Ph. (2017). Partitioning of hydrophobic organic contaminants between polymer and lipids for two silicones and low density polyethylene. Chemosphere 186, 948-957. http://dx.doi.org/10.1016/j.chemosphere.2017.08.044

Smedes, F. (2018). Silicone-water partition coefficients determined by cosolvent method for chlorinated pesticides, musks, organo phosphates, phthalates and more. Chemosphere 210, 662-671. https://doi.org/10.1016/j.chemosphere.2018.07.054

Smedes, F. (2019). SSP silicone-, lipid- and SPMD-water partition coefficients of seventy hydrophobic organic contaminants and evaluation of the water concentration calculator for SPMD. Chemosphere 223, 748-757.

Smedes, F., Sobotka, J., Rusina, T.P., Fialová, P., Carlsson, P., Kopp, R., Vrana, B. (2020). Unraveling the Relationship between the Concentrations of Hydrophobic Organic Contaminants in Freshwater Fish of Different Trophic Levels and Water Using Passive Sampling. Environ. Sci. Technol. 54, 7942-7951

Smith, K.E.C., G.J. Oostingh, and P. Mayer (2010). Passive Dosing for Producing Defined and Constant Exposure of Hydrophobic Organic Compounds during in Vitro Toxicity Tests. Chemical Research in Toxicology 23(1): p. 55-65.

Stiles, R., Yang, I., Lippincott, R.L., Murphy, E., Buckley, B. (2008). Measurement of drinking water contaminants by solid phase microextraction initially quantified in source water samples by the USGS, Environ. Sci. Technol. 42, 2976-2981. https://doi:10.1021/es071804i

Taguchi, Y. and Noguchi, T. (2007). Drastic Changes in the Ligand Structure of the Oxygen-Evolving Mn Cluster upon Ca2+ Depletion as Revealed by FTIR Difference Spectroscopy. Biochim. Biophys. Acta - Bioenerg., 1767 (6), 535-540. https://doi.org/10.1016/j.bbabio.2006.11.002

Tanwar S., Di Carro M., Ianni C., Magi E. (2015). Occurrence of PCPs in Natural Waters from Europe, in: Handb. Environ. Chem. M.S. Díaz-Cruz, D. Barceló (Eds.): pp. 41-53. https://doi:10.1007/698

Tell J., Caldwell D.J., Haner A., Hellstern J., Hoeger B., Journel R., Mastrocco F., Ryan J.J., Snape J., Straub J.O. et al. (2019). Science-based targets for antibiotics in receiving waters from pharmaceutical manufacturing operations. Integrated Environmental Assessment and Management. 15(3):312-319.

Tessier, A., and Turner, D.R. (1995). Metal Speciation and Bioavailability in Aquatic Systems, vol.3. IUPAC Series. Wiley. 696p.

Tousova Z., Oswald P., Slobodnik J., Blaha L., Muz M., Hu M., Brack W., Krauss M., Di Paolo C., Tarcai Z., et al. (2017). European demonstration program on the effect-based and chemical

identification and monitoring of organic pollutants in European surface waters. Science of the Total Environment 601: p. 1849-1868.

Trumbore, S.E., and Druffel, E.R.M. (1995). Carbon isotopes for characterizing sources and turnover of non-living organic matter. R. G. Zepp, & C. Sonntag (Eds.). Role of Non-Living Organic Matter in the Earth's Carbon Cycle. 7-22.

US EPA (2018). https://ecotox.ipmcenters.org/

US EPA (2019). https://cfpub.epa.gov/ecotox/

Valenta, P., Duursma, E.K., Merks, A.G.A., Rützel, H., and Nürnberg, H.W. (1986). Distribution of Cd, Pb and Cu between the dissolved and particulate phase in the Eastern Scheldt and Western Scheldt estuary. Science of The Total Environment 53, 41-76.

Van Daele, M., Bertrand, S., Meyer, I., Moernaut, J., Vandoorne, W., Siani, G., Tanghe, N., Zakariou, G., Pino, M., Urrutia, R. & De Batist, M. (2016). Late Quaternary evolution of Lago Castor (Chile, 45.6S): Timing of the deglaciation in northern Patagonia and evolution of the southern westerlies during the last 17 kyr. Quaternary Science Reviews, 133, 130-146. https://doi.org/10.1016/j.quascirev.2015.12.021

Vanryckeghem, F. (2020). Novel active and passive sampling approaches for monitoring contaminants of emerging concern in the marine environment. PhD Thesis, Ghent University, Ghent, Belgium.

Vergeynst, L., Haeck, A., De Wispelaere, P., Van Langenhove, H., Demeestere, K. (2015). Multi-residue analysis of pharmaceuticals in wastewater by liquid chromatography-magnetic sector mass spectrometry: method quality assessment and application in a Belgian case study. Chemosphere 119, S2-S8. https://doi.org/10.1016/j.chemosphere.2014.03.069

Vergeynst, L., K'oreje, K., De Wispelaere, P., Harinck, L., Van Langenhove, H., Demeestere, K. (2017). Statistical procedures for the determination of linearity, detection limits and measurement uncertainty: a deeper look into SPE-LC-Orbitrap mass spectrometry of pharmaceuticals in wastewater. J. Hazard. Mater. 323, 2-10. https://doi.org/10.1016/j.jhazmat.2016.05.077

Vermeirssen E.L.M., Dietschweiler C., Escher B.I., Van Der Voet J., Hollender J. (2012). Transfer kinetics of polar organic compounds over polyethersulfone membranes in the passive samplers pocis and chemcatcher, Environ. Sci. Technol. 46 6759-6766. https://doi:10.1021/es3007854

Weigel S., Kuhlmann J., Hühnerfuss H. (2002). Drugs and personal care products as ubiquitous pollutants: Occurrence and distribution of clofibric acid, caffeine and DEET in the North Sea, Sci. Total Environ. 295 131-141. https://doi.org/10.1016/S0048-9697(02)00064-5

Weston D.P., Chen D., Lydy M.J. (2015). Stormwater-related transport of the insecticides bifenthrin, fipronil, imidacloprid, and chlorpyrifos into a tidal wetland, San Francisco Bay, California, Sci. Total Environ. 527-528 18-25. doi: https://doi.org/10.1016/j.scitotenv.2015.04.095

Wormser G.P., Keusch G.T., Heel R.C. (1982). Co-trimoxazole (Trimethoprim-sulfamethoxazole): An updated review of its antibacterial activity and clinical efficacy, Drugs. 24 459-518. https://doi:10.2165/00003495-198224060-00002

Wu, S., Jia, A., Daniels, K. D., Park, M., Snyder, S. A. (2019). Trace Analysis of Corticosteroids (CSs) in Environmental Waters by Liquid Chromatography-Tandem Mass Spectrometry. Talanta, 195, 830-840. https://doi.org/10.1016/j.talanta.2018.11.113

Zhang, H., and Davison, W. (1995). Performance Characteristics of Diffusion Gradients in Thin Films for the in-situ Measurement of Trace Metals in Aqueous Solution. Anal. Chem. 67, 3391-3400.

Zhang, L.-P., Wang, X.-H., Ya, M.-L, Wu, Y.-L., Li, Y.-Y., Zhang, Z. (2014). Levels of Endocrine Disrupting Compounds in South China Sea. Mar. Pollut. Bull., 85 (2), 628-633. https://doi.org/10.1016/j.marpolbul.2013.12.040

GLOSSARY

α-MEM	alpha-Minimal Essential Medium
AA-EQS	Annual Average Environmental Quality Standard
AF	Assessment Factor
AGC	Automatic Gain Control
ANOVA	Analysis of Variance
APCI	Atmospheric Pressure Chemical Ionisation
APS	ammonium persulfate
ASE	Accelerated Solvent Extraction
ASTM	American Society for Testing and Materials
a.u.	arbitrary unit
BFR	Brominated Flame Retardant
BPNS	Belgian Part of the North Sea
CBs	Chlorinated Biphenyls
CCAP	Culture Collection of Algae and Protozoa
CEC	Contaminants of Emerging Concern
CLO	Clothianidin
COHERENS	Coupled Hydrodynamic Ecological model for Regional Shelf seas
DBL	Diffusive Boundary Layer
DF	Detection Frequency
DGT	Diffusive Gradient in Thin films
DOM	Dissolved Organic Matter
DMEM	Dulbecco's Modified Eagle Medium
DVB	Divinylbenzene
E1	Estrone

E2	17 β -estradiol
E3	Estriol
EE2	17-alpha-ethinyl-estradiol
EA	Elemental Analyzer
EDC	Endocrine Disrupting Chemical
Eq.	Equation
EQS	Environmental Quality Standard
ERA	Environmental Risk Assessment
ERCM	Environmentally Relevant (Organic) Contaminant Mixture
ERE-CALUX	Estrogen Responsive Elements - Chemically Activated Luciferase gene expression
EU	European Union
FBS	Foetal Bovine Serum
FTIR	Fourier transform infrared
FWHM	Full Width at Half Maximum
GES	Good Environmental Status
GMF	glass-microfibre filters
HCB	Hexachlorobenzene
HDPE	High Density Polyethylene
HESI	Heated Electrospray Ionization
HLB	Hydrophilic Lipophilic Bond
HOC	Hydrophobic Organic Compounds
HPLC	High Performance Liquid Chromatography
HRMS	High-Resolution Mass Spectrometry
IAEA	International Atomic Energy Agency
ICP-MS	Inductively Coupled Plasma Mass Spectrometry

IDL	Instrumental Detection Limit
IMI	Imidacloprid
IQL	Instrumental Quantification Limit
IRMS	Isotope Ratio Mass Spectrometry
IUPAC	International Union of Pure and Applied Chemistry
LDPE	Low Density Polyethylene
LDR	Larval Development Ratio
LOEC	Lowest-observed Effect Concentration
MDL	Method Detection Limit
ME	Matrix suppression or Enhancement factor
MoS	Margin of Safety
MQL	Method Quantification Limit
MRCC	Marine Rescue and Coordination Centre
MR-EPS	multi-ratio equilibrium passive sampling
MSFD	Marine Strategy Framework Directive
ND-EPS	Non-depletive equilibrium passive sampling
NIR	Near Infrared
NOEC	No-observed Effect Concentration
NPR	Nominal Particle Retention
o-DGT	organic Diffusive Gradient in Thin films
OPP	Office of Pesticide Programs
PAE	Phthalic Acid Esters
PAHs	Polycyclic Aromatic Hydrocarbons
PBS	Phosphate Buffered Saline
PCPs	Personal Care Products

PE	Process Efficiency
PeCB	Pentachloro benzene
PES	Polyether sulfone
PhACs	Pharmaceuticals
PNEC	Predicted No Effect Concentration
POC	Particulate Organic Carbon
POP	Persistent Organic Pollutant
PRC	Performance Reference Compound
PRM	Parallel Reaction Monitoring
PS	Passive sampler
psu	practical salinity unit
PTFE	Polytetrafluoroethylene
RE	Extraction Recovery
REF	relative enrichment factor
RMSE	Root-Mean-Square of the relative Errors
RQ	Risk quotient
RSD	Relative Standard Deviation
SAD	Shipping Assistance Division
SC	Sampling campaign
SD	Standard Deviation
SI	Supplementary Information
SpD	Speedisk passive samplers
SPE	Solid Phase Extraction
SPM	Suspended Particulate Matter
SR	Silicone Rubber

STEPS Simple Teabag Equilibrium Passive Sampler

TCP Thiacloprid

TEMED Tetramethyl Ethylene Diamine

TIE Toxicity identification Evaluation

TMX Thiamethoxam

TU toxic unit

UHPLCUltra-High Performance Liquid Chromatography

US EPA United States Environmental Protection Agency

UV Ultra-Violet

WBL water boundary layer

WFD Water Framework Directive

WP Work Package

WWTP Wastewater treatment plant